Department of Experimental Neurology
University of Ulm
Head: Prof. Dr. A.C. Ludolph



Microtubule stabilization facilitates axon regeneration in central nervous system

Dissertation submitted in partial fulfillment of the requirements for the degree of “Doctor Human biologie” (Dr.biol.hum) of the Medicine Faculty, University of Ulm

Vetrivel Sengottuvel

Rasipuram, Tamilnadu, India

2012

Dean: Prof. Dr. Thomas Wirth

First supervisor: Prof. Dr. Dietmar Fischer

Second supervisor: Prof. Dr. Uwe Knippschild

Day doctorate awarded: 22 June 2012

To my parents and teachers

Contents

Contents…….. i
Abbreviations……. iii
1. Introduction…… 1
1.1 General introduction……. 1
1.2 Factors affecting axon regeneration in CNS…….…… 1
1.3 Anatomical organization of the retina and visual pathways of rats…….…….. 6
1.4 The optic nerve as a model system for CNS regeneration……. 9
1.5 Measures toward improvement of axon regeneration in CNS……..... 10
1.6 Microtubules - assembly and dynamics……. 13
1.7 Paclitaxel – a therapeutic drug……... 16
1.8 Thesis objective(s)…….. 17
2. Materials and methods……..... 18
2.1 Materials……. 18
2.1.1 Chemicals and reagents…….. 18
2.2 Experimental methods…… 22
2.2.1 Optic nerve crush, LI, and Taxol treatment of the optic nerve…… 22
2.2.2 Preparation of CNS myelin extract (CME)……. 23
2.2.3 BCA protein estimation assay……..... 24
2.2.4 Preparation of dissociated mixed retinal cultures…….. 25
2.2.5 Treatments of adult rat retinal cultures *in vitro*…….. 25
2.2.6 Immunocytochemistry and RGC neurite outgrowth analysis……. 26
2.2.7 PC12 cell cultures and neurite outgrowth analysis…….…… 27
2.2.8 Preparation of retinal lysate for western blot analysis……..... 28
2.2.9 Western blot assay……. 28
2.2.10 PC12 cell cultures and Rho activity assay……... 31
2.2.11 Quantification of growth cone size……. 31
2.2.12 Tissue preparation for cryo-sectioning and immunohistochemistry…….. 33
2.2.13 Quantification of axons in the optic nerve and RGCs in retinal cross sections…... 34
2.2.14 Quantification of macrophages……... 34
2.2.15 Measurement of GFAP-free gap at the lesion site…….. 35
2.2.16 Primary astrocyte cultures and Taxol treatment…… 36
2.2.17 Measurement of CSPG expression……. 37

3. Results…….. 39
3.1 Taxol improves neurite outgrowth of adult RGCs in a concentration dependent manner……..... 39
3.2 Taxol synergistically enhances neurite outgrowth in a combinatorial treatment and overcomes myelin inhibition…….. 41
3.3 Taxol improves neurite outgrowth of PC12 cells and overcomes myelin inhibition.... 43
3.4 Taxol overcomes CSPG inhibition of neurite outgrowth……..... 45
3.5 Taxol prevents myelin induced growth cone collapse/shrinkage independent of RhoA activation……..... 47
3.6 Taxol treatment enhances optic nerve regeneration *in vivo*…….. 53
3.7 Taxol promotes early axonal sprouting *in vivo*……. 58
3.8 Taxol treatment at the lesion site does not affect the intrinsic regenerative state of RGCs…….. 60
3.9 Taxol affects the migration of peripheral macrophages at the lesion site……. 63
3.10 Taxol delays the astrocytic cellular responses around the lesion site…….. 65
3.13 Taxol delays the proliferation of primary astrocytes *in vitro*…….. 67
3.14 Taxol reduces CSPG expression at the lesion site……..... 69
4. Discussion……..... 72
4.1 General discussion……. 72
4.2 Relevance of Taxol concentrations to improve axon regeneration……..... 73
4.3 Modalities of Taxol mediated axon regeneration……..... 74
4.4 Taxol desensitizes growth cone toward myelin and CSPGs inhibition…….. 75
4.5 Taxol impedes glial scar formation……..... 76
5. Summary……. 79
6. Reference(s)…….. 81
7. Acknowledgements…….. 96
8. Curriculum Vitae……. 97

Abbreviations

BBB	Blood brain barrier
BCA	Bicinchoninic acid
BSA	Bovine serum albumin
C-domain	Central domain
CME	CNS myelin extract
CNS	Central nervous system
CNTF	Ciliary neurotrophic factor
CSPG	Chondroitin sulphate proteoglycans
CRMP-2	Collapsing response mediator protein 2
CTB	Cholera toxin subunit beta
DMEM	Dulbecco's modified eagle's medium
ECL	Enhanced chemiluminescence
F-actin	Filamentous actin
EGFR	Epidermal growth factor
GAP43	Growth associated protein 43
GDP	Guanosine di phosphate
GFAP	Glial fibrillary acidic protein
GPI	Glycosyl phosphatidyl-inositol
GTP	Guanosine tri phosphate
Ig	Immunoglobulin
KIF2	Kinesin family member 2
LGN	Lateral geniculate nucleus
LI	Lens injury

LIF	Leukemia inhibitory factor
LINGO-1	leucine rich repeat and Ig domain-containing, NgR1 interacting protein
MAG	Myelin associated glycoprotein
MIL	Myelin inhibitory ligands
MT	Microtubule
MTs	Microtubules
NGF	Nerve growth factor
NgR	Nogo receptor
Omgp	Oligodendrocyte myelin glycoprotein
ON	Optic nerve
ONC	Optic nerve crush
PBS	Phosphate buffered saline
P-domain	Peripheral domain
PirB	Paired immunoglobulin like receptor beta
PKC	Protein kinase C
PTN	Pretectal nucleus
PTPσ	Protein tyrosine phosphatase-sigma
PNS	Peripheral nervous system
$p75^{NTR}$	p75 Neurotrophin receptor
RGCs	Retinal ganglion cells
RhoA	Ras homologue gene family, member A
RhoGDI	Rho guanine dissociation factor
RhoGEF	Rho Guanine exchange factor
ROCK	Rho-associated protein kinase
SC	Superior colliculus
STAT3	Signal transducers and activators of transcription 3
TGFβ	Transforming growth factor beta

TROY	another tumor necrosis factor receptor family member
T-zone	Transition zone

1. Introduction

1.1 General Introduction

Nervous system - the master regulator in the body receives stimuli from external as well as internal environment, coordinates the input signals, provides feedback responses to the stimuli and thereby governs various functions necessary to maintain homeostasis. The mammalian nervous system is composed of two anatomically distinct types: the central nervous system (CNS) and peripheral nervous system (PNS). The CNS comprises the various compartments of the brain, spinal cord, retina and the optic nerve. The PNS consists of all the nerves that are not part of the CNS and relays the information from CNS to the effector organs, muscles or glands. PNS and CNS vary in their axon regenerative capabilities, while the PNS neurons display significant levels of regeneration, the mature CNS neurons has very limited regenerative potential. This affects the normal functions in the system and leads to debilitating conditions after traumatic CNS injuries and plethora of neurodegenerative diseases like Alzheimer's disease, Parkinson disease, Multiple sclerosis. Therefore, research on strategies to augment axon regeneration and survival of CNS neurons after injury/neurodegeneration assumes great significance and interest.

1.2 Factors affecting axon regeneration in CNS

1.2.1 Myelin inhibitors

The ligands derived from myelin components of the CNS - Nogo, myelin-associated glycoprotein (MAG), oligodendrocyte myelin glycoprotein (Omgp) are inhibitory toward axon regeneration after injury (Schwab et al., 1993; Filbin, 2003; Yiu and He, 2006) [Fig. 1]. Nogo belongs to the reticulon family of transmembrane proteins usually located in the endoplasmic reticulum, although it has been also found on oligodendrocyte surface and innermost loop of myelin membrane (Chen et al., 2000; GrandPre et al., 2000; Prinjha et al., 2000; Huber et al., 2002; Wang et al., 2002c). Nogo consists of three different isoforms – Nogo - A, B and C; and the structural analysis of Nogo isoforms revealed two inhibitory domains – Nogo-66 (a 66-amino acid loop) that is present in all the isoforms and amino-Nogo (a unique amino terminal region) located only in Nogo-A (Prinjha et al., 2000; Oertle et al., 2003). However, both domains inhibit neurite

outgrowth of CNS neurons. MAG, the first myelin ligand described belongs to immunoglobulin (Ig) super family and is located on the periaxonal membrane as well as on paranodal loops (Lai et al., 1987). MAG exhibits a dual phenomenon toward neurite outgrowth based on the age of animals. MAG promotes neurite outgrowth of embryonic and neonatal neurons whereas inhibits outgrowth of adult neurons, suggesting a transition in its properties around the time of birth (Johnson et al., 1989; McKerracher et al., 1994; Mukhopadhyay et al., 1994; Cai et al., 2001). MAG is also a sialic acid binding protein that interacts with sialoglycolipids (gangliosides) like GT1b expressed on neuronal surface and inhibits neurite outgrowth (DeBellard et al., 1996; Collins et al., 1997). GT1b mediated inhibition can also occur independent of MAG when they are clustered through addition of anti-GT1b antibodies, possibly through the interaction of clustered GT1b to p75 neurotrophin receptor ($p75^{NTR}$) and the resultant activation of downstream signaling cascades (Vinson et al., 2001; Vyas et al., 2002; Yamashita et al., 2002). OMgp is a glycosylphosphatidyl-inositol (GPI) anchored protein present in the membranes of paranodal loops that cover the nodes of Ranvier and has a putative role in prevention of collateral branching (Mikol et al., 1990; Huang et al., 2005). OMgp has been also implicated in neurite outgrowth inhibition and growth cone collapse (Kottis et al., 2002; Wang et al., 2002b). The myelin associated proteins like semaphorins and ephrins that are involved in axon path finding and guidance during development also plays a negative role toward regeneration in mature CNS (Yiu and He, 2006).

1.2.2 Signaling of myelin inhibitors

The receptor binding and downstream signaling activation of myelin inhibitory ligands (MIL) are quite complex considering the variance in the ligands that are part of myelin (Fig. 1). Nogo receptor (NgR), a GPI-linked protein can bind to most of the MIL – Nogo isoforms, OMgp, MAG (Fournier et al., 2001). There are different homologues of NgR that exists in neurons – NgR1, NgR2 and NgR3 (Lauren et al., 2003; Pignot et al., 2003). However, NgR lacks the intracellular domain and therefore requires co-receptors for signal transduction. The co-receptors that bind to NgR1 for downstream signaling activation are $p75^{NTR}$, another tumor necrosis factor receptor family member (TROY), as well as leucine rich repeat and Ig domain-containing, NgR1 interacting protein (LINGO-1) (Wang et al., 2002a; Wong et al., 2002; Mi et al., 2004; Park et al., 2005; Shao et al., 2005). $p75^{NTR}$ is not expressed in most of the mature neurons, wherein TROY/LINGO forms a complex with NgR to activate receptor signaling. Recently, PirB (paired immunoglobulin-

like receptor B) has been characterized as another receptor for Nogo, MAG and OMgp (Atwal et al., 2008). The binding of MIL to the NgR receptor complex, for instance to the $p75^{NTR}$, results in transphosphorylation of $p75^{NTR}$ which leads to the release of bound ras homologue gene family guanine dissociation factor (RhoGDI). This factor facilitates the transformation of ras homologue gene family-member A- guanosine di phosphate [RhoA-GDP] (inactive state) into RhoA-guanosine tri phosphate [RhoA-GTP] (active state) by Rho guanine exchange factor (RhoGEF). RhoA-GTP then elicits the sequential phosphorylation of molecules that lie downstream of RhoA/Rho-associated protein kinase (ROCK) signaling cascade – ROCK, Lim kinase1/2 and, cofilin which causes actin depolymerization and growth cone collapse ultimately leading to axon growth inhibition (Mueller, 1999; Tang, 2003; Berry et al., 2008).

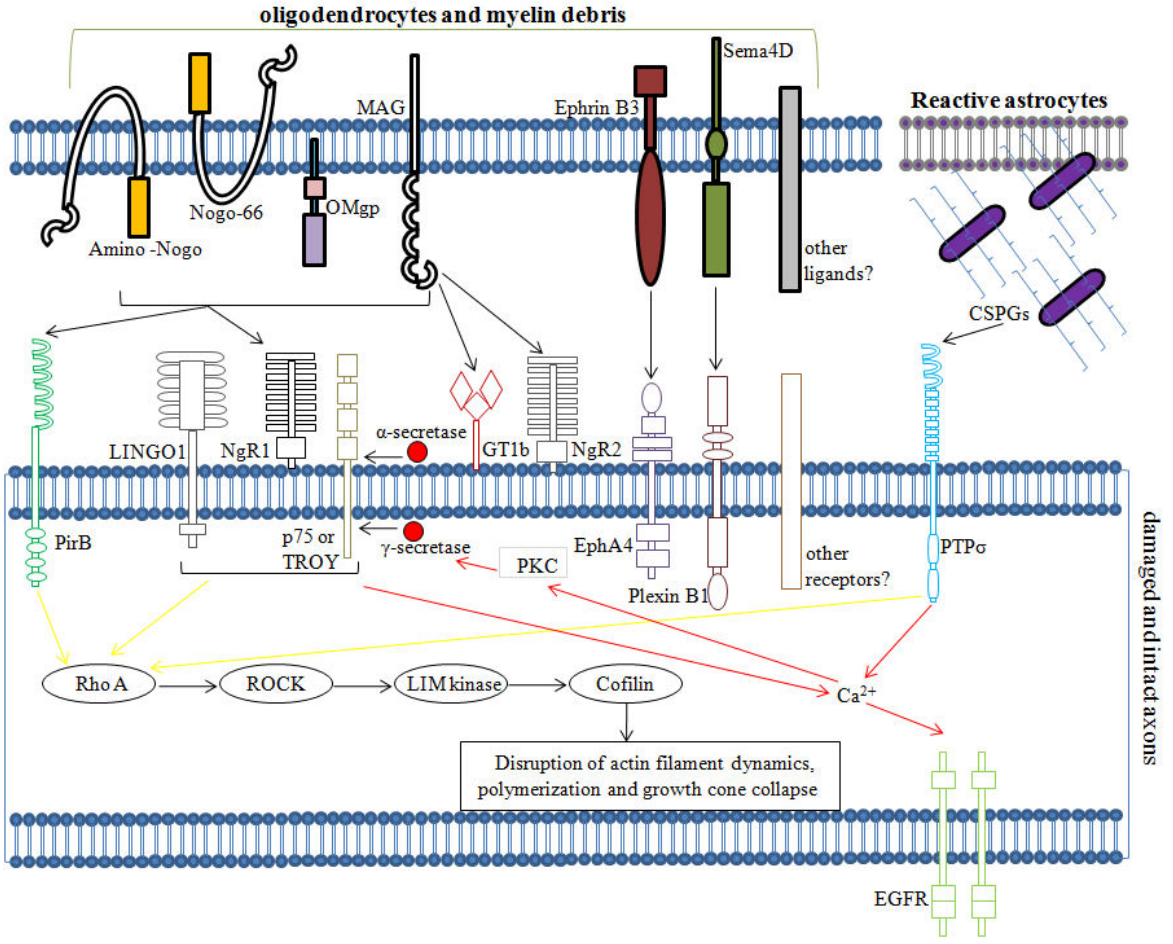

Fig. 1. Glial inhibitors and intracellular signaling mechanisms. Intact oligodendrocytes and cellular debris present at the CNS injury site contribute to the myelin associated inhibitory molecules which include Nogo, MAG, OMgp, ephrins and semaphorins. CSPGs are derived from reactive astrocytes. Receptor binding of the inhibitory ligands activate the

downstream signaling cascade (yellow arrows) through Rho/ROCK pathway (black arrows) leading to actin depolymerization and inhibition of axon growth. In addition, intracellular increase in Ca^{2+} levels activate protein kinase C (PKC) which is necessary for the cleavage of p75 neurotrophin receptor by γ-secretase or transactivation of the EGFR (red arrows) and contribute to impaired axon regeneration. [Conceived and re-drawn from: (Filbin, 2003; Yiu and He, 2006; Berry et al., 2008)]

1.2.3 Glial scar

Glial scar that forms around the CNS injury site along with the plethora of molecules released from scar forming cells inhibits axon regeneration (Silver and Miller, 2004; Fitch and Silver, 2008). The events and cellular types that contribute to glial scar formation include reactive astrocytes, meningeal fibroblasts, activated microglia and infiltrating macrophages from the blood stream. Reactive astrocytes are characterized by cellular hypertrophy, proliferation and strong increase in glial fibrillary acidic protein expression (GFAP) which occurs immediately after injury (McKeon et al., 1991; Fitch and Silver, 2008). In contrast to MIL whose levels remain unchanged after injury, reactive astrocytes lead to increased expression and release of chondroitin sulphate proteoglycans (CSPGs) - neurocan, phosphocan, aggrecan, brevican, versican into the extracellular matrix along with other inhibitory molecules like ephrin, tenascin C (McKeon et al., 1995; Asher et al., 2001; Jones et al., 2003). CSPGs in general consist of a protein core and chondroitin sulphate side chains which differ not only in their protein component but also with the pattern, number and length of sulphation of side chains (Margolis and Margolis, 1993; Grimpe and Silver, 2002). Recently, transmembrane protein tyrosine phosphatase-sigma (PTPσ) as well as transmembrane leukocyte common antigen-related phosphatase (LAR) has been identified as the receptors for CSPGs (Shen et al., 2009; Fisher et al., 2011). Similar to MIL signaling, CSPG molecules activate the RhoA/ROCK pathway and its downstream effectors to inhibit axon regeneration (Monnier et al., 2003) [Fig. 1]. It has been also reported that the intracellular influx of Ca^{2+} after p75 receptor complex binding of MIL or CSPGs-receptor interaction leads to transactivation of epidermal growth factor receptor (EGFR) and inhibition of neurite outgrowth (Koprivica et al., 2005) [Fig. 1]. Meningeal fibroblasts release semaphorins after CNS injury which interacts with neuropilin/plexin receptor expressed on scar forming cells and neuronal growth cones to promote scar formation and inhibition of axon growth respectively (Pasterkamp et al., 1998; Pasterkamp et al., 1999; Whitford and Ghosh, 2001).

1.2.4 Role of macrophages and microglia

After CNS injury, activated microglial cells and macrophages from blood stream that infiltrate the lesion site due to the breakdown of blood-brain barrier also contribute to the inflammatory response and glial scar formation (Fitch and Silver, 1997). These cells release inflammatory cytokines (e.g. tumor necrosis factor alpha), nitrogen monoxide and other molecules like transforming growth factor beta (TGFβ) which upregulates the expression of inhibitory CSPGs in the lesion site after CNS injury (DiProspero et al., 1997; Fitch et al., 1999). Macrophages have been also reported to cause axon retraction and formation of dystrophic growth cones around the lesion site after spinal cord injury (Horn et al., 2008; Busch et al., 2009). Therefore, macrophages act as another significant barrier to CNS axon regeneration. In addition, after CNS injury, influx of serum protein – fibrinogen occurs which acts as ligand to β3 integrin on neurons and transactivates the EGFR leading to RhoA activation and inhibition of neurite outgrowth (Schachtrup et al., 2007).

1.2.5 Axon regeneration in the PNS vs CNS

CNS has limited axon regenerative potential as compared to the PNS. In response to injury, axons of PNS can regenerate efficiently which might be associated with the rapid clearance of the cellular debris, reduced scar formation and intrinsic potential of PNS neurons toward regeneration (Chen et al., 2007; Vargas and Barres, 2007). PNS axons are myelinated by Schwann cells which play a pro-active role in myelin clearance and have the capability to proliferate and dedifferentiate after injury and also readily remyelinate the regenerating axons (Fawcett and Keynes, 1990; Fernandez-Valle et al., 1995; Akassoglou et al., 2002). In addition, macrophages are actively recruited by Schwann cells to expedite the debris clearance at the PNS injury site (Shamash et al., 2002). The scenario is completely different in the CNS environment. Firstly, CNS suffers from the lack of efficient clearance of debris which could be attributed to the insufficient capacity of microglial cells and macrophages to perform phagocytosis at the lesion site (Kuhlmann et al., 2002). Microglial cells do display an activated phenotype after CNS injury; nevertheless their phagocytic activity is subdued (Skoff and Vaughn, 1971; Barron, 1995). The myelin ensheathing cells of CNS axons are oligodendrocytes which have negligible potential for efficient myelin clearance and undergo programmed cell death after loss of contact with axons (Ludwin, 1990; Barres et al., 1993). Hence, the injured axon tips at the

CNS are exposed to inhibitory myelin components as well as the glial scar molecules which adversely affect axon regeneration.

1.2.6 Intrinsic growth state of CNS neurons

Adult CNS neurons lack the intrinsic capability to regenerate axons after injury (Goldberg et al., 2002b; Goldberg et al., 2002a; Park et al., 2008; Moore et al., 2009). This could be attributed to the CNS environment as well as differential cellular response of CNS neurons to injury which includes the expression of putative transcription factors that play a positive role in axon regeneration, protein synthesis and axon transport (Sun and He, 2010). For instance, 90% of the retinal ganglion cells undergo apoptosis 14 d after optic nerve injury (Berkelaar et al., 1994; Garcia-Valenzuela et al., 1994; Fischer et al., 2000). All these factors cumulatively abrogates axon regeneration in the CNS resulting in several debilitating disorders after traumatic CNS injuries and neurodegeneration which occurs in the case of Multiple Sclerosis, Alzheimers disease, or Parkinsons disease.

1.3 Anatomical organization of the retina and visual pathways of rats

1.3.1 Retinal layers

Retina consists of multiple layers generally outlined as nuclear and plexiform layers, along with epithelial/limiting membrane layer (Fig. 2). Retinal pigment epithelium is the innermost layer of the retina that regulates exchange of nutrients and waste between the retina and choroid capillaries. Adjacent to retinal pigment epithelial layer, the photoreceptors – rods and cones are located. The nuclei of the photoreceptors are located at the outer nuclear layer. The rods are the predominant photoreceptors in the rat retina and cones account for ~1% of the total photoreceptors. Photoreceptors convert the light stimuli into electrochemical signals and transmit these to the dendrites of bipolar and horizontal cells at the outer plexiform layer. Cell bodies of the bipolar cells, horizontal cells and amacrine cells are located in the inner nuclear layer and the axons of bipolar cells form synapses with the dendrites of retinal ganglion cells at the inner plexiform layer. Horizontal and amacrine cells regulate the photoreceptor output at the outer plexiform layer and the signal transmission that occurs between bipolar cells and retinal ganglion cells at the inner plexiform layer, respectively. The ganglion cell layer consists of retinal ganglion cells and astrocytic processes that extend from the nerve fiber layer. Axons of retinal ganglion cells

form the nerve fiber layer which enters into the optic nerve, and the end plates of Müller cells, the unique glial cells of the retina interlocks itself to form the inner limiting membrane which separates the retinal layers from the vitreous body.

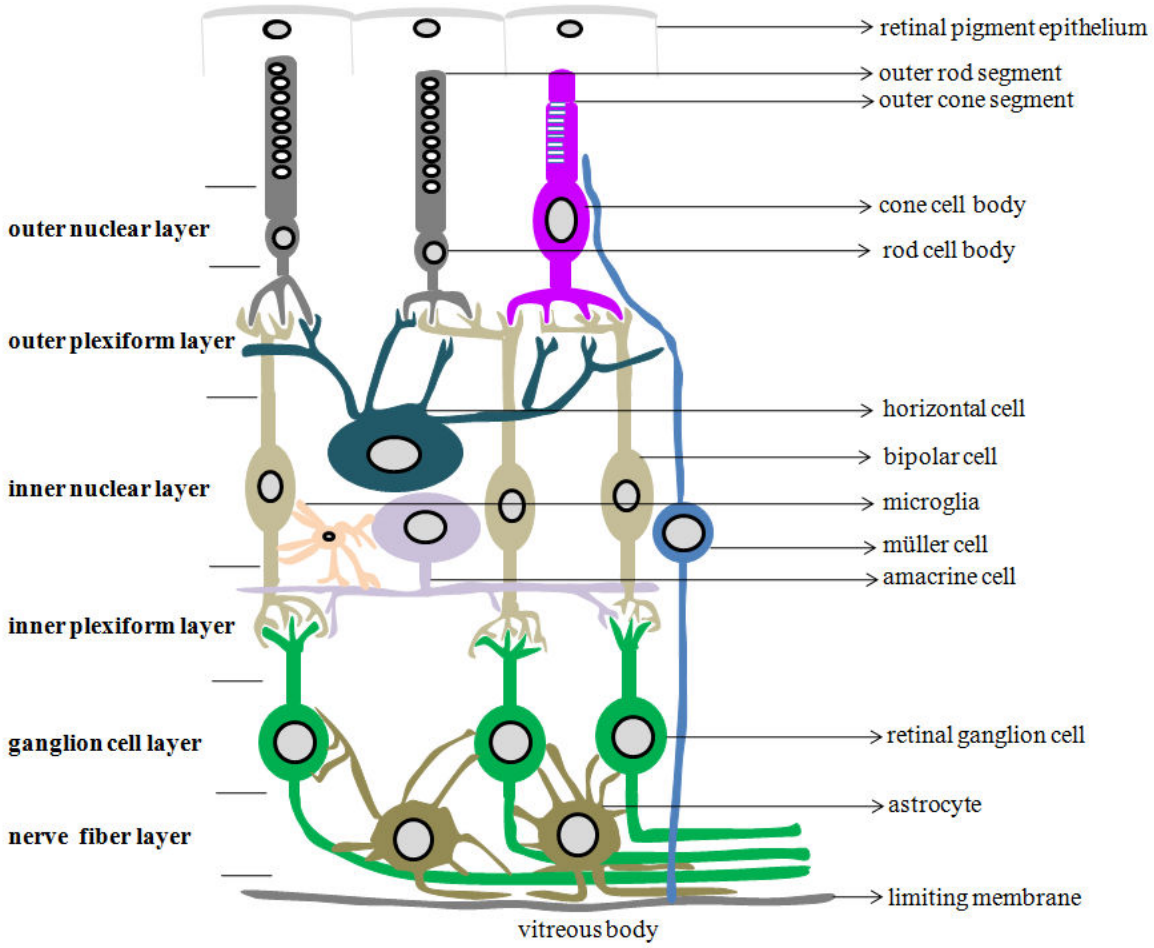

Fig. 2. Schematic representation of the anatomical organization of rat retinal layers. Cell bodies of neurons and interneurons are present at the nuclear layers while the synaptic connections are laid out at the plexiform layers. Retinal ganglion cells in the ganglion cell layer then send out axons to the optic nerve through the nerve fiber layer. Retinal glial cells comprise of astrocytes which intertwine with the nerve fiber layer and Müller cells whose processes extend through the whole retinal layers and form the limiting membrane along with astrocytic processes. Microglial cells are also present in the retina. [Conceived and re-drawn from: (Berry et al., 2008)].

1.3.2 Organization of visual pathways

Retinal ganglion cell axons then carry the information from retinal cell layers along the length of the optic nerve (Fig. 3). The optic nerves from the left and right eyes join to form the optic chiasm. At the chiasm, approximately 10% of temporal axons of the retina from each eye remain ipsilateral, while the nasal axons and rest of the temporal axons decussates and projects onto the contralateral optic tract. Hence, the optic tract generally comprises of axons derived from both eyes. The target areas of the axons present in the optic tract are ipsilateral lateral geniculate nucleus (LGN), superior colliculus (SC) and pretectal nucleus (PTN). Some of the nerve fibers leave the optic tract before entering the LGN and connects with the SC and also forms synapses at the PTN. SC in turn relays information to motor nuclei in brain stem/cord for visually guided movements. PTN transports the information to brain stem ocular autonomic and motor nuclei for the maintenance of pupillary light reflex/accomodation. LGN located in the thalamus of the brain, is the primary relay center for transmitting information onto the visual cortex. Visual cortex is situated in the occipital lobe of the brain where the higher order processing and interpretation of visual input signals occur (Berry et al., 2008).

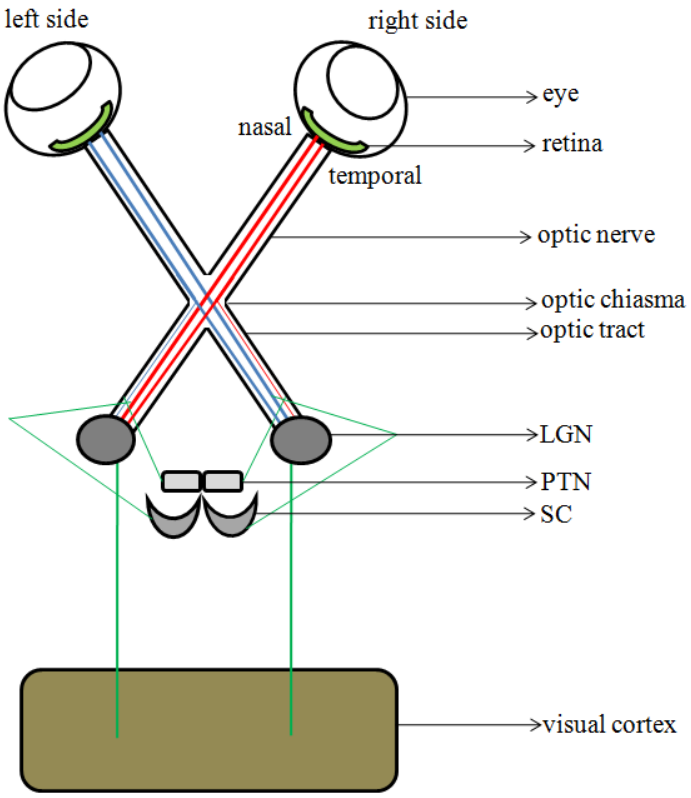

Fig. 3. Schematic representation of rat visual pathways. Retinal ganglion cell axons

from left and right eyes travel along the optic nerve. Cross-over of nasal and most of the temporal retinal ganglion cell axons (e.g. red lines – axons from right eye) occurs at optic chiasm and enters contralateral optic tract while the rest of the temporal axons remains ipsilateral. Some axons (thin green lines) synapse at the PTN or SC before entering the LGN. Axons from LGN innervate the visual cortex for processing of input signals.

1.4 The optic nerve as a model system for CNS regeneration

The retina and the optic nerve are constituents of the CNS. The retinal layers consist of relatively few neuronal subtypes and the axons that populate the optic nerve emanates exclusively from the retinal ganglion cells, the projecting neurons of the retina. Optic nerve transection/crush clearly demarcates the proximal and distal optic nerve fibers at the lesion site and disconnects retinal ganglion cells from their central targets. This clear demarcation allows deciphering the specific effects on axon regeneration which occurs from the proximal stump. Since, there are no interneurons present in the optic nerve which is not the case with other CNS injury models like spinal cord, the complications that might arise due to collateral damage to the connecting structures does not occur after optic nerve injury. Hence, a detailed and specific analysis of the effects of injury to the retinal ganglion cell axons could be identified. Optic nerve transection/crush can be performed without disrupting the blood supply to the retina. The central retinal artery and vein involved in the blood supply to the retina are located inside the dural sheath and enter the optic nerve tissue close to the eye. Damage to these blood vessels would result in ischemia and retinal ganglion cell death. Therefore, mechanical disruption farther from the site of entry of blood vessels into the optic nerve tissue alleviates this problem. In addition, glial response that arises due to optic nerve transection/crush or LI can be easily deciphered considering the distinct glial cells that populate the retina or optic nerve. Treatment of compounds or adeno associated viral transduction of retinal ganglion cells can be easily performed through intravitreal injections without causing extensive tissue damage. The localization of retinal ganglion cells in the highly ordered anatomical organization of the retina allows for an accurate quantitative assessment of these neurons. The localization of retinal ganglion cell axons outside the skull makes it easily accessible for surgical procedures. All these features described above renders the optic nerve as a classical model system for studying axonal regeneration and neurodegeneration (David and Aguayo, 1981; Vidal-Sanz et al., 1987; Aguayo et al., 1991; Villegas-Perez et al., 1993; Berry et al., 2008).

1.5 Measures toward improvement of axon regeneration in CNS

1.5.1 Overcoming inhibitory molecules and their downstream signaling pathways

The several classes of inhibitory molecules derived from myelin as well as glial scar have been targeted to enhance axon regeneration in CNS. Neutralization of MIL through application of ligand-specific antibodies improves regeneration of axons after CNS injury (Schnell and Schwab, 1990, 1993; Brosamle et al., 2000; Freund et al., 2006). Treatment with an antagonist peptide against the NgR has also been shown to improve axon regeneration (GrandPre et al., 2000; Li et al., 2004; Li et al., 2005). MIL associated inhibition can be circumvented through overexpression of dominant negative form of NgR which competes for ligand binding, thereby compromises the inhibitory signaling activation and results in enhanced axon regeneration after optic nerve injury (Fischer et al., 2004a). These studies suggest that blockade of MIL or its receptor interaction can promote axon regeneration. However, the efficacy of these strategies to obtain significant level of axon regeneration remains ambiguous. It has been reported that NgR knockout mice displays only modest axon regeneration after spinal cord injury (Kim et al., 2004; Zheng et al., 2005). In addition, mice lacking the inhibitory myelin components - Nogo A/B or Nogo A/B/C or Nogo/MAG/OMgp did not significantly enhance axon regeneration after CNS injury *in vivo* (Zheng et al., 2003; Lee et al., 2010). Recently, sulfatide component of myelin lipid has also been described to inhibit neurite outgrowth of retinal ganglion cells (RGCs). However, genetic deletion of sulfatide pathway enzymes alone did not promote axon regeneration *in vivo* (Winzeler et al., 2011). Hence, the extent of MIL contribution toward impaired CNS axon regeneration could not be clearly ascertained due to the complexity and variability of inhibitory molecules.

CSPGs have been directly targeted through intrathecal administration of chondroitinase ABC enzymes which degrade these inhibitory proteoglycans (Schreyer and Skene, 1993; Moon et al., 2001; Bradbury et al., 2002; Steinmetz et al., 2005). This strategy partially overcomes the barrier caused by glial scar components and leads to enhanced axon regeneration. MIL/CSPGs as well as cell surface gangliosides activates RhoA/ROCK signaling pathway and causes neurite outgrowth inhibition *in vitro* as well as insufficient axon regeneration *in vivo* (Yamashita et al., 2002; Filbin, 2003; Monnier et al., 2003; Yiu and He, 2006; Berry et al., 2008). Hence, RhoA/ROCK pathway through which

most of the signal transduction of CNS inhibitory ligands occurs is blocked through overexpression of RhoA inactivator ADP-ribosyl transferase in RGCs which results in improved axon regeneration after optic nerve injury (Lehmann et al., 1999; Fischer et al., 2004b). Also pharmacological inhibition of ROCK, which is a downstream effector of RhoA enhances regeneration of axons after CNS injury (Dergham et al., 2002; Fournier et al., 2003). Another treatment paradigm involves peripheral nerve grafting at the optic nerve transected site which provides a permissive bridge for the CNS neurons to regenerate within the PNS environment (David and Aguayo, 1981). Nevertheless, the extent of axon regeneration achieved by either inhibition of myelin components/CSPGs or the activated downstream signaling cascades does not lead to complete functional recovery after CNS injuries. These results suggest the presence of additional CNS inhibitors or alternate inhibitory signaling activation mechanisms. Moreover, the failure of strategies that compromise the inhibitory environment at the injury site to improve axon regeneration could also be attributed to the insufficient intrinsic inability of CNS neurons to regenerate axons after injury (Goldberg et al., 2002b; Goldberg et al., 2002a; Goldberg, 2004; Sun and He, 2010).

1.5.2 Stimulating the intrinsic growth state

Several approaches have been pursued to activate the intrinsic regenerative state of CNS neurons. In spinal cord injury model, conditioning lesion performed at the peripheral axons enhances the regeneration of central axons (Richardson and Issa, 1984; Schreyer and Skene, 1993). In case of optic nerve injury model, puncturing the lens of the eye [lens injury (LI)] activates the intrinsic regenerative state of RGCs and improves axon regeneration after optic nerve injury (Fischer et al., 2000; Leon et al., 2000; Lorber et al., 2005; Pernet and Di Polo, 2006). The effects of LI are mediated through the release of β/γ-crystallins, which are structural proteins of the ocular lens. The crystallins induces the expression of several axon growth stimulating factors/proteins; for instance, the ciliary neurotrophic factor (CNTF) and leukemia inhibitory factor (LIF) from astrocytes and Müller cells (Muller et al., 2007; Fischer et al., 2008; Leibinger et al., 2009; Muller et al., 2009). LI can be simulated by intravitreal injections of lens-derived β/γ–crystallins or yeast cell wall extract zymosan or Toll-like receptor agonist - Pam_3Cys (Hauk et al., 2008; Hauk et al., 2009; Lorber et al., 2009). Receptor interaction and signaling activation of the cytokines - CNTF and LIF are mediated through the formation of heteromeric receptor complex consisting of gp130 receptors along with specific receptors for CNTF/LIF (Davis

et al., 1993; Heinrich et al., 2003). The receptor complex formation results in auto-tyrosine phosphorylation and activation of downstream signaling pathways including the janus kinase/signal transducer and activator of transcription 3 (JAK/STAT3)-, phosphoinositid-3-kinase/activated protein kinase (PI3K/AKT)- and mitogen activated protein kinase/ extracellular-signal-regulated-kinase (MAPK)- pathways leading to changes in gene expression necessary for axon regeneration (Heinrich et al., 2003; Bauer et al., 2007; Muller et al., 2007; Leibinger et al., 2009; Muller et al., 2009).

Exogenous application of the recombinant CNTF has been shown to improve regeneration of axons in the optic nerve (Cui et al., 2003; Muller et al., 2007; Lingor et al., 2008; Muller et al., 2009). In addition, AAV-mediated overexpression of CNTF also enhances axon regeneration in the optic nerve (Leaver et al., 2006a; Leaver et al., 2006b; Hellstrom et al., 2011). Constitutive activation of the PI3K/AKT/mTOR (mammalian target of rapamycin) signaling pathway achieved through the depletion of either phosphatase and tensin homolog (PTEN) or tuberous sclerosis protein 1 (TSC1), allows axons to regenerate over long distances after optic nerve injury and also provides significant neuroprotection to RGCs (Park et al., 2008; Kurimoto et al., 2010). Suppressor of cytokine signaling 3 (SOCS3) is a negative regulator of the JAK/STAT3- pathway activation which limits the expression of genes that are paramount for axon regeneration (Fischer et al., 2004c; Miao et al., 2006). Depletion of SOCS3 *per se* enhances optic nerve regeneration after the intravitreal application of CNTF (Smith et al., 2009). Moreover, cumulative depletion of PTEN as well as SOCS3 results in extensive axon regeneration when compared to the levels achieved after the depletion of these negative regulators individually (Sun et al., 2011). Activated macrophages found in the inner eye after LI has also been reported to contribute to the improved axon regeneration observed due to LI (Yin et al., 2003; Cui et al., 2009). Hence, there exists a lively discussion in the field about the principal contributors of the beneficial effects of LI (Cui et al., 2008; Fischer, 2008, 2010). LI also offers neuroprotection to the RGCs which otherwise begins to undergo apoptosis 5 days after optic nerve crush. However, LI *per se* is still not sufficient to attain extensive axon regeneration. This necessitates the requirement of identifying novel therapeutic strategies and application of combinatorial treatments to achieve significant axon regeneration in CNS which could ultimately lead to functional recovery.

1.6 Microtubules - assembly and dynamics

Microtubules (MTs) are one of the basic cytoskeletal components of the cell which maintain cell shape, support cell motility, and facilitate intracellular transport of proteins and organelles. MTs also play an important role during cell division by arrangement of spindle fibers. MTs are made up of the globular protein known as tubulin which in turn consists of two closely related subunits – α-tubulin and β-tubulin, each having a molecular weight of 55KDa. Also a third type of tubulin – γ-tubulin is specifically localized in the centrosome and nucleates the growing microtubule subunits. α and β tubulin heterodimers polymerize through head to tail interactions to form linear protofilaments. During the process of polymerization, GTP-bound to β-tubulin (at E-site or exchangeable site) is hydrolyzed and result in β-tubulin with GDP at the E-site which is non-exchangeable. GTP is also bound to the α-tubulin, but is not hydrolyzed and hence, non-exchangeable (known as N-site GTP). Thirteen linear protofilaments associate laterally to form the MTs (Fig. 4).

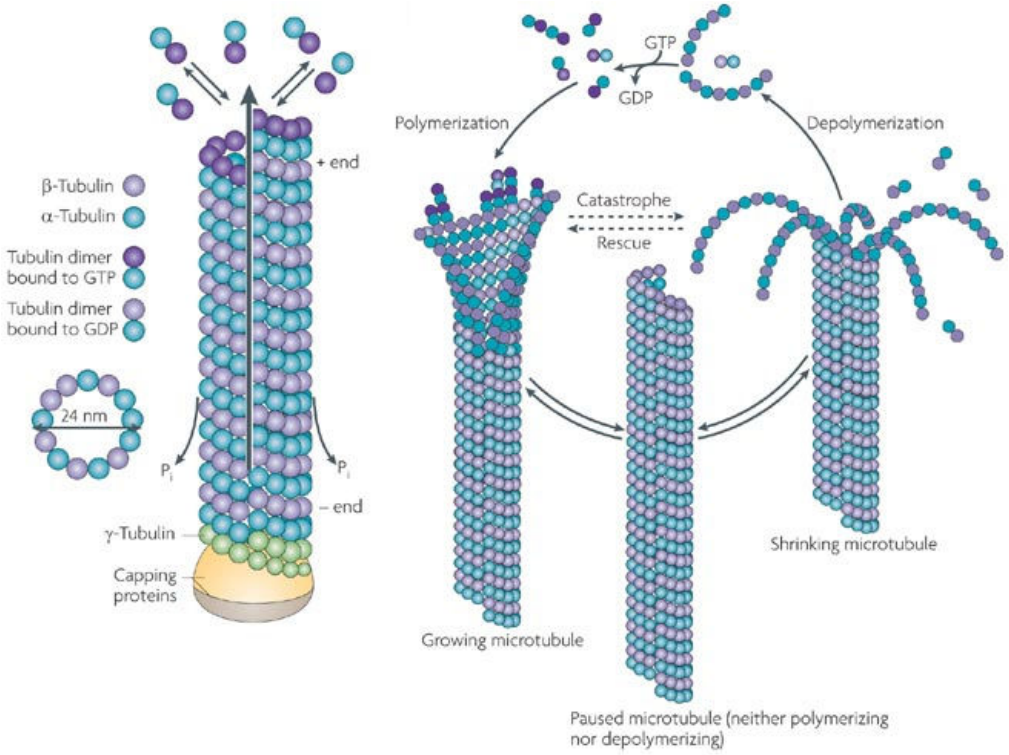

Fig. 4. Microtubule assembly, organization and dynamics. MTs are made up of heterodimers of α and β-tubulin subunits arranged as linear protofilaments and 13 of which associate laterally to form polymers of MTs. MTs exists in a dynamic state of assembly and disassembly in accordance with the GTP-cap at the growing end and the availability of free GTP-bound tubulin. [Source: (Conde and Caceres, 2009)]

MTs are dynamic structures which are constantly in a state of assembly (growth/polymerization) or disassembly (catastrophe/depolymerization) within the cell (Fig. 4). The growth or catastrophe of MTs is determined by the rate of addition of GTP-bound tubulin at the plus end compared to GTP hydrolysis. A rapid addition of GTP-bound tubulin allows the MTs to retain a GTP-cap at the plus end which promotes polymerization. Whereas, lack of free GTP-bound tubulin slows down the polymerization rate and leads to rapid GTP-hydrolysis at the plus end which results in microtubule depolymerization. This alternating phase of growth and catastrophe is described as microtubule dynamics or dynamic instability. Microtubule dynamics is essential for the cytoskeleton to forage the cell periphery and transport the cargo (proteins, vesicles etc.,) to the necessary locus. The intracellular transport utilizes the polar state of MTs to deliver cargos through motor transport proteins – kinesin (anterograde transport) and dyenin (retrograde transport) in an energy dependent process. Microtubule assembly and dynamics are closely regulated by stabilizing and destabilizing factors/proteins localized in (and/or distributed) around the MTs. The microtubule associated protein 2 (MAP-2) and collapsing response mediator protein 2 (CRMP-2) confers MTs stabilization and assembly respectively. In contrast, kinesin family member 2 (KIF-2) and stathmin instigates depolymerization of MTs (Conde and Caceres, 2009).

MTs along with actin filaments form the key cytoskeletal components of neuronal growth cones. Growth cones are broad, highly dynamic structures located at the axon tips that can be delineated into distinct domains based on its structure derived due to the arrangement of actin, MTs and organelles etc., (Fig. 5). MTs that are stabilized by MAPs exist as parallel bundles in the axonal shaft. Defasciculation of MTs occurs at the central domain (C-domain) which enters into the transition zone and peripheral domain (T-zone and P-domain) as individual filaments to explore the growth cone periphery along the filamentous actin (F-actin) bundles. C-domain encompasses both stable as well as dynamic MTs along with several organelles, vesicles and actin arcs. Actin arcs consist of anti-parallel bundles of F-actin and myosin. Actin arcs generate compressive forces that coral the unbundled MTs and promote microtubule bundling in the growth cone wrist. The T-zone comprises the dynamic MTs, actin arcs in addition to the rear of F-actin bundles from filopodial extensions which gets terminated at this locus and is severed into short filaments. The P-domain mainly includes the actin bundles which line the filopodial extensions and the branched F-actin filaments which form the lamellipodia-like veils. Moreover, some population of dynamic MTs are also located in the P-domain.

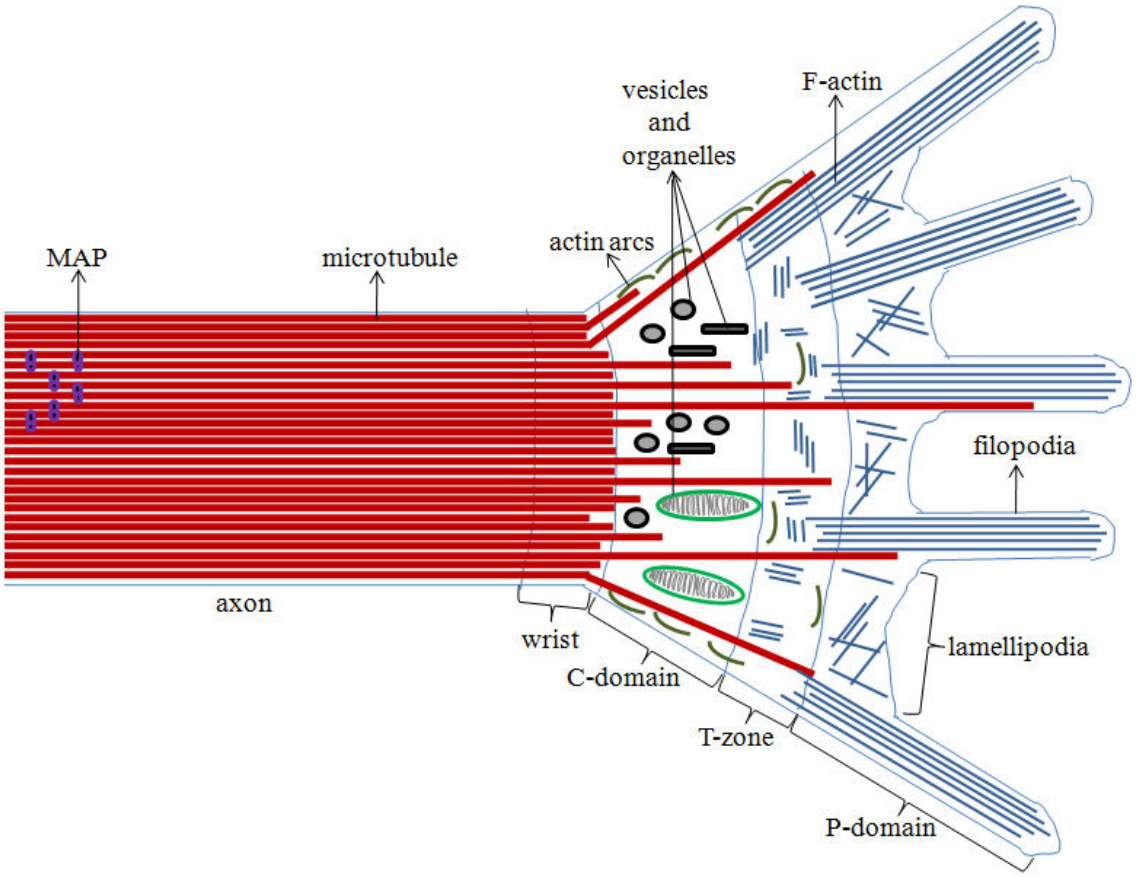

Fig. 5. Schematic representation of the organization of cytoskeleton in the growth cone. P-domain and T-zone are mainly the actin rich regions of the growth cone with defasciculated MTs traversing dynamically to support axonal growth and transport. C-domain contains vesicles/organelles and MTs undergo defasciculation at this region. Actin arcs regulate the bundling of MTs at the growth cone wrist. MAPs interact laterally and stabilize the MTs at the axon shaft. [Conceived and re-drawn from: (Geraldo and Gordon-Weeks, 2009)].

Axonal growth imparts morphological alterations on the growth cone which can be delineated into three phases: protrusion, engorgement and consolidation. During protrusion, elongation of filopodia and lamellipodia occurs which could be attributed to F-actin polymerization. The engorgment phase involves the shift of the C-domain and F-actin arcs towards the new growth region together with the invasion of MTs (including the newly synthesized dynamic MTs) and population of the site with vesicles and organelles. Finally, consolidation of growth occurs through the formation of new axonal shaft by compaction of the region that was previously the base of C-domain over the MTs. The three phases described above occurs sequentially to promote axon extension and requires

dynamic involvement of both microtubule and actin cytoskeletal components. It has been reported that the application of microtubule depolymerizing drugs which abrogates the entry of dynamic MTs into filopodial extensions of P-domain prevents growth cone turning (Challacombe et al., 1997). In addition, selective microtubule depolymerization on one side of the growth cone through application of gradients of microtubule depolymerizing drugs results in growth cone to turn away from that side. In contrast, selective polymerization of MTs on one side of growth cone by microtubule polymerization drugs causes growth cone to turn toward that side (Buck and Zheng, 2002). Microtubule dynamics abrogated through treatment with low doses of vinblastine has been shown to prevent axon elongation (Tanaka et al., 1995). However, microtubule stabilization has been reported to induce axon formation and splaying of MTs into growth cones which potentiates axon growth (Tanaka et al., 1995; Witte et al., 2008). Moreover, enhanced transport of organelles on MTs and synthesis of proteins to facilitate growth could be observed during axon formation (Bradke and Dotti, 1997). These studies suggest an important role of microtubule stabilization and dynamics to support axon formation and growth.

1.7 Paclitaxel - a therapeutic drug

Paclitaxel, also known as Taxol, is a microtubule stabilizing compound isolated from the bark of the pacific yew tree, *Taxus brevifolia*. Taxol binds to the β-tubulin subunit of MTs and induces a conformational change which promotes MTs stabilization/polymerization. Taxol is widely used in the treatment of different types of cancer (Vyas and Kadow, 1995). Taxol at high dosages used in cancer therapy leads to hyper-stabilization of MTs and disrupts microtubule dynamics completely. This affects the orientation and assembly of spindle fibers necessary for cell division which ultimately blocks the proliferation of tumor cells. Interestingly, at low nanomolar concentrations, Taxol selectively increases the assembly of tubulin subunits at the growing/plus ends of MTs without suppressing microtubule dynamics (Derry et al., 1995; Derry et al., 1997).

1.8 Thesis objective(s)

CNS injury exposes the damaged axon tip to a milieu of inhibitory components derived from myelin and CSPGs. This results in destabilization of actin cytoskeletal filaments leading to actin depolymerization (Berry et al., 2008). Consequently, microtubule disassembly/disorientation occurs and forms retraction bulb like structures, which impedes successful regeneration of axons (Mimura et al., 2006; Erturk et al., 2007). Hence, stabilization of MTs toward assembly/polymerization by application of low concentrations of Taxol might promote regeneration of axons and also alleviate the negative influence of inhibitory myelin/CSPGs on the tips of the injured axons. Taxol has been reported to overcome the myelin inhibition on neurite outgrowth of postnatal cerebellar granule neurons *in vitro* (Erturk et al., 2007). However, the beneficial effect of Taxol to promote neurite outgrowth of adult CNS neurons *in vitro* or enhance axon regeneration *in vivo* after CNS injury has not yet been described. Hence, the objective(s) for my thesis project are as follows:

- Can microtubule stabilization by Taxol promote neurite outgrowth of PC12 cells and adult RGCs *in vitro*.
- Does Taxol act synergistically with other combinatorial treatments to enhance neurite outgrowth of RGCs *in vitro*.
- If Taxol can promote neurite outgrowth of adult RGCs, whether it can also overcome the inhibition on neurite outgrowth by inhibitory CNS myelin and CSPGs.
- What are the mechanisms underlying the enhanced neurite outgrowth and disinhibitory effects on inhibitory substrates.
- Whether Taxol application can be used as a therapeutic strategy *in vivo*, either alone or in combination with other treatments to enhance axon regeneration after optic nerve injury.
- If the improved axon regeneration *in vivo* can also be achieved through Taxol treatment by alternate application routes.
- Does Taxol modulate the components of glial scar around the injury site to promote axon regeneration.

2. Material and Methods

2.1 Materials

2.1.1 Chemicals and reagents

Acrylamide solution	Bio rad
Ammonium per sulphate (APS)	Sigma
Aprotinin	Chemicon
B-27 supplement	Invitrogen
β-mercaptoethanol	Sigma
Bromophenol blue	Pharmacia Biotech
Bovine Serum Albumin	PAA Laboratories GmbH
Chloral hydrate	Sigma
Cholera toxin subunit beta conjugated-	
-with Alexa Fluor® 488	Invitrogen
Chondroitinase ABC	Sigma
Ciliary neurotrophic factor (rat)	Serotec
4´,6-diamidino-2-phenylindole (DAPI)	Sigma
Distilled water (sterile)	Fresenius
Donkey serum	Millipore
Dithiothreitol (DTT)	Invitrogen
Dulbecco's modified eagles medium	Sigma
Ethylenediaminetetraacetic acid (EDTA)	Sigma
Enhanced chemiluminescence (ECL)-	
-detection reagents	Amersham Biosciences
ECL advance blocking agent	Amersham Biosciences
Fetal bovine serum	Invitrogen
Glycerine	J.T.Baker
Glycine	AppliChem
Hydrochloric acid (HCl)	Riedel-de Häen
Horse serum	Invitrogen
Isopropanol	Roth
Ketamine	WDT

Laminin	Sigma
L-cysteine	Sigma
Leupeptin	Chemicon
L-glutamine	Gibco
Magnesium chloride ($MgCl_2$)	Invitrogen
Methanol	Merck
Mowiol	Roth
Nerve growth factor	Sigma
Neurocan	R&D systems
Nocodazole	Sigma
Paclitaxel	LC laboratories
Papain	Worthington
Paraformaldehyde	Sigma
Penicillin/Streptomycin	Biochrom
Phalloidin–tetramethyl rhodamine--isothiocyanate	Sigma
Phosphate buffered saline	Gibco
Phenylmethylsulfonyl fluoride (PMSF)	Chemicon
poly-D-Lysine	Sigma
Potassium chloride (KCl)	AppliChem
Potassium dihydrogen phosphate (KH_2PO_4)	Sigma
pre-stained protein marker	Fermentas
Protease inhibitor cocktail	Calbiochem
Skimmed milk powder	Roth
Sodium chloride (NaCl)	Sigma
Sodium deoxychelate	Sigma
Sodium dihydrogen phosphate (NaH_2PO_4)	Sigma
Sodium dodecyl sulphate	USB
Sodium fluoride (NaF)	Sigma
Sodium orthovandate (Na_3VO_4)	Sigma
Sucrose	Sigma
Tetramethylethylenediamine (TEMED)	Sigma
Tris	Sigma
Triton X-100	Sigma
Trypsin EDTA (1X)	PAA

Tween-20	Sigma
Xylazine	Alverta

2.1.2 Kits and additional reagents

Bicinchoninic acid (BCA) Protein Assay kit	Pierce
Glutathione sepharose™ 4B	GE Healthcare
Tissue Tek (O.C.T compound)	Sakura

2.1.3 Antibodies

Mouse anti-βIII-tubulin (Tuj I)	Babco
Mouse anti-rat CD-68 (ED1)	Serotec
Mouse anti-CS-56	Sigma
Rabbit anti-rat CNTF	Serotec
Sheep anti-GAP43	a gift from Dr Benowitz, Harvard--Medical School, Boston, USA
Rabbit anti-GFAP	Santa cruz Biotechnology
Mouse anti-RhoA (sc-418)	Santa cruz Biotechnology
Rabbit anti-rat phospho STAT3 (Tyr 705)	Cell Signaling Technology
Anti-mouse IgG horseradish peroxidase conjugated	Sigma
Anti-rabbit IgG horseradish peroxidase conjugated	Sigma
Anti-sheep/goat IgG horseradish peroxidase conjugated	Sigma
Alexa Fluor® donkey anti-mouse 488	Molecular Probes
Alexa Fluor® donkey anti-mouse 594	Molecular Probes
Alexa Fluor® donkey anti-rabbit 594	Molecular Probes
Alexa Fluor® donkey anti-sheep 594	Molecular Probes

2.1.4 Consumable materials

Blotting paper	Bio-Rad
Cell strainer (40 μm; Falcon)	BD Biosciences Discovery labware
Centrifuge tubes	Beckman Coulter
Coverslips	VWR International

Dissection scissors	Fine Science Tools
Filter (0.22 µm)	Sarstedt
Forceps (Dumont)	Fine Science Tools
Four-well plates	Nunc International
Gelfoam	Pharmacia
Glass slides	Superfrost Plus, Fischer
Hyperfilm™ ECL	Amersham Biosciences
Injection needle	Aesculap
Microcapillary tube	World Precision Instruments
Nitrocellulose membrane	Amersham Biosciences
Pasteur pipette	Sarstedt
Pipette tips (10, 200, 1000 µl)	Sarstedt
Pipettes (10, 25 ml)	Sarstedt
Plastic tubes (500, 1000 µl)	Eppendorf
Scalpel	Aesculap
Surgical blades	Braun
Suture threads	Fine Science Tools
Syringes (1, 20 ml)	BD Biosciences Discovery labware
Test tubes (15, 50 ml)	Sarstedt
Tissue culture flask (75 cm^2)	Nunc
Tissue culture petri dish (10 cm^2)	Sarstedt

2.1.5 Technical equipment and software

Cell culture incubator	Hera safe, Heraeus
Centrifuges	Biofuge, Heraeus
	Megafuge, 1.OR, Heraeus
	Ultracentrifuge, Sorvall
Cryostat	Leica CM3050S
Fluorescent microscopy	Zeiss
Incubator (shaker)	Eppendorf
Light microscopy	Leica
pH-meter	Hanna Instruments
Spectrophotometer	Eppendorf

Vortex	VWR International
Water bath	Kotterman
Weighing balance	Sartorius
Western blot apparatus	Bio-Rad
-80°C freezer	Heraeus
Software	Adobe Photoshop
	Microsoft Office XP
	NIH ImageJ
	Endnote

2.2 Experimental methods

2.2.1 Optic nerve crush, LI, and Taxol treatment of the optic nerve

All surgical procedures were performed by Prof. Dr. Fischer and approved by the relevant local authorities (Regierungspräsidium Tübingen, Germany). Adult female Sprague Dawley rats (weighing 200–230 g) were anesthetized by intraperitoneal injections of ketamine (60–80 mg/kg) and xylazine (10–15 mg/kg), and a 1–1.5 cm incision was made in the skin above the right orbit. The optic nerve was surgically exposed under an operating microscope. The dural sheath was longitudinally opened. The nerve was crushed 1 mm behind the eye for 10 s using a jeweler's forceps, avoiding injury to the retinal artery. The vascular integrity of the retina was verified by fundoscopic examination after surgery. LI was induced by a retrolenticular approach, puncturing the lens capsule with the tip of a microcapillary tube. For the application of PBS or Taxol at the lesion site of the optic nerve, we used a rectangular formed piece of gelfoam with side lengths of ~2 mm, which was longitudinally opened and completely soaked with a solution of either phosphate buffered saline (PBS) [137 mM NaCl, 2.7 mM KCl, 8 mM NaH_2PO_4 and 2 mM KH_2PO_4 pH 7.4] or different concentrations of Taxol (1, 10, 100, and 1000 μM). These pieces of gelfoam were then carefully placed around the lesion site of the optic nerve in a way that parts of the proximal optic nerve stump and ~1 mm of the distal nerve were covered (Fig. 6). For the application of PBS or Taxol into the vitreous body, we injected 5 μl of either PBS or Taxol (1 μM) into the vitreous body after retrieving the same volume from the anterior chamber. The skin was sutured with 4-0 silk suture threads after surgery and the animals were provided with food and water *ad libitum*.

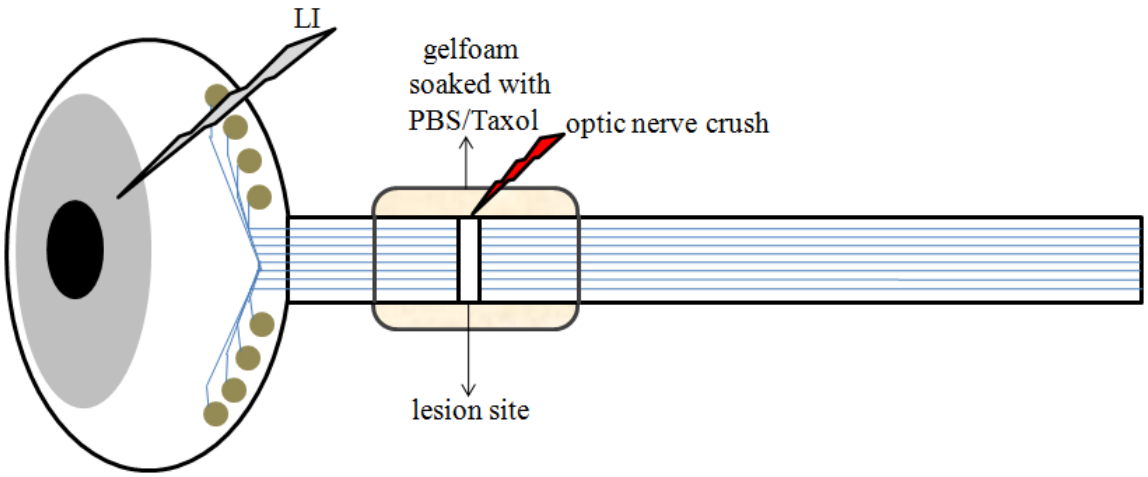

Fig. 6. Schematic representation of an LI, optic nerve crush, and the lesion site applied with gelfoam soaked in Taxol/PBS solutions.

2.2.2 Preparation of CNS myelin extract (CME)

CME was prepared as described previously (Ahmed et al., 2005). Rats (weighing 200-230g) were killed by a lethal overdose of chloral hydrate solution (14%). The brain tissue was dissected out and a 10% homogenate of finely chopped brain tissue in ice cold solution of 0.32 M sucrose, 1 mM EDTA, pH 7.0 was prepared. The homogenate was centrifuged at 800 x *g* for 10 min at 4°C and the supernatant was collected in a separate tube. The cell pellet was resuspended again to the original volume of 10% homogenate with ice-cold solution of 0.32M sucrose, 1 mM EDTA, pH 7.0 and the centrifugation step was repeated. The supernatants from both steps were then pooled together and centrifuged again at 13,000 x *g* for 20 min. The resulting pellet was resuspended in 0.9 M sucrose to the original volume of 10% homogenate and 1-2 ml of 0.32 M sucrose was carefully added as an overlay. The gradient layers were then centrifuged at 20,000 x *g* for 60 min and the white interface layer was collected and resuspended in 20 volumes of 0.32 M sucrose. Centrifugation of the resuspended white interface layer was performed at 13,000 x *g* for 25 min to precipitate the myelin fraction and the pellet was diluted in 25 volumes of pure water and incubated on ice for 30 min. Finally the diluted myelin fraction was centrifuged at 20,000 x *g* for 25 min and the pellet containing the pure myelin fraction was resuspended in a small volume of water and stored as aliquots at -80°C until further use. The protein content of CME was measured using the bicinchoninic acid protein estimation assay by dissolving an aliquot of CME with 10% SDS (to prevent interference of lipids during protein estimation) which was further diluted to <1% SDS for the assay.

2.2.3 BCA protein estimation assay

Bicinchoninic acid (BCA) provides a sensitive, detergent-compatible tool for colorimetric detection and quantification of protein which involves two important steps. Firstly, proteins facilitate a reduction reaction which converts Cu^{2+} to Cu^{1+} in an alkaline medium (Biuret reaction). Then two molecules of BCA chelate with one molecule of cuprous cation, Cu^{1+} and results in the development of a purple colored reaction product which exhibits strong absorbance at a wavelength of 562 nm. Bovine serum albumin (BSA), a well known protein was prepared at different dilutions (0, 5, 25, 50, 125 and 250 µg/ml) [Table. 1] to obtain a standard curve and used as a reference to estimate the protein concentrations of unknown sample. BCA working reagent was prepared by mixing 50 parts of BCA Reagent A with 1 part of BCA Reagent B (50:1, Reagent A:B). Protein standards/unknown samples were prepared in triplicates and for each reaction mixture, 100 µl of standard/unknown sample was added to 2 ml of BCA working reagent in separate tubes and incubated at 60°C for 30 min. Optical density measurement of standards/samples was performed at 562 nm to determine the protein concentration of unknown sample.

Tube no.	**Final BSA concentration** (µg/ml)	**Volume and source of BSA**	**Volume of diluent** (H_2O)
A	250	100 µl of *stock solution	700 µl
B	125	400 µl of tube A dilution	400 µl
C	50	300 µl of tube B dilution	450 µl
D	25	400 µl of tube C dilution	400 µl
E	5	100 µl of tube D dilution	400 µl
F	0	0	400 µl

(*Stock solution = 2 mg/ml BSA in H_2O)

Table. 1. Preparation of diluted BSA standards

2.2.4 Preparation of dissociated mixed retinal cultures

The retinal cell cultures were prepared as described previously (Grozdanov et al., 2010) [Fig. 7]. In brief, tissue culture plates (four-well plates) were coated with poly-D-lysine (0.1 mg/ml; molecular weight, <300,000 Da), rinsed with distilled water, and air dried. Wells were then coated with laminin (20 µg/ml), rinsed with Dulbecco's modified eagles medium (DMEM). To prepare retinal cell cultures, rats (weighing 200–230 g) were killed by an overdose of chloral hydrate solution (14%). Retinas were rapidly dissected from the eyecups and incubated at 37°C for 30 min in a digestion solution containing papain (16.4 U/ml) and L-cysteine (0.3 µg/ml) in DMEM. Retinas were then rinsed with DMEM and triturated in 2 ml of DMEM. To remove cell fragments or factors released from the cells, the cell suspension of one retina was immediately adjusted with DMEM to a volume of 50 ml. Cells were then centrifuged at 900 x *g* for 5 min, and the pellet was carefully resuspended in 6 ml of DMEM containing B27 supplement (1:50) and penicillin/streptomycin (1:50). Dissociated cells were then passed through a cell strainer (40 µm). Cell suspension, 300 µl, was added into each well (coated with poly-D-Lysine and laminin) resulting in a low density of cells. Cultures were arranged in a pseudorandomized manner on the plates to avoid any potential bias during the evaluation procedures and at least three independent experiments were performed to verify the results.

2.2.5 Treatments of adult rat retinal cultures *in vitro*

For testing the neurite outgrowth promoting effects of Taxol and/or CNTF, mixed retinal cultures from normal adult rats were prepared and cells were untreated or treated with 0.5, 1, 3, 10, and 50 nM Taxol in the medium. CNTF was added at a concentration of 200 ng/ml. In addition, disinhibitory effects on neurite outgrowth were tested after treatment of retinal cultures with CME or neurocan in the medium. CME was applied to cultures at a preoptimized concentration [~10 µg/ml] (Ahmed et al., 2009). Neurocan was added at a concentration of 5 µg/ml as described previously (Inatani et al., 2001). Cultures were incubated as indicated in the figures, and then fixed; immunostained and neurite outgrowth was evaluated as described later.

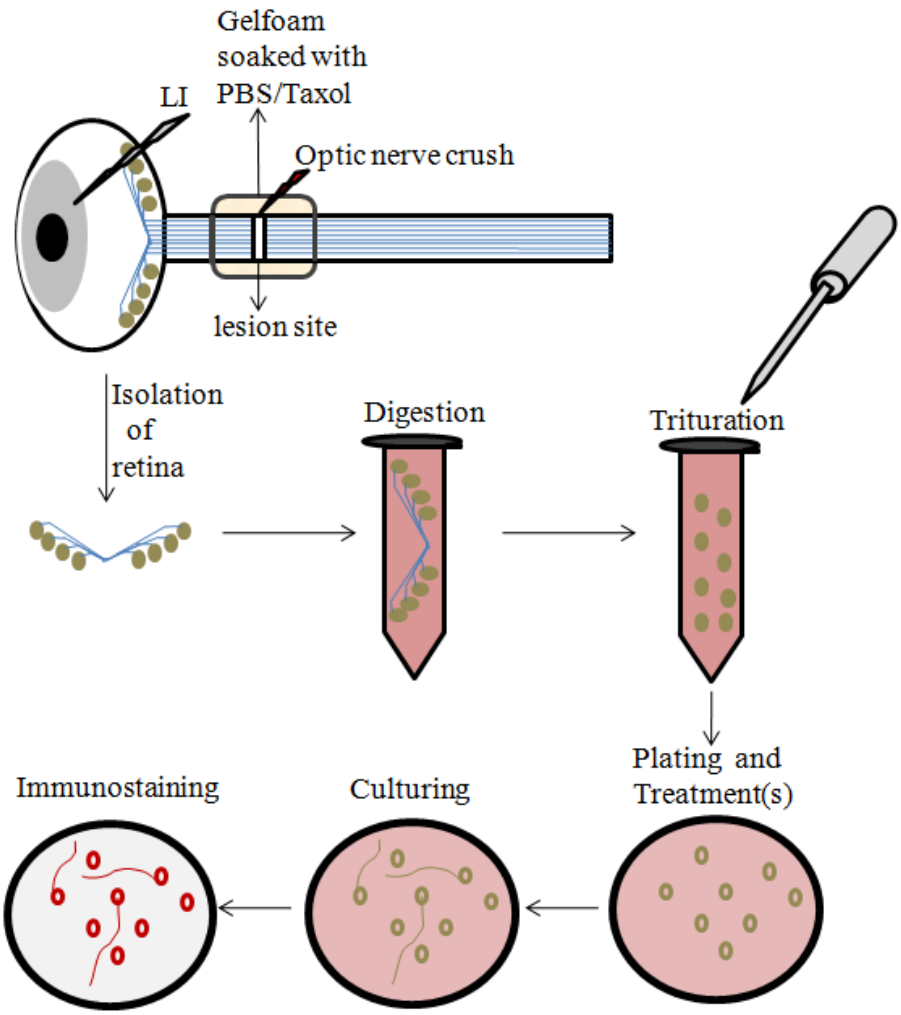

Fig. 7. Schematic overview of the preparation of dissociated retinal cultures. Retinas from untreated or *in vivo* treated animals were isolated and treated *in vitro* with compounds/growth factors. Cells were cultured; immunostained and RGC neurite outgrowth/survival analysis was performed.

2.2.6 Immunocytochemistry and RGC neurite outgrowth analysis

Retinal cell cultures were fixed with a paraformaldehyde solution (4%) for 30 min and methanol for 10 min at room temperature. Cultures were treated with blocking buffer (2% BSA in PBS and 0.1 % Tween-20) for 30 min at room temperature. Immunocytochemical staining was performed with a βIII-tubulin antibody (TUJ-1) (1:2,000) diluted in the blocking buffer for 2 h at room temperature. βIII-tubulin is a phenotypic marker for RGCs (Fournier and McKerracher, 1997; Cui et al., 2003; Fischer et al., 2004a; Fischer et al., 2004b; Lorber et al., 2005; Muller et al., 2007). After incubation with the βIII-tubulin antibody, cultures were rinsed 3 x 10 min in PBS and then treated

with the secondary antibody conjugated to Alexa Flour® 488 (1:1,000) for 1 h at room termperature. Cultures were rinsed 3 x 10 min in PBS and all RGCs with regenerated neurites in wells (four-well tissue culture plates) were photographed under a fluorescent microscope (200X). The neurite length of RGCs was determined using the NIH ImageJ software. Furthermore, the total number of βIII-tubulin positive RGCs with an intact nucleus (detected by DAPI staining) per well was quantified to test for potential neurotoxic or neuroprotective effects after each treatment. Values for neurite outgrowth were determined by the sum of the neurite length per well divided by the total number of RGCs per well, resulting in the average neurite length per RGC. The neurite length values were then normalized to the respective control groups as indicated. The normalized neurite length values were averaged per case, and then averaged across all similarly treated groups to obtain a group means and SE as described previously (Muller et al., 2007; Muller et al., 2009). The significances of intergroup differences were evaluated using a one-way ANOVA test, followed by corrections for multiple *post hoc* tests (Bonferroni–Holm, Tukey's).

2.2.7 PC12 cell cultures and neurite outgrowth analysis

PC12 cells (a cell line derived from pheochromocytoma of rat adrenal medulla) were cultured in 5% fetal bovine serum plus 10% horse serum in DMEM (PC12 cell medium) on poly-D-lysine-coated 10 cm^2 dishes (0.1 mg/ml; molecular weight, <300,000 Da). To prepare cells for neurite outgrowth experiments, cultures were treated with 3 ml of Trypsin-EDTA (1X) and incubated at 37°C for 3 min to remove the cells adhered to the substrate. PC12 cell medium was then added to the cells to neutralize trypsin digestion. Cells were collected and centrifuged at 900 x *g* for 5 min. The supernatant was removed and cell pellet was resuspended in PC12 medium and the cells were plated into four well plates. Cells were then exposed to 100 ng/ml nerve growth factor (NGF), Taxol (3 nM), and/or CME (~10 μg/ml). After 72 h, cultures were fixed with a paraformaldehyde solution (4%) and methanol for 30 min and 10 min respectively at room temperature. Cultures were then blocked with a blocking buffer and prepared for immunocytochemical staining with a βIII-tubulin antibody (TUJ-1) (1:2,000) as described in the procedures for mixed retinal cultures. PC12 cells with neurites were photographed under a fluorescent microscope (200X). To measure the effects of Taxol and CME on neurite outgrowth, the length of the longest neurite of PC12 cells was determined using the NIH ImageJ software. The neurite length values were then normalized to the respective control groups as indicated. The

normalized neurite length values were averaged per case, and then averaged across all similarly treated groups to obtain a group means and SE. The significances of intergroup differences were evaluated using a one-way ANOVA test, followed by corrections for multiple *post hoc* tests (Bonferroni-Holm, Tukey's). Each experiment was repeated at least three times.

2.2.8 Preparation of retinal lysate for western blot analysis

For retinal lysate preparation, retinas from rats that had been subjected to ONC/LI together with the application of gel foam soaked in a solution of Taxol (1 μM) or PBS at the lesion site were dissected and collected in lysis buffer (20 mM Tris/HCl, pH 7.5, 10 mM KCl, 250 mM sucrose, 10 mM NaF, 1 mM DTT, 0.1 mM Na_3VO_4, 1% Triton X-100, and 0.1% SDS) with 1:100 protease inhibitor cocktail. Retinas were homogenized and centrifuged at 5,000 rpm for 10 min at 4°C. The supernatants were collected and stored at -20°C until further analysis by western blot assay.

2.2.9 Western blot assay

Sodium dodecyl sulphate-polyacrylamide gel electrophoresis (SDS-PAGE) is a widely used method for separation of proteins. The denaturing conditions in the presence of SDS and β-mercaptoethanol dissociate the proteins into subunits and coats with negative charges (SDS). This results in a uniform charge to mass ratio and allows the proteins to migrate in the electric field based on their mass/size. Two layers of gels were used, stacking gel with a large pore size helps to concentrate all the proteins (irrespective of their mass) and resolving gel with lower pore size (determined by the ratio of acrylamide added) allows protein separation to occur according to their relative molecular mass.

The gel cast apparatus was cleaned and assembled. 10% acrylamide resolving gel was prepared according to the recipe (Table. 2 and 3) and the contents were poured into the gel cast apparatus. Immediately 1-2 ml of isopropanol was added on top of the gel to prevent air from interfering with the cross-linking reaction and the gel was allowed to polymerize for ~15 min. In the mean time, 4% acrylamide stacking gel contents were prepared (Table. 2 and 3). Once the polymerization of resolving gel was complete, isopropanol was removed using blotting paper. The stacking gel contents were then

carefully overlaid on the resolving gel and a gel comb was inserted. This was allowed to polymerize for ~10 min and the comb was removed (after the gel was set).

Contents	Resolving gel (10%)	Stacking gel (4%)
H_2O	3125 µl	1500 µl
Acrylamide (30%)	2500 µl	375 µl
Resolving gel buffer (pH 8.8) Stacking gel buffer (pH 6.8)	1875 µl -	- 625 µl
SDS (10%)	75 µl	25 µl
TEMED	12.5 µl	3.75 µl
APS (40%)	6.25 µl	7.5µl

Note: APS was added and mixed well just before pouring the contents into the gel appara--tus, since cross-linking reaction starts after its addition.

Table. 2. Recipes for the preparation of resolving and stacking gels.

The gel assembly was taken out of the casting apparatus, placed into the gel tank and running gel buffer was added into the tank such that it covers the top of the gel. Protein samples were prepared for separation by mixing with an equal volume of 2X sample buffer (Laemmli buffer), boiled at 95°C for 5 min and loaded into the wells (pre-stained protein ladder [standard] was also loaded to detect the appropriate size of proteins). Gels were then electrophoresed at 100V constant while the proteins migrate in the stacking gel and increased to 200V constant for separation to occur at the resolving gel until the bromophenol blue reaches the bottom of the gel.

After SDS-PAGE, proteins were transferred to nitrocellulose membranes. Nitrocellulose membranes were cut to the correct size for the gel and prepared for transfer by soaking in the transfer buffer along with sponges and blotting paper. Gel assembly was taken out of the electrophoresis tank and gels were carefully removed from the glass plates. The gel and nitrocellulose membrane was sandwiched between two stacks of blotting paper and one layer of sponge on a transfer cassette. The transfer cassette was then placed into the electrophoresis tank along with an ice pack and cold transfer buffer was added. Electrophoresis was then performed at 50V constant for 2 h.

Buffer/Solution	Contents
Resolving gel buffer	1.5 M Tris/HCl, pH 8.8 in distilled water
Stacking gel buffer	1 M Tris/HCl, pH 6.8 in distilled water
40% APS	400 mg of APS powder dissolved in 1 ml of distilled water
2X Sample buffer (Laemmli buffer)	200 mM Tris/HCl, 6% SDS, 20% Glycerine, 0.1% Bromophenol blue, 4% β-mercaptoethanol in distilled water
Running gel buffer	25 mM Tris, 192 mM Glycine, 0.1% SDS in distilled water
Transfer buffer	25 mM Tris, 192 mM Glycine, 20% Methanol in distilled water
Tris-buffered saline/Tween-20	20 mM Tris, 137 mM NaCl, 0.1% Tween-20, pH 7.6 in distilled water
5% skimmed milk (blocking) buffer	5 g of skimmed milk powder dissolved in 100 ml of Tris-buffered saline/Tween-20 in distilled water
2% ECL Advance blocking buffer	2 g of ECL Advance blocking agent dissolved in 100 ml of Tris-buffered saline/Tween-20 in distilled water

Table. 3. Recipes for the buffers and solutions used in western blot assay.

Immunoblotting was performed on the nitrocellulose membranes after protein transfer. The membranes were blocked in either 5% skimmed milk buffer or 2% ECL advance blocking buffer in Tris-buffered saline/Tween-20 for 2 h at room temperature. They were then processed for immunostaining with an antiserum against rat phospho-STAT3 (1:5,000), antibody against CNTF (1:5,000), a monoclonal antibody against rat tubulin (1:1,000), or an antibody against RhoA (1:5,000) which were prepared in blocking buffer and incubated for overnight at 4°C. Membranes were washed 3 x 10 min with Tris-buffered saline/Tween-20 to remove unbound antibodies and then incubated for 2 h at room temperature with anti-rabbit, anti-goat, or anti-mouse IgG secondary antibodies conjugated with horseradish peroxidase diluted at 1:80,000 in blocking buffer. Membranes were washed 3 x 10 min with Tris-buffered saline/Tween-20. The membranes were then incubated with ECL or ECL advance detection reagents (equal volume of reagents A and B) for 2 or 5 min respectively. The signals from antigen–antibody complexes were then detected on Hyperfilm™ ECL. Western blots were repeated at least two times to confirm results.

2.2.10 PC12 cell cultures and Rho activity assay

PC12 cells were cultured in PC12 cell medium and differentiated after treatment with NGF (100 ng/ml) for 48 h on poly-D-lysine-coated 10 cm^2 dishes (0.1 mg/ml; molecular weight, <300,000 Da). Then some cultures were treated with Taxol (3 nM) for another 3 h. After that, CME (~10 µg/ml) was added to the medium of some cultures for 10 min. [Note: The affinity precipitation and immunoblotting for RhoA was performed by Mariana Pfreimer]. Cells were then rinsed with Tris buffered saline (50 mM Tris/HCl, pH 7.5, and 150 mM NaCl) and lysed by the addition of 500 µl of Rho–radioimmunoprecipitation assay lysis buffer [50 mM Tris/HCl, pH 7.2, 500 mM NaCl, 1% Triton X-100, 10 mM $MgCl_2$, 0.5% sodium deoxycholate (dissolved in distilled H_2O), 0.1% SDS, 10 µg/ml aprotinin, 10 µg/ml leupeptin, and 1mM PMSF] and passing them 10 times through a 18 gauge needle. After centrifugation at 15,800 x *g* for 10 min, the supernatants were incubated with 20–50 µg of Sepharose bound glutathione *S*-transferase (GST) proteins containing the RhoGTPase binding domain Rhotekin (RBD) for 45 min at 4°C by gently shaking, followed by five washing steps with Rho–RBD washing buffer (50 mM Tris/HCl, pH 7.2, 150 mM NaCl, 1% Triton X-100, 10 mM $MgCl_2$, 10 µg/ml aprotinin, 10 µg/ml leupeptin, and 0.1 mM PMSF). Activated RhoA protein was analyzed by western blot assay as described above. The films were scanned and the band intensity was measured using the NIH ImageJ software. All values in the histograms have been corrected against the total RhoA band densities in lysates. Data obtained from three independent experiments were normalized and are represented as the mean ± SEM.

2.2.11 Quantification of growth cone size

Dissociated mixed retinal cells were cultured on coverslips (coated with poly-D-lysine and laminin) for 3 d and then some of the cultures were treated with Taxol (3 nM) for 3 h (Fig. 7). Half of the cultures were then exposed to CME (~10 µg/ml) for 10 min. Cultures were fixed with a paraformaldehyde solution (4%) and RGCs were immunostained with a βIII-tubulin antibody (TUJ1) (1:2,000) as described in the procedures for mixed retinal cell cultures. In addition, cultures were then stained for actin cytoskeleton with phalloidin–tetramethyl rhodamine isothiocyanate (100 ng/ml diluted in PBS) for 40 min at room temperature. The phalloidin staining was performed to improve the visualization of full growth cone. Cultures were then rinsed 3 x 10 min with PBS and the coverslips were inverted onto glass slide (with the side containing the stained cells

facing the glass slide) placed with a drop of mowiol. Growth cones (at least 400 per treatment group) were then photographed under a fluorescent microscope (1000X). The area of growth cone was analyzed using NIH ImageJ software as described below:

- A reference image with scale bar (in µm) photographed at 1000X magnification (such that a complete square was drawn with the scale bar) was opened in the ImageJ software (Fig. 8). The free hand area selection tool of the software was used to mark the perimeter of the scale bar to determine the area in pixels.

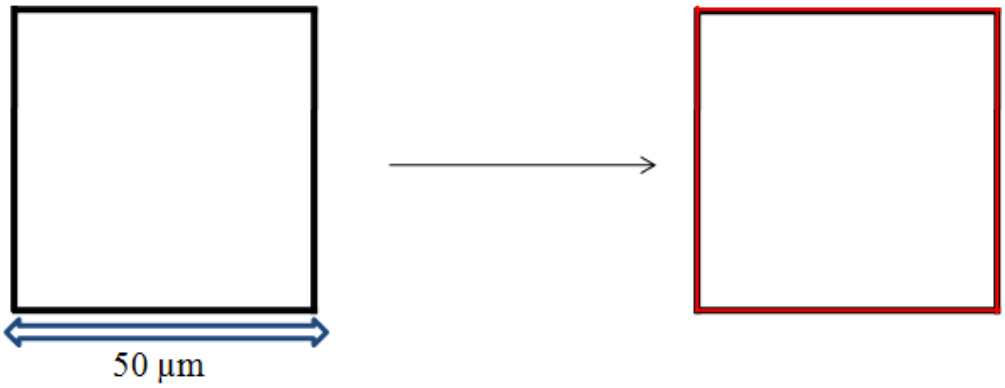

Fig. 8. Schematic representation of a reference image with the scale bar drawn as square (black square). The perimeter of the square was marked to determine the area in pixels (red line over black square)

- Likewise, all the images to be analyzed were opened in the software and the perimeter of the growth cone was marked using the free hand area selection tool to obtain the area in pixels (Fig. 9).

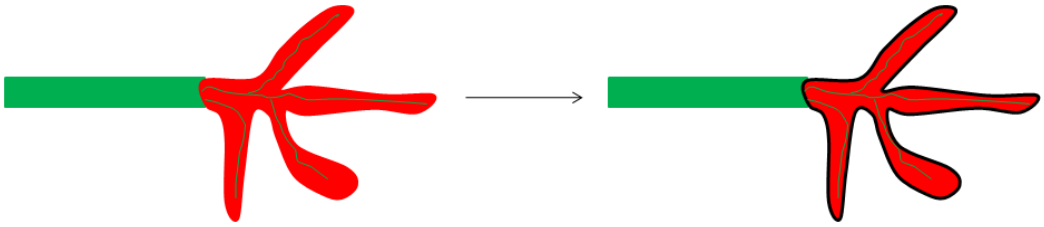

Fig. 9. Schematic representation of a RGC growth cone with axon and dynamic MTs (after tubulin staining) depicted in green color and growth cone (after phalloidin-tetramethyl rhodamine isothiocyanate staining) in red colour. The perimeter of the growth cone was marked (black line) to determine the area in pixels.

- The area of growth cone in μm^2 was derived by the following formula:

$$\text{Area of growth cone} = \frac{\text{Area of growth cone (in pixels)} \times \text{square length of scale bar (in } \mu m)}{\text{Area of scale bar (in pixels)}}$$

To confirm the results, experiments were repeated at least two times. The significances of intergroup differences were evaluated using a one-way ANOVA test, followed by corrections for multiple *post hoc* tests (Bonferroni-Holm, Tukey's).

In other growth cone experiments, PC12 cells were differentiated with NGF (100 ng/ml) for 3 d. Additionally, PC12 cells were either untreated or treated with Taxol (3 nM) for 3 h and half of the cultures were then exposed to CME (~10 µg/ml) for 10 min. Cells were then fixed, stained with βIII-tubulin antibody and phalloidin–tetramethyl rhodamine isothiocyanate and growth cone sizes were measured as described above for RGCs.

2.2.12 Tissue preparation for cryo-sectioning and immunohistochemistry

Rats were anesthetized and perfused through the heart with cold saline (PBS) followed by 4% paraformaldehyde and killed. Eyes with the optic nerve segments attached were dissected free from connective tissue, postfixed (in 4% paraformaldehyde) overnight, and transferred to 30% sucrose at 4°C for 6 h. [Note: The cryo-sectioning procedures were performed by Anastasia Andreadaki]. The tissue was embedded in Tissue-Tek O.C.T compound and frozen at -20°C. Frozen sections of optic nerves were cut longitudinally on a cryostat, thaw-mounted onto coated glass slides and stored at −20°C until further use. For immunostaining, Tissue-Tek O.C.T compound was displaced from optic nerve sections after incubation with PBS for 10-15 min and then fixed in methanol for 10 min. Optic nerve sections were blocked in the blocking buffer (2 % BSA and 5% donkey serum in PBS containing 0.1% Tween-20) for 30 min at room temperature. Sections were probed with sheep anti-GAP-43 antibody (1:1,000) or βIII-tubulin antibody (TUJ1) (1:2,000) in blocking buffer or other relevant antibodies, overnight at 4°C and rinsed 3 x 10 min in PBS. Secondary antibodies included an anti-sheep/anti-mouse IgG conjugated to Alexa Fluor® 488/Alexa Fluor® 594 (1:1,000; Molecular Probes) which were then incubated to

the sections for 1 h at room temperature. Fluorescent sections were rinsed 3 x 10 min in PBS, covered using Mowiol and analyzed under a fluorescence microscope.

2.2.13 Quantification of axons in the optic nerve and RGCs in retinal cross sections

Regeneration of axons was quantified 14 d after surgery as described previously (Leon et al., 2000; Fischer et al., 2004b; Muller et al., 2007; Hauk et al., 2008; Leibinger et al., 2009). In brief, under 400X magnification, the number of GAP-43-positive axons extending ≥0.5, ≥1, ≥1.5, and ≥2 mm from the injury site in six sections per case were counted, normalized to the cross-sectional width of the optic nerve. These data were used to calculate the total numbers of regenerating axons in each animal (Leon et al., 2000; Muller et al., 2007; Hauk et al., 2008; Hauk et al., 2010). For each experimental group, at least five animals were used. Additionally, the length of the longest axon of each section was measured, and also the numbers of βIII-tubulin positive cells, RGCs per section were counted. Measurements were averaged per case, and then averaged across all similarly treated animals to obtain a group means and SE as described previously (Muller et al., 2007). The significance of intergroup differences was evaluated using a one-way ANOVA test, followed by corrections for multiple *post hoc* tests (Bonferroni-Holm, Tukey's).

To measure axon sprouting 1 and 3 d after optic nerve crush, animals received an intravitreal injection of 2 µl of cholera toxin subunit beta (CTB) conjugated with Alexa Fluor® 488 (Invitrogen) simultaneously with surgery, because GAP-43 expression in RGCs was still too low to clearly detect axons 3 d after optic nerve crush (Park et al., 2008; Smith et al., 2009). The quantification of axons that had sprouted into the distal part of the injured optic nerve was performed as described before for GAP-43-positive axons, except that the CTB positive axons were counted at distances ≥50 and ≥100 µm beyond the lesion site.

2.2.14 Quantification of macrophages

Rat optic nerve sections from animals that had undergone optic nerve crush and treated with either gel foam soaked in a solution of Taxol (1 µM) or PBS at the lesion site for 2, 24 and 72 h were stained with a polyclonal antibody against CD68 (ED1, 1:500). The number of macrophages (~1 mm) around the lesion site was counted for each optic nerve section, averaged per case, and then averaged across all similarly treated animals (n = 4) to obtain a group means and SE. Each experimental group consisted of at least four

animals. The significance of intergroup differences was evaluated using a one-way ANOVA test, followed by corrections for multiple *post hoc* tests (Bonferroni-Holm, Tukey's).

2.2.15 Measurement of GFAP-free gap at the lesion site

Rat optic nerve sections from animals that had undergone optic nerve crush and either treated with gel foam soaked in a solution of Taxol (1 μM) or PBS at the lesion site for 3 and 14 d were stained with a monoclonal antibody against GFAP (1:100). The area without appreciable staining for GFAP, both proximal and distal to the lesion site, was measured using the NIH ImageJ software as follows:

- A reference image with scale bar (in μm) photographed at 100X magnification (such that a complete square was drawn with the scale bar) was opened in the ImageJ software (e.g. Fig. 8). The free hand area selection tool of the software was used to mark the perimeter of the scale bar to determine the area in pixels.
- Likewise, all the images to be analyzed were opened in the ImageJ software and the perimeter of the GFAP staining free area of the images was marked using the free hand area selection tool to obtain the area in pixels (Fig. 10).

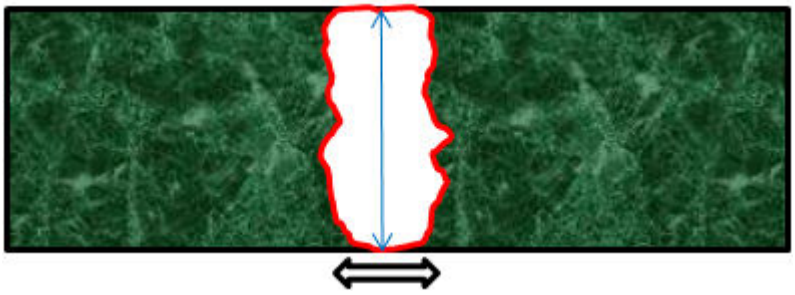

Fig. 10. Schematic representation of an optic nerve section stained for GFAP (green texture) containing GFAP-free area (unshaded region) at the lesion site 3 d after optic nerve crush. The perimeter of GFAP-free area was marked (red line) and the width of optic nerve section was measured (blue line) to determine the length of the GFAP-free gap (double headed open arrow).

- The area of GFAP staining free area cone in μm^2 was derived by the following formula:

$$\text{Area of GFAP staining free area} = \frac{\text{Area of GFAP free area (in pixels) x square length of scale bar } (\mu m)}{\text{Area of scale bar (in pixels)}}$$

- The length of the GFAP staining free gap (in μm) was then derived by the formula:

$$\text{Length of GFAP staining free area} = \frac{\text{Area of GFAP staining free area (in sq.}\mu m)}{\text{Width of the optic nerve section (in } \mu m)}$$

The obtained values of gap length per section were averaged per case and then averaged across all similarly treated animals (n = 4) to obtain a group means and SE. The significance of intergroup differences was evaluated using a one-way ANOVA test, followed by corrections for multiple *post hoc* tests (Bonferroni-Holm, Tukey's).

2.2.16 Primary astrocyte cultures and Taxol treatment

Primary cell cultures of astrocytes were prepared from postnatal (4-d-old) C57BL/6 mice. [Note: The astrocyte cultures were prepared by Dr. Anke Witting]. Cerebra of the pups were dissected aseptically, and the meninges were removed. Cortices were homogenized in ice-cold PBS with Pasteur pipette. The homogenate was washed two to three times in PBS by centrifugation at 2,000 x *g* for 5 min. The cell pellet was resuspended in DMEM containing 10% fetal bovine serum, 1% L-glutamine, and 1% penicillin/streptomycin solution and cultured in poly-D-lysine-coated 75 cm^2 culture flasks for 14 d until monolayers reached confluence. Confluent cultures were vigorously agitated to dislodge oligodendrocytes and microglia. The astrocytes remain attached to the culture flask which were then trypsinized and re-plated in poly-D-lysine coated four-well plates. Cultures were incubated until they reached confluency. Scratch injury was then performed on confluent primary astrocyte cultures using a sterile plastic tip with a diameter of 0.5 mm. Cultures were untreated or exposed to different concentrations of Taxol (3, 10, 50, and 100 nM) and incubated for another 24 h. Cells were then fixed with 4%

paraformaldehyde and methanol for 30 and 10 min respectively and blocked in a blocking buffer for 30 min at room temperature. Immunostaining was performed with a monoclonal antibody against GFAP (1:100) for 2 h at room temperature, and the cells were washed 3 x 10 min with 1X PBS. Cells were then incubated with a secondary antibody, anti-rabbit IgG conjugated to Alexa Fluor® 594 (1:1,000) and washed 3 x 10 min with 1X PBS. Images were taken under 200X magnification at different sites of scratch injury for all the culture conditions. The width of the unclosed injury site was measured using NIH ImageJ software as described below:

- A reference image with a scale bar (in μm) photographed at 200X magnification was opened in the ImageJ software. The line tool of the software was then used to calibrate and apply the length of the scale bar for all the images to be analyzed.
- Images of the scratch injury site after different treatment conditions were opened and width of the unclosed injury site (in μm) was determined.

The obtained values from width of the unclosed injury site were averaged per case and then averaged across all similarly treated conditions (n = 3) to obtain a group means and SE. The significance of intergroup differences was evaluated using a one-way ANOVA test, followed by corrections for multiple *post hoc* tests (Bonferroni-Holm, Tukey's).

2.2.17 Measurement of CSPG expression

After an optic nerve crush, animals were applied with the gel foam soaked in a solution of either Taxol (1 μM) or PBS at the lesion site for 2, 24, or 72 h. Rat optic nerve sections from these animals were taken and stained with CS-56 antibody (a monoclonal antibody against the glycosaminoglycan portion of native CSPGs, 1:100). Optic nerve sections from the animals of the different groups (n = 4 per group) were stained simultaneously, and images were taken in a single session at the same exposure time. The staining intensity for CSPGs was measured in all optic nerve sections using NIH ImageJ software as described below:

- All the images to be analyzed were opened and converted into gray scale images in the ImageJ software.
- First, a reference image of an optic nerve section (from control animals – 2 h after optic nerve crush and PBS treatment) was taken and the rectangular area selection

tool was used to select an area distal to the lesion site (~500 µm in length) such that it covers the entire width of the optic nerve section (Fig. 11 A). The CSPG staining intensity of the selected region was measured which was then used to normalize the values obtained in other experimental conditions.

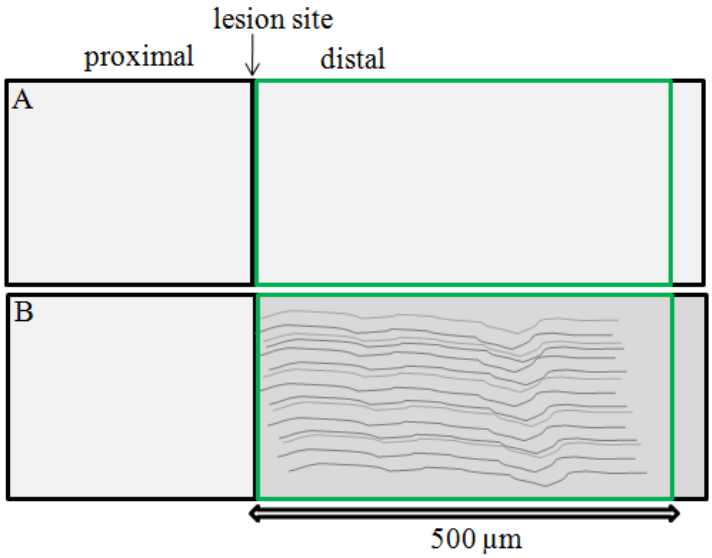

Fig. 11. Schematic representation of optic nerve sections stained for CS-56 (CSPGs) from either control animals (A) or 3 d after optic nerve crush and PBS treatment (B). Staining intensity of an equal area distal to the lesion site (marked in green line) was measured in both cases.

- The area selection settings from reference image was retained and used to analyze the staining intensity of equal area distal to the lesion site from all the other optic nerve sections (Fig. 11 B).

The measured intensities were averaged per case and then averaged across all similarly treated animals to obtain a group means and SE. The significance of intergroup differences was evaluated using a one-way ANOVA test, followed by corrections for multiple *post hoc* tests (Bonferroni-Holm, Tukey's). To verify the specificity of the CSPG staining, optic nerve sections were exposed to chondroitinase ABC in digestion buffer (50 mM Tris, pH 8.0, 60 mM sodium acetate and 0.02% BSA) at 0.3 U for 10 h at 37°C and then washed 3 x 10 min with 1X PBS and stained for CSPGs.

3. Results

3.1 Taxol improves neurite outgrowth of adult RGCs in a concentration dependent manner

Taxol differentially alters microtubule (MT) dynamics and polymerization in cells or purified tubulin subunits based on the concentrations in which it is applied (Derry et al., 1995; Derry et al., 1997; Chuckowree and Vickers, 2003). Hence, we tested different concentrations of Taxol to evaluate its effect on RGC neurite outgrowth on normal adult rat primary dissociated retinal cell cultures. We treated these cultures either in the absence or presence of Taxol at 0.5, 1, 3, 10 and 50 nM concentrations. In untreated controls, RGCs showed minimal neurite outgrowth after 72 h in culture. Neurite length of RGCs was significantly increased in the groups treated with low nanomolar concentrations of Taxol (0.5 – 3 nM), with the strongest effect observed at a concentration of 3 nM (Fig. 12 A, B). The beneficial effects of Taxol on neurite outgrowth could not be detected at a concentration of 10 nM and neurite length was strongly decreased at a concentration of 50 nM compared to untreated controls. Importantly, Taxol did not affect the survival of RGCs on the various concentrations tested in the study, which indicates that it was not neurotoxic (Fig. 12 C). These results clearly suggest that Taxol can exert positive effects on neurite outgrowth of RGCs only at low nanomolar concentrations.

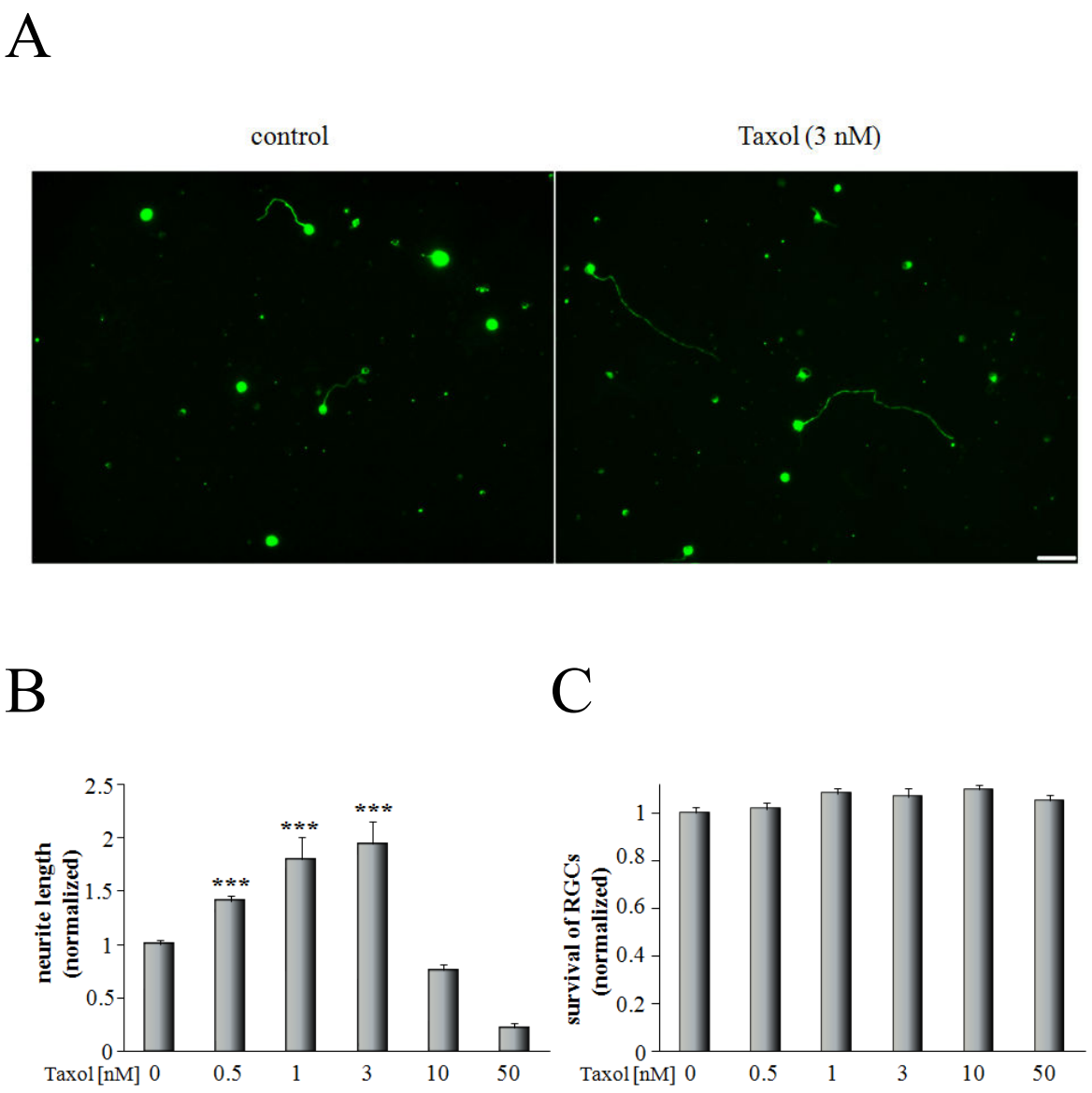

Fig. 12. Taxol associated increase in neurite outgrowth is concentration dependent. A. Representative images of βIII-tubulin positive RGCs with regenerated neurites that were cultured in the absence (control) or presence of Taxol (3 nM). Scale bar = 50 µm. B. Quantification of neurite length of RGCs which were either untreated or treated with Taxol for 3 d in culture. Taxol at low nanomolar concentrations markedly increased outgrowth, while neurite outgrowth was drastically reduced at a concentration of 50 nM. Treatment effects: ***$p < 0.001$. C. RGC survival was not affected in any of the Taxol concentrations tested *in vitro*.

3.2 Taxol synergistically enhances neurite outgrowth in a combinatorial treatment and overcomes myelin inhibition

We observed that the neurite outgrowth of both normal as well as *in vivo* growth stimulated RGCs was significantly increased after Taxol treatment [Fig. 12 A, B], (Sengottuvel et al., 2011). CNTF has been reported to markedly enhance neurite outgrowth of RGCs *in vitro* (Jo et al., 1999; Muller et al., 2007; Lingor et al., 2008; Leibinger et al., 2009; Muller et al., 2009; Hauk et al., 2010). Therefore, we tested whether Taxol can also improve neurite growth of RGCs concomitantly with CNTF. Dissociated retinal cell cultures from adult rats were prepared which were then untreated (controls) or treated with CNTF (200 ng/ml) and/or Taxol (3 nM). Consistent with previous studies, mean neurite length of RGCs was increased ~2 fold after CNTF treatment compared to untreated controls. Moreover, Taxol treatment *per se* increased the neurite outgrowth of RGCs to similar levels achieved after CNTF treatment. In addition, a combinatorial treatment of Taxol and CNTF significantly increased the neurite outgrowth of RGCs compared to either treatment alone, which indicates that both treatments functioned synergistically (Fig. 13 A, B).

CNS myelin inhibits neurite outgrowth of normal adult as well as CNTF treated RGCs (Logan et al., 2006; Ahmed et al., 2009). Hence, we examined whether Taxol can overcome myelin inhibition on neurite outgrowth of RGCs. To test this possibility, we prepared dissociated retinal cell cultures and treated these cells with CME. As reported in previous studies, we observed that the neurite length of RGCs was significantly reduced in the presence of CME in control as well as CNTF treated groups. Taxol treatment *per se* or a combinatorial treatment of Taxol and CNTF completely overcame myelin inhibition and RGCs showed similar neurite length comparable to the groups cultured on normal substrate (Fig. 13 A, B). These data denote that Taxol negated the influence of inhibitory myelin and enhanced neurite outgrowth of RGCs.

A

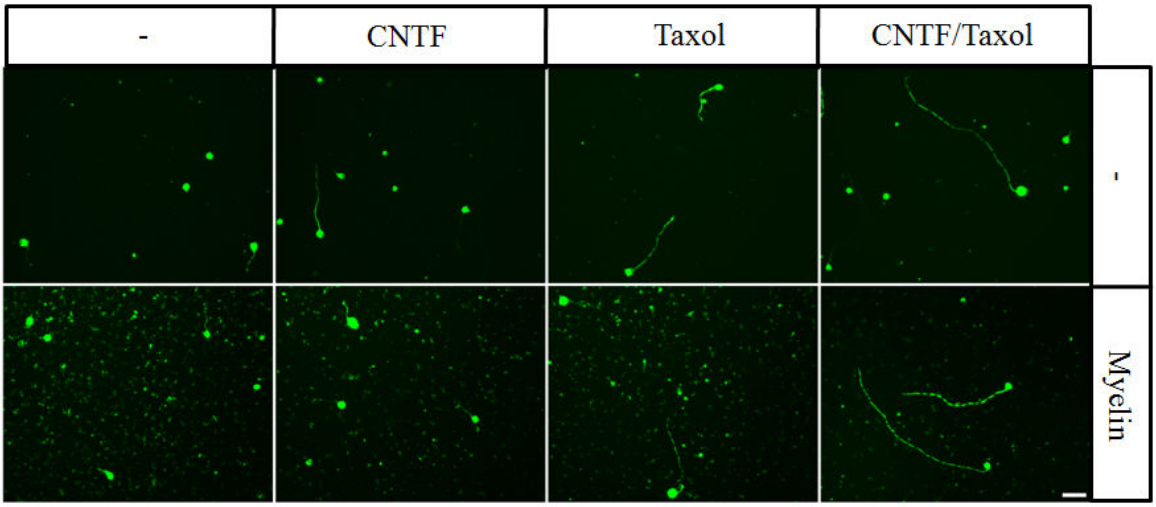

B

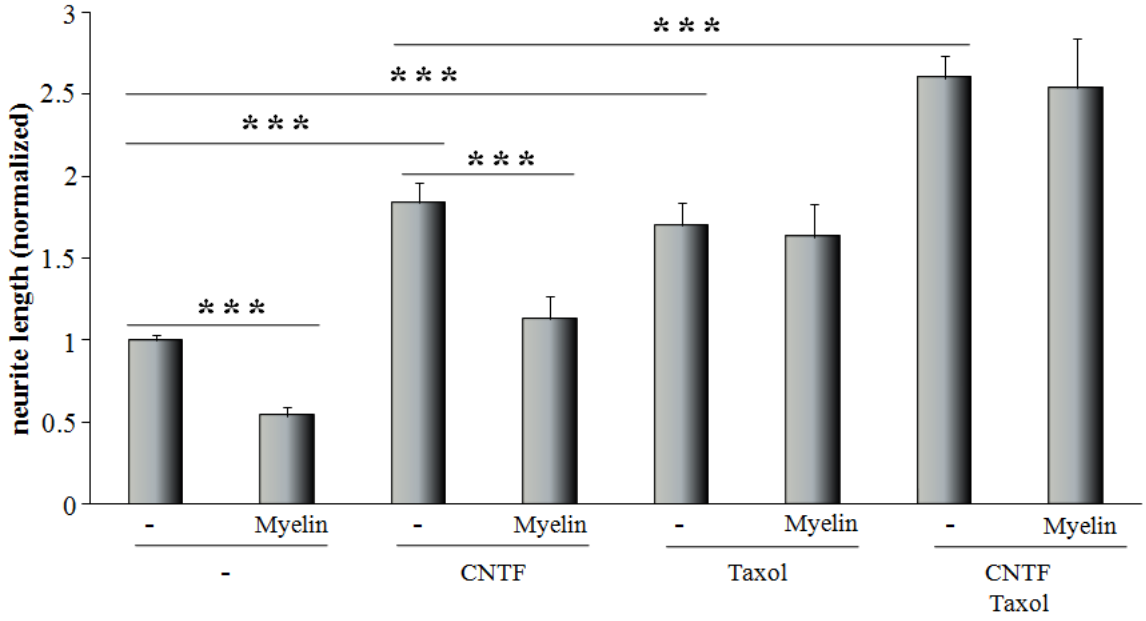

Fig. 13. Taxol synergistically increases neurite outgrowth along with CNTF and also overcomes myelin inhibition. A. Representative images of βIII-tubulin positive RGCs with regenerated neurites after 3 d in culture from untreated (-), CNTF (200 ng/ml), Taxol (3 nM) or Taxol + CNTF treated mixed retinal cultures. All the above groups were also cultured in the presence of CNS myelin extract (Myelin). Scale bar = 50 µm. B. Quantification of neurite length of the groups described in A. Taxol (3 nM) increased neurite length to similar levels as CNTF and also acts in combination to further improve

neurite outgrowth. Disinhibited neurite outgrowth after myelin treatment can be observed only in Taxol treated groups. Treatment effects: ***$p < 0.001$.

3.3 Taxol improves neurite outgrowth of PC12 cells and overcomes myelin inhibition

PC12 cells are useful model system to evaluate neurite outgrowth owing to their differentiation into neuronal morphology after NGF treatment. Moreover, PC12 cells also respond to myelin inhibition and display reduced neurite length (Lehmann et al., 1999; Fournier et al., 2003). To confirm the neurite outgrowth results obtained in RGCs, PC12 cells were differentiated (with NGF) and the cultures were grown in the absence (controls) or presence of Taxol (3 nM). Half of the groups were also treated with CME. Neurite length was increased ~2-fold in PC12 cells treated with Taxol compared to untreated controls. In addition, differentiated PC12 cells exposed to CME resulted in significantly decreased neurite length, whereas Taxol treated cells exhibit disinhibited neurite outgrowth (Fig. 14 A, B). These data demonstrate that Taxol can also overcome myelin inhibition in other neuron-like cells and promote neurite outgrowth.

A

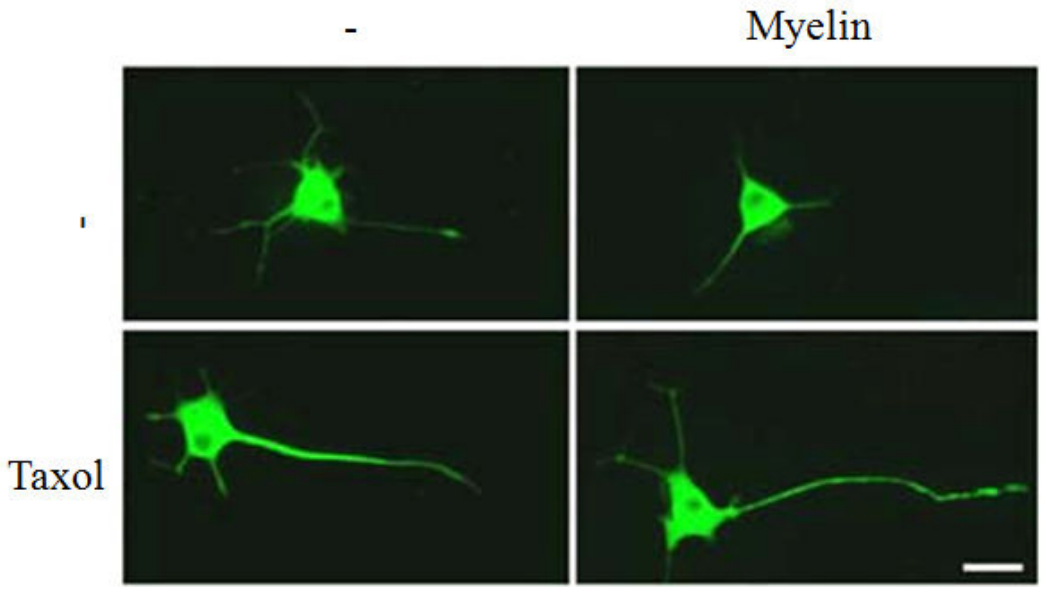

B

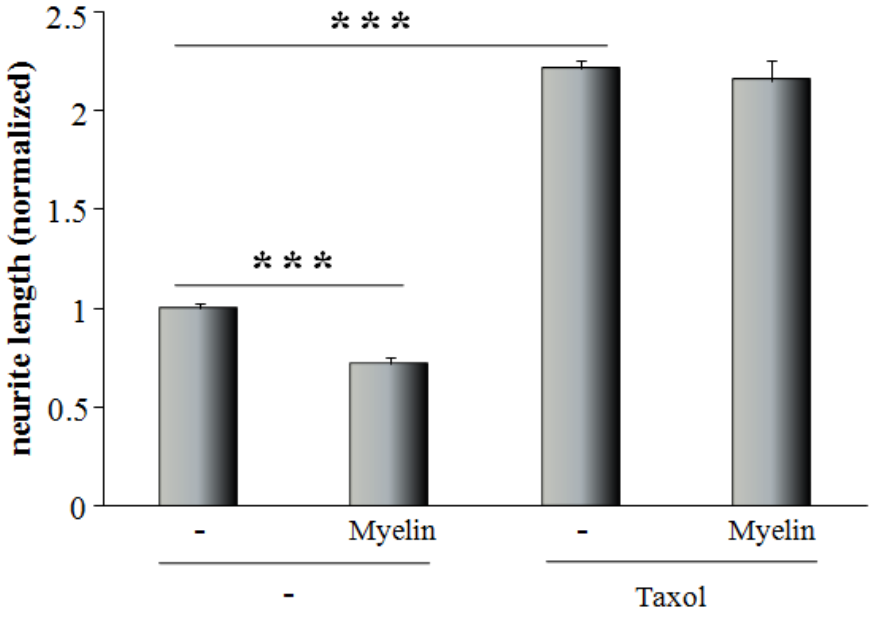

Fig. 14. Taxol also increases neurite outgrowth of PC12 cells and overcomes myelin inhibition. A. Differentiated PC12 cells cultured in the absence (-) or presence of Taxol (3 nM)/CNS myelin extract (Myelin) for 3 d and stained with βIII-tubulin to observe neurite outgrowth. Scale bar = 50 μm. B. Quantification of neurite length of groups described in A. Treatment effects: ***$p < 0.001$.

3.4 Taxol overcomes CSPG inhibition of neurite outgrowth

CSPGs consist of various inhibitory molecules/proteins like neurocan, aggrecan, brevican, versican and reduces neurite outgrowth of CNS neurons (McKeon et al., 1991; McKeon et al., 1995; Monnier et al., 2003). Hence, we investigated whether Taxol can also overcome neurocan (one of the prominent CSPG inhibitory proteins) mediated decrease in neurite outgrowth of RGCs. We prepared dissociated mixed retinal cultures which were either untreated (controls) or treated with Taxol (3 nM). In addition, the cells were also grown in the absence or presence of neurocan at a concentration of 5 µg/ml in the culture medium. Consistent with previous reports (Inatani et al., 2001), neurocan significantly decreased the neurite length of RGCs in controls, whereas additional Taxol treatment overcame the neurocan mediated reduction in neurite outgrowth of RGCs (Fig. 15 A, B). The refractory phenomenon of Taxol treatment toward neurocan as well as myelin inhibition on neurite outgrowth suggests that the effect of Taxol occurred downstream of common inhibitory receptor pathways activation.

A

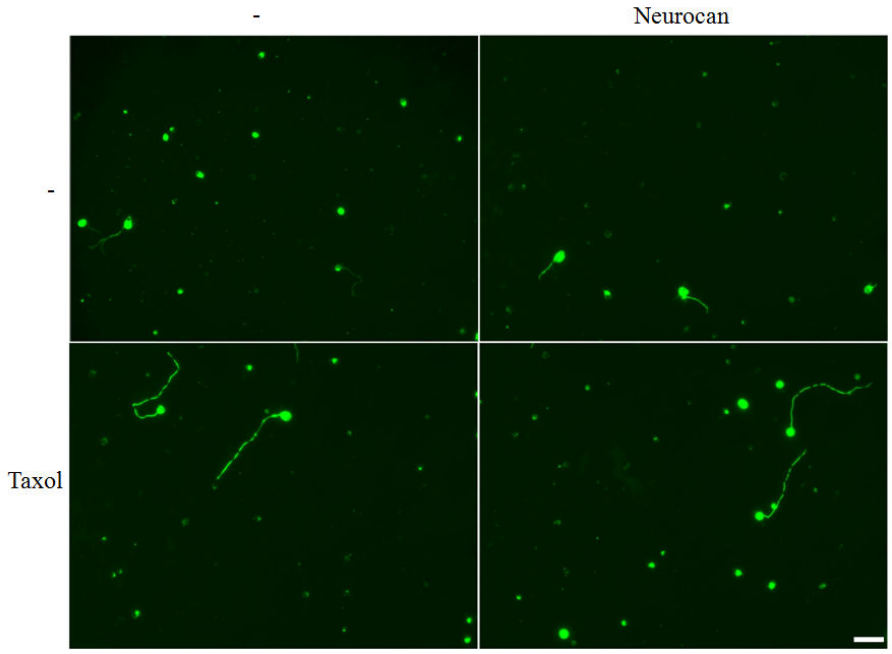

B

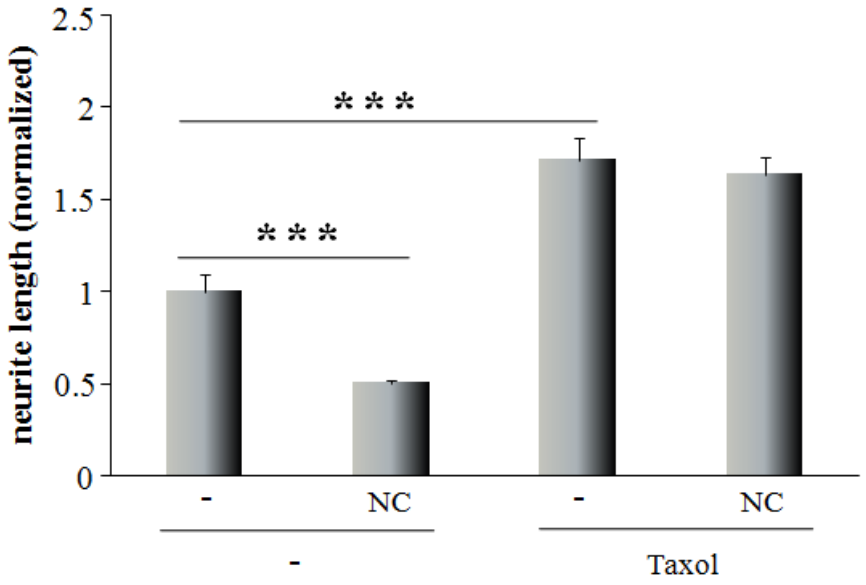

Fig. 15. Taxol overcomes neurocan mediated inhibition of neurite outgrowth on RGCs. A. βIII-tubulin positive RGCs with regenerated neurites in untreated (-) or Taxol (3 nM) treated mixed retinal cell cultures after 3 d. Neurocan [NC] (5 µg/ml) was added to half of the cultures in the culture medium. Scale bar = 50 µm. B. Quantification of neurite length of groups described in A. Treatment effects: ***$p < 0.001$.

3.5 Taxol prevents myelin induced growth cone collapse/shrinkage independent of RhoA activation

3.5.1 Taxol prevents growth cone collapse of RGCs

Growth cone collapse/shrinkage occurs in CNS neurons exposed to myelin (Bandtlow et al., 1993; Loschinger et al., 1997; Fournier et al., 2002; Wong et al., 2003). We found that the myelin as well as CSPGs mediated neurite outgrowth inhibition of RGCs in culture could be circumvented after Taxol treatment. Hence, we tested whether Taxol might stabilize the growth cones and modulate the inhibitory responses of RGCs toward myelin. Dissociated mixed retinal cells were cultured for 72 h which were then untreated or treated with Taxol (3 nM) for 3 h. Half of the groups were also exposed to CME for 10 min. Significant reduction in growth cone size was observed in untreated RGCs exposed to CME. However, after Taxol treatment the CME induced reduction in growth cone size was markedly ameliorated and RGCs showed similar growth cone size comparable to controls (Fig. 16 A, B). This data indicates that Taxol desensitized RGC growth cones toward inhibitory myelin.

A

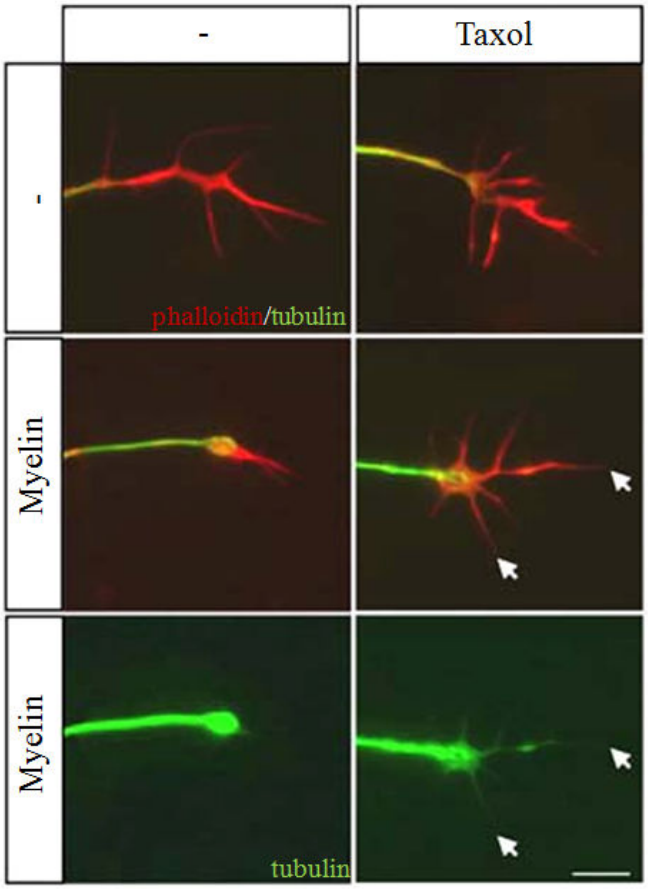

B

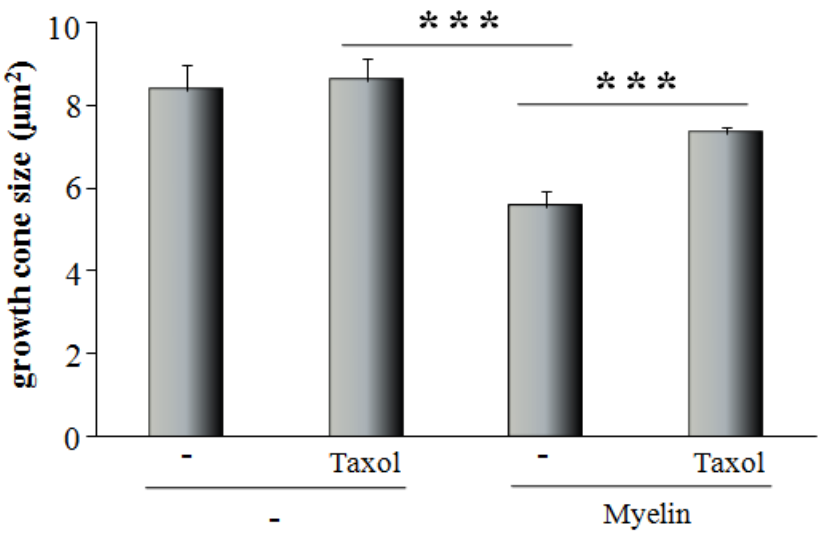

Fig. 16. Taxol prevents growth cone shrinkage/collapse of RGCs. A. βIII-tubulin

positive regenerated neurites of RGCs with phalloidin stained growth cones after 3 d in culture, untreated (-) or Taxol (3 nM) treated for 3 h. Half of the groups were cultured in the presence of CNS myelin extract (Myelin) for 10 min. Scale bar = 2 μm. B. Measurement of growth cone sizes of all the groups indicated in A. Treatment effects: ***p < 0.001.

3.5.2 Taxol prevents growth cone collapse of PC12 cells

To extend the results obtained in RGCs on growth cone size, we cultured PC12 cells and differentiated these cells with NGF for 3 d. Cells were untreated or treated with Taxol (3 nM) for 3 h and half of the cultures were then exposed to CME for 10 min. Similar to the results obtained in RGCs, growth cone size of untreated PC12 cells was significantly reduced after CME exposure, whereas Taxol treatment significantly alleviated the reduction in growth cone size (Fig. 17 A, B). These data confirm that Taxol prevented growth cone collapse/shrinkage, possibly through stabilization of MTs located in the growth cones.

A

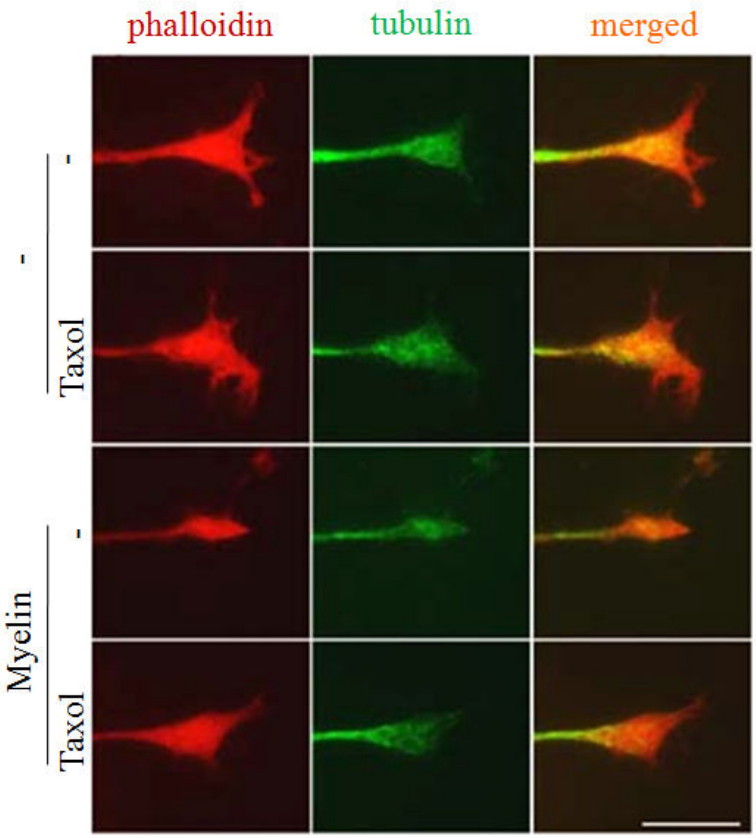

B

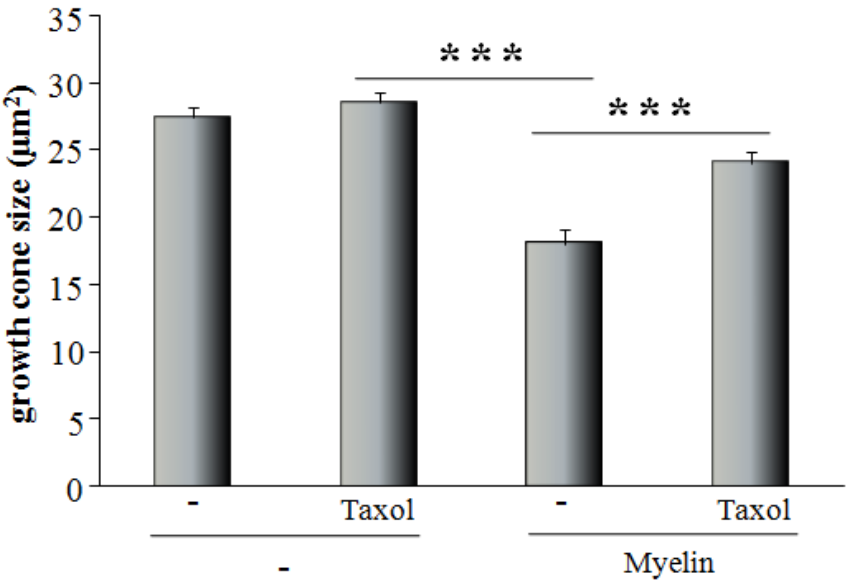

Fig. 17. Taxol stabilizes growth cones of PC12 cells from myelin induced shrinkage/collapse. A. PC12 cells were differentiated with NGF for 3 d and cultures were

untreated (-) and/or treated with Taxol (3 nM)/CNS myelin extract (Myelin) for 3 h and 10 min respectively. PC12 cells were stained with βIII-tubulin and phalloidin to demarcate the soma/axon and growth cone. Scale bar = 10 μm. B. Growth cone area analysis of all the groups indicated in A. Growth cone collapse occurs after myelin exposure while Taxol treatment prevents this phenomenon. Treatment effects: ***$p < 0.001$.

3.5.3 Taxol treatment does not affect myelin induced RhoA activation

RhoA/ROCK signaling is one of the common inhibitory pathways that are activated after receptor binding of MIL in the CNS (Filbin, 2003; Yiu and He, 2006; Berry et al., 2008). It has been reported that the myelin inhibition on neurite outgrowth could be significantly reduced by blocking RhoA/ROCK signaling pathway (Dergham et al., 2002; Fournier et al., 2003). To test whether Taxol alleviates the inhibitory effects of myelin by influencing RhoA activation, we differentiated PC12 cells for 3 d which were then untreated or treated with Taxol (3 nM) for 3 h. In addition, half of the cultures were also exposed to CME for 10 min. Cells were then lysed and RhoA-GTP was affinity precipitated with GST-RBD. RhoA levels were determined by immunoblotting [Note: The affinity precipitation and immunoblotting was performed by Mariana Pfreimer]. RhoA-GTP was strongly induced only in the groups exposed to CME [lane(s) 3, 4 compared to lane(s) 1, 2] (Fig. 18 A, B). However, RhoA-GTP expression was not notably altered after Taxol treatment either in the absence [between lanes(s) – 1 and 2] or presence of CME [between lane(s) – 3 and 4] compared to untreated controls (Fig. 18 A, B). These data demonstrate that Taxol enhanced neurite outgrowth through desensitization/stabilization of neuronal growth cones toward myelin inhibition without significantly altering RhoA activation.

A

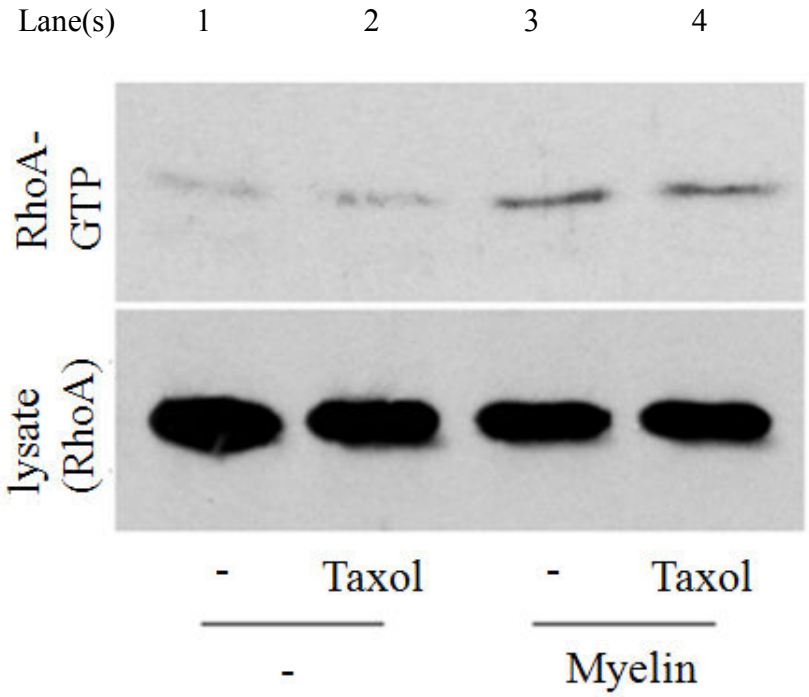

B

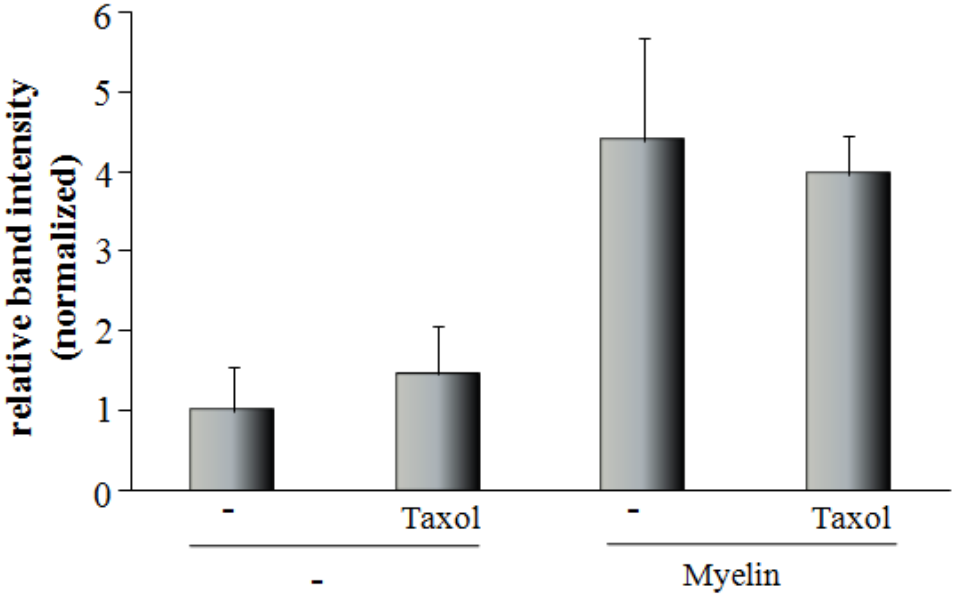

Fig. 18. Myelin induced RhoA activation was not altered after Taxol treatment as detected through Rho activity assay. A. Immunoblot of PC12 cell lysates after affinity precipitation with Sepharose beads containing GST-RBD to detect RhoA-GTP from cells that were cultured in the presence of NGF for 3 d and untreated (-) or treated with Taxol (3 nM) for 3 h. Half of the cultures were exposed to CNS myelin extract (Myelin) for 10 min.

Lane 1: Untreated PC12 cells. Lane 2: Taxol treated PC12 cells. Lane 3: PC 12 cells treated with Myelin only. Lane 4: PC12 cells treated with Taxol and Myelin. B. Quantification of RhoA-GTP band intensity normalized to loading control (RhoA) after three independent experiments.

3.6 Taxol treatment enhances optic nerve regeneration *in vivo*

3.6.1 Taxol treatment enhances optic nerve regeneration in a concentration dependent manner

Damage to the optic nerve axons (e.g. ONC) results in very limited regeneration and more than 90% of RGCs undergo apoptosis 14 days after injury (Berkelaar et al., 1994; Garcia-Valenzuela et al., 1994; Berry et al., 2008). However, markedly improved axon regeneration could be attained when ONC was combined with LI and also significantly higher numbers of RGCs survive the injury (Fischer et al., 2000). We observed that Taxol treatment improved the neurite outgrowth of RGCs as well as PC12 cells and also overcame myelin and CSPGs inhibition *in vitro*. We therefore investigated whether the beneficial effects of Taxol could be harnessed to facilitate regeneration of axons in the rat optic nerve injury model *in vivo*. Considering that only low nanomolar concentrations of Taxol enhanced neurite outgrowth *in vitro* and higher concentrations adversely affected neurite outgrowth, in initial studies we tested different concentrations of Taxol (1, 10, 100 and 1000 μM) along with PBS (controls) to determine the appropriate concentration required to improve axon regeneration. After ONC, Gelfoam soaked with a solution of Taxol or PBS was applied directly around the lesion site of the optic nerve (Fig. 6). LI was also performed to stimulate the intrinsic regenerative state of RGCs and enhance RGC survival. We found that the regeneration of axons increased inversely in relation to the concentrations of Taxol applied, with the lowest tested concentration (1 μM) leading to strongest regeneration (Fig. 19 A). Moreover, all the concentrations of Taxol tested in our study showed increased axon regeneration compared to controls. RGC survival was not affected in any of the Taxol concentrations tested in our study and remained similar to the numbers observed in controls (Fig. 19 B).

A

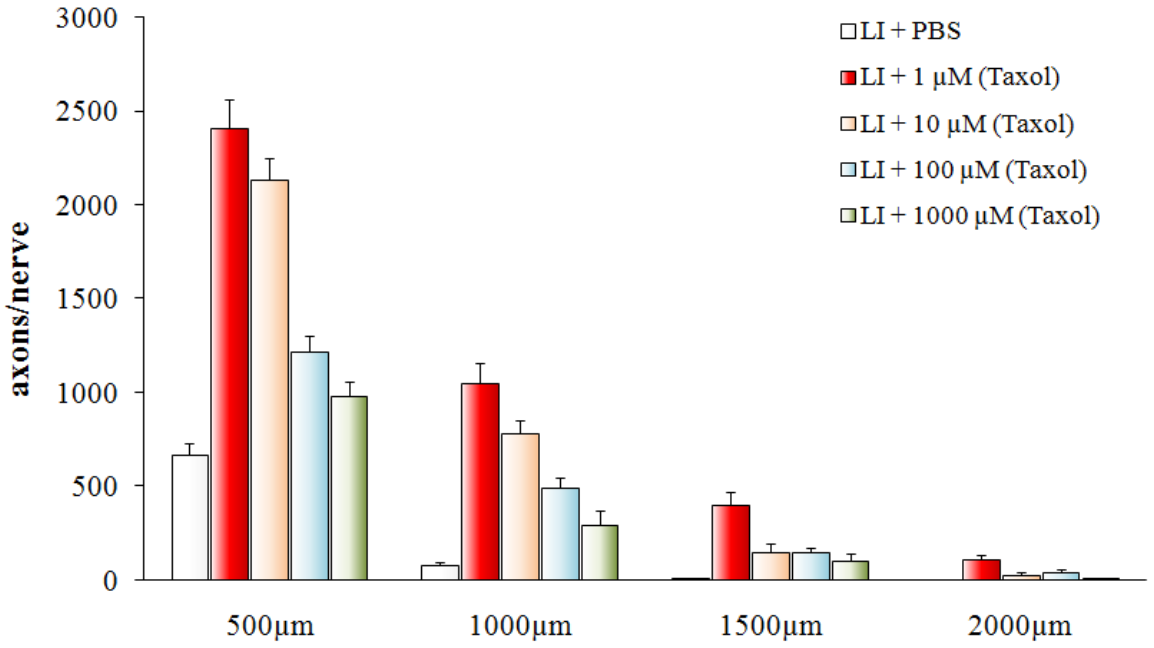

B

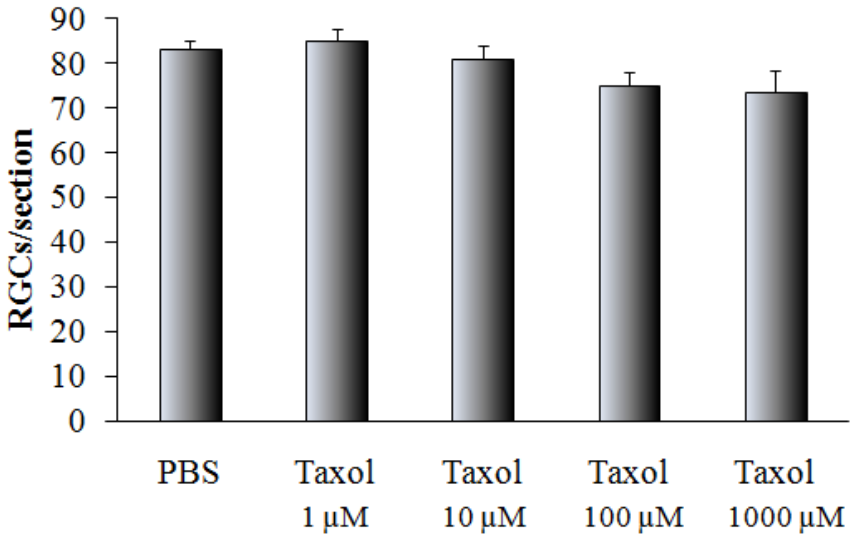

Fig. 19. Taxol enhances optic nerve regeneration *in vivo* at low concentrations of Taxol. A. Quantification of axon regeneration in the optic nerve 500 – 2000 µm beyond the lesion site, 14 d after ONC+LI and treatment of the lesion site with gel foam soaked in solutions of PBS/Taxol (1, 10, 100 and 1000 µM). The number of axons were counted and extrapolated to the whole optic nerve. B. Quantification of RGC survival (βIII-tubulin positive RGCs) after the above mentioned treatments.

3.6.2 Taxol treatment enhances optic nerve regeneration synergistically with LI

Taxol was used at a concentration of 1 μM for further experiments which resulted in more than 4-fold and 15-fold increase in number of axons that regenerated 0.5 mm and 1 mm beyond the lesion site respectively compared to LI and PBS treated groups. Significant levels of axon regeneration could also be observed at 1.5 and 2 mm beyond the lesion site in Taxol treated animals, with almost no discernable regeneration found in PBS treated animals at these distances (Fig. 20 A, B). The average length of the longest regenerating axons reached a distance up to 2.17 ± 0.8 mm after Taxol (1 μM) and LI treatment. However, LI and PBS treated animals displayed an average length of only 1.1 ± 0.05 mm (Fig. 20 D). This indicates that Taxol enhanced axon regeneration *in vivo* along with measures that stimulate the intrinsic regenerative state of RGCs.

We also examined whether Taxol treatment without an additional LI could improve axon regeneration. Animals that had been subjected to ONC and PBS treatment at the lesion site exhibited only minimal regeneration. However, ONC and Taxol treatment at the lesion site significantly increased (although the regeneration achieved was not extensive as in the case after LI treatment) the numbers of regenerating axons compared to PBS treated animals (Fig. 20 A, B). In Taxol treated groups the average length of longest regenerating axons reached up to 0.89 ± 0.12 mm, whereas, PBS treated controls showed an average length of only 0.58 ± 0.08 mm (Fig. 20 D). The survival of RGCs was not altered after Taxol application either in the absence or presence of LI (Fig. 20 C). This demonstrates that Taxol treatment at the optic nerve lesion site enhanced axon regeneration without affecting the LI induced beneficial effects on RGC survival.

A

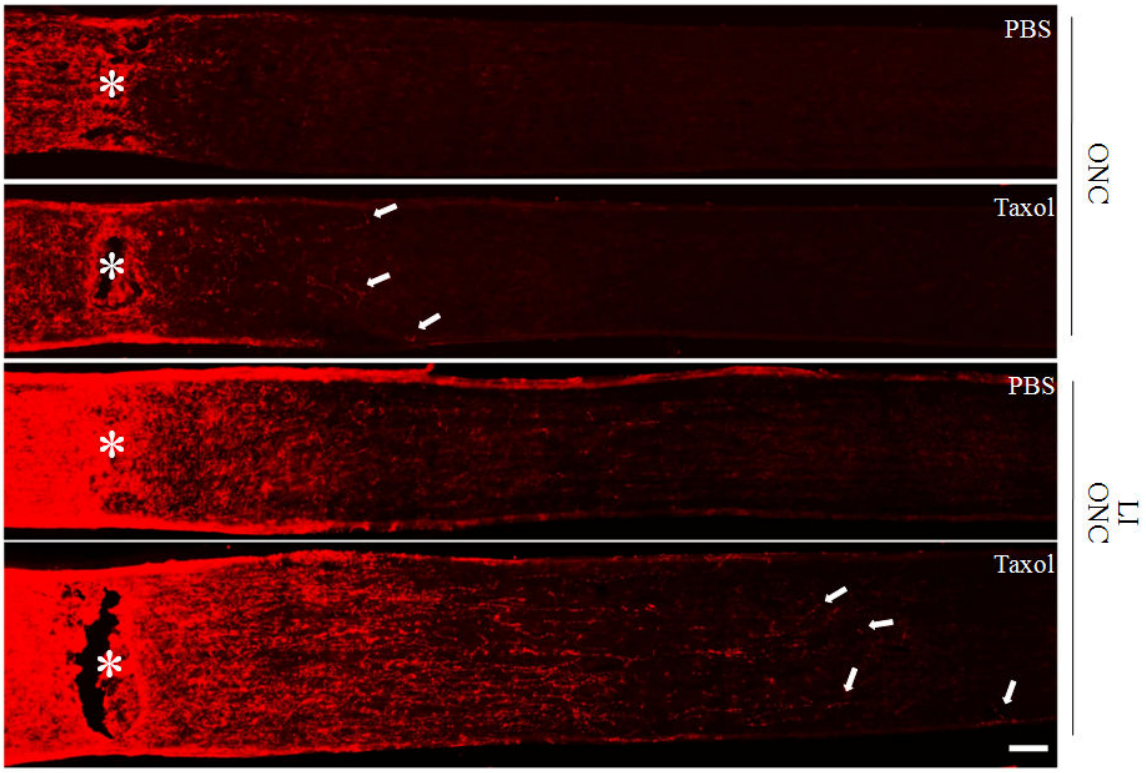
PBS
Taxol
PBS
Taxol
ONC
LI ONC

B

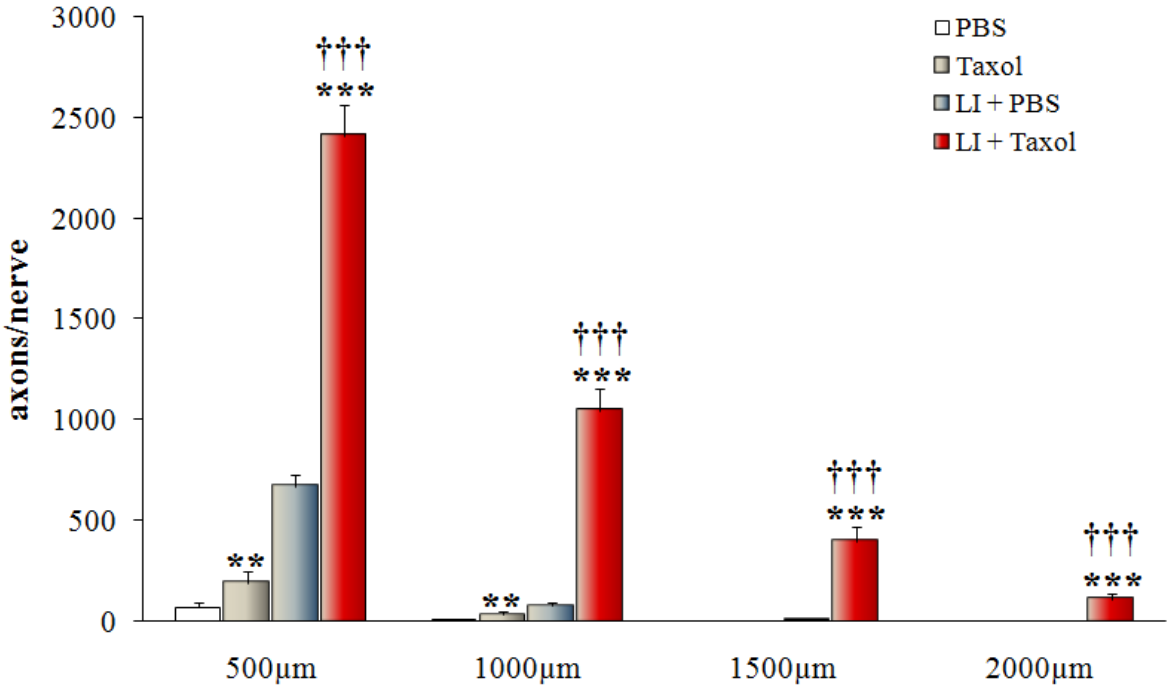
axons/nerve
3000
2500
2000
1500
1000
500
0
PBS
Taxol
LI + PBS
LI + Taxol
500μm
1000μm
1500μm
2000μm

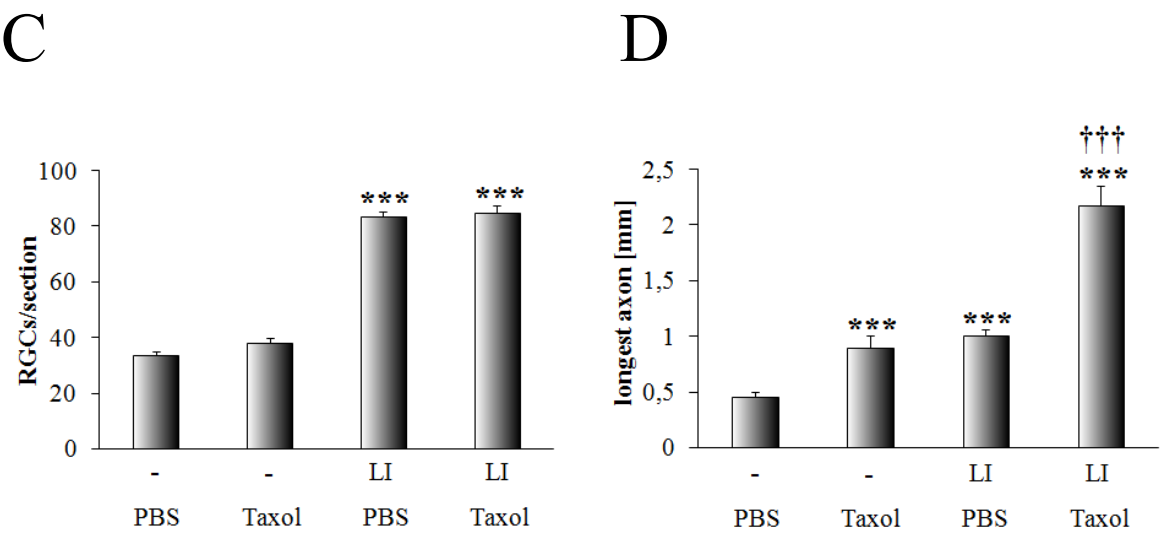

Fig. 20. Taxol enhances optic nerve regeneration *in vivo* synergistically with inflammatory stimulation (LI). A. Longitudinal sections of optic nerve (ON) stained with GAP-43, 14 d after ONC/LI and additional treatment of the lesion site with gel foam soaked in PBS/Taxol (1 µM) solutions as indicated. Asterisks denote the lesion site and arrows indicate the longest regenerating axons. Scale bar = 100 µm. B. Quantification of axon regeneration in the optic nerve 500-2000 µm beyond the lesion site, 14 d after ONC/LI. Treatment effects: ***$p < 0.001$, **$p < 0.01$ compared to PBS treated group; †††$p < 0.001$- compared to PBS and LI treated group. C. Quantification of RGC survival (βIII-tubulin positive RGCs) in the groups indicated in A. Treatment effects: ***$p < 0.001$ compared to PBS treated group. D. Quantification of the longest axons per section of the groups indicated in A. Treatment effects: ***$p < 0.001$ compared to PBS treated group; †††$p < 0.001$ compared to PBS and LI treated group.

3.7 Taxol promotes early axonal sprouting *in vivo*

We next analyzed the effects of Taxol on initial axon sprouting at 1 and 3 days after ONC *in vivo*. The lesion site of rats were treated with gel foam soaked in a solution of Taxol (1 µM) or PBS and the anterograde neuronal tracer, CTB was injected at the time of surgery. CTB injection was required due to the low levels of GAP-43 expression 3 d after ONC which could not be detected by immunostaining. At 1 d after ONC, axons terminated at the proximal end of the lesion site and axonal growth was not observed beyond the crush site in animals that received either PBS or Taxol treatment. However, 3 d after ONC and Taxol treatment substantial number of CTB-positive regenerating axons had already grown beyond the lesion site and the longest axonal sprouts showed a noticeable length of up to 400 µm (Fig. 21 A, B, C). In contrast, only very little axonal sprouting could be found in PBS-treated controls. We also examined whether intravitreal injections of Taxol could catapult axonal sprouting similar to the application of Taxol at the ON lesion site. However, no axonal sprouting could be achieved after intravitreal injections of Taxol as in the case of PBS treatment (Fig. 21 A, B, C). These data denote that Taxol exerted its beneficial effects on axonal sprouting by directly acting at the regenerating axon tips rather than on the cell body of RGCs.

A

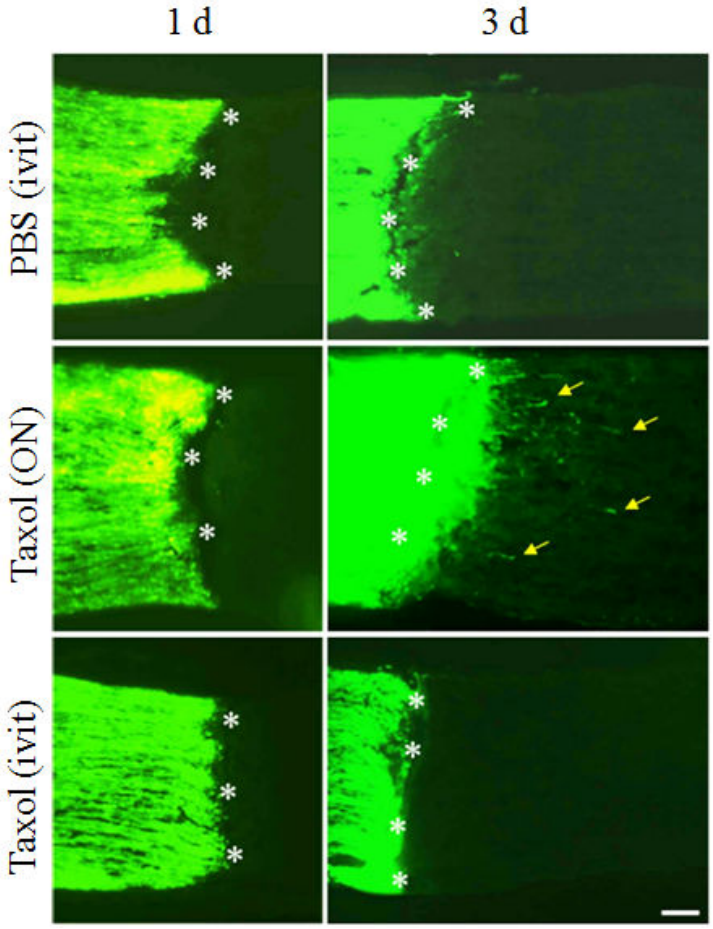

B

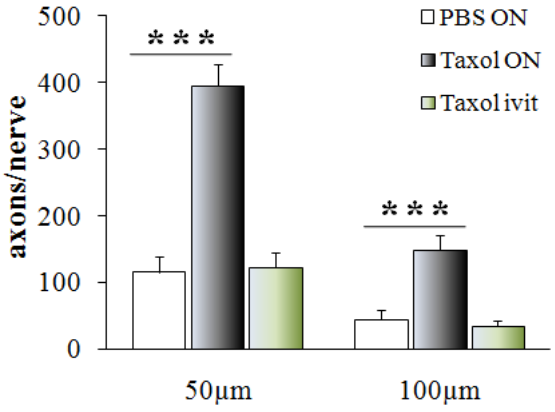

C

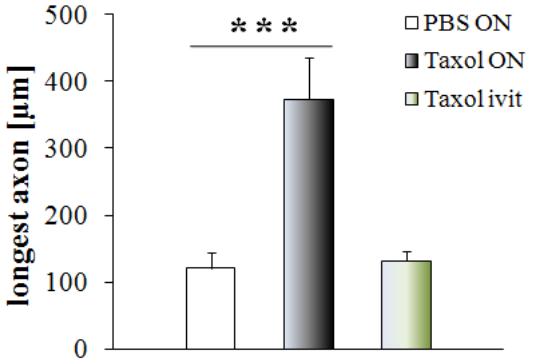

Fig. 21. Taxol promotes intial axon sprouting *in vivo*. A. Longitudinal sections of ON sections 1 d or 3 d after ONC and treatment of the lesion site with gelfoam soaked with a solution of PBS/Taxol (1 µM) or intravitreal injections of Taxol (1 µM). Axons were

anterogradely labeled with CTB. Asterisks indicate the lesion site and arrows denote the axon sprouts beyond the lesion site. Scale bar = 100 µm. B. Quantitative analysis of axonal sprouting 50 and 100 µm beyond the lesion site after treatment of the lesion site with PBS/ Taxol or intravitreal injections of Taxol as described in A. Treatment effects: ***$p < 0.001$. C. Quantification of the longest axons per section of all the groups indicated in A. Treatment effects: ***$p < 0.001$.

3.8 Taxol treatment at the lesion site does not affect the intrinsic regenerative state of RGCs

Taxol application at the ON lesion site improved axon regeneration *in vivo* either alone or synergistically with LI. Hence, we examined whether Taxol directly or indirectly affected the intrinsic regenerative state of RGCs. Gelfoam soaked with a solution of PBS or Taxol (1 µM) was applied at the lesion site of the ON and LI was performed in half of the rats to activate the intrinsic regenerative state of RGCs. Dissociated mixed retinal cultures were prepared 5 d after surgery and incubated for 1 d in culture to determine the spontaneous neurite outgrowth of RGCs as described before (Lorber et al., 2005; Muller et al., 2007; Leibinger et al., 2009; Muller et al., 2009). Consistent with earlier studies, neurite length was significantly increased after LI compared to ONC alone. Taxol treatment at the ON lesion site with or without additional LI did not notably alter neurite outgrowth of RGCs compared to the correspondingly treated PBS groups (Fig. 22 A, B). This indicates that local application of Taxol at the ON lesion site does not affect the intrinsic regenerative state of RGCs.

A

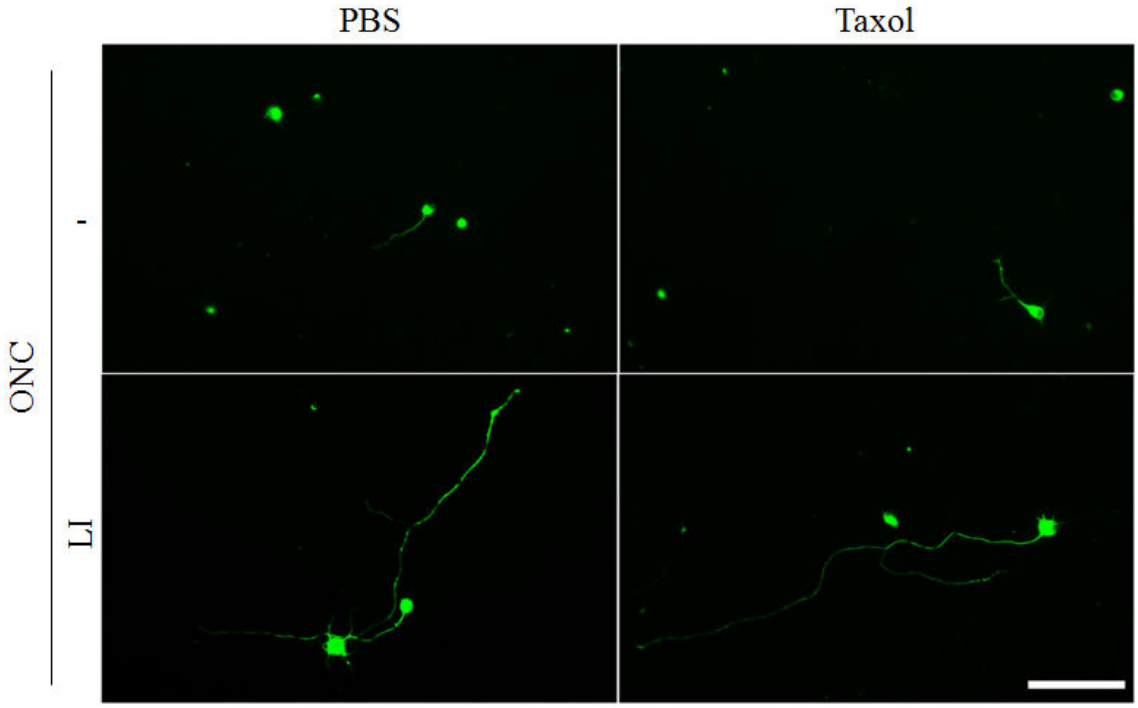

B

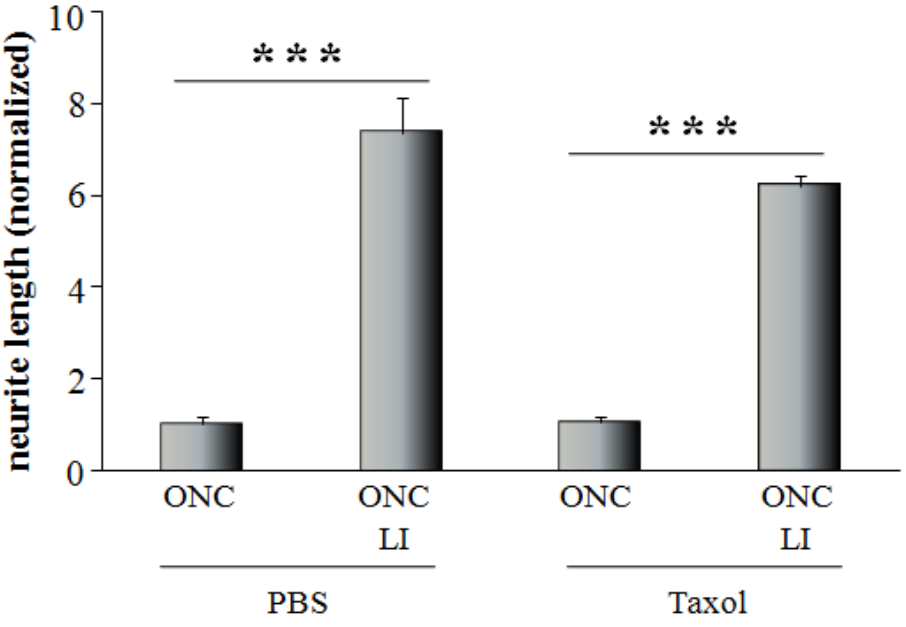

Fig. 22. Taxol does not affect the intrinsic regenerative state of RGCs. A. βIII-tubulin positive RGCs with regenerated neurites after 1 d in culture from mixed retinal cultures of rats that had received ONC/LI and the lesion site treated with either gelfoam soaked in a

solution of Taxol (1 µM) or PBS for 5 d. Treatment effects: ***p < 0.001. Scale bar = 50 µm. B. Quantification of spontaneous neurite outgrowth of RGCs from groups described in A. Treatment effects: ***p < 0.001.

Several genes (expressing cytoskeletal proteins, transcription as well as growth factors etc.,.) are activated after stimulation of the intrinsic regenerative state of RGCs by ONC+LI which are essential for improved axon regeneration (Fischer et al., 2004b). The higher expression levels of some of the genes observed after ONC+LI include - Growth associated protein-43 (GAP-43), cytokines - CNTF, LIF and signal transduction proteins like pSTAT3 (Muller et al., 2007; Leibinger et al., 2009). We analyzed the expression of CNTF and pSTAT3 from the retinal lysates of rats that had been subjected to ONC with or without LI and additionally treated the lesion site with Taxol (1 µM) or PBS for 5 d. We found that the expression levels of optic nerve regeneration associated genes - CNTF and pSTAT3 were not affected after Taxol treatment at the lesion site compared to the corresponding PBS controls (Fig. 23). These data confirm that Taxol facilitates axon regeneration without influencing the intrinsic regenerative state of RGCs.

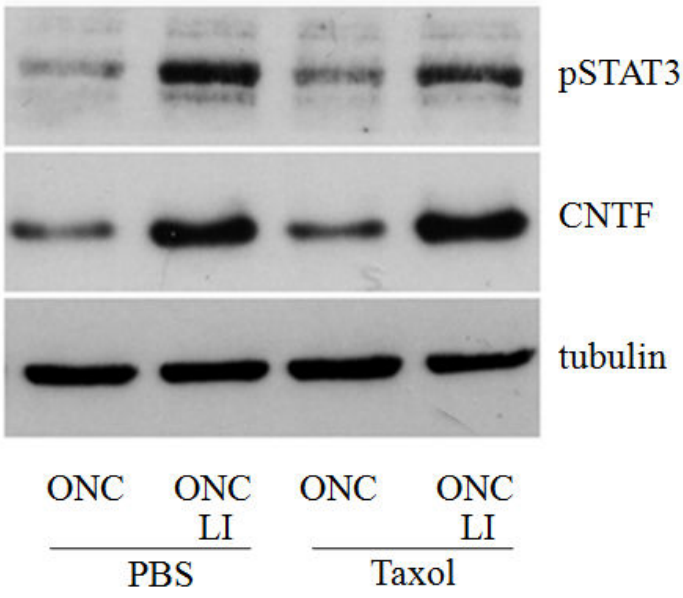

Fig. 23. Taxol does not affect the expression of genes necessary for the stimulation of intrinsic regenerative state of RGCs. Western blot analysis of retinal lysates obtained from rats that received ONC/LI and the lesion site treated with either gelfoam soaked in a solution of Taxol (1 µM) or PBS for 5 d. CNTF and pSTAT3 were probed with specific antibodies and tubulin served as a loading control.

3.9 Taxol affects the migration of peripheral macrophages at the lesion site

Macrophages that infiltrate the CNS lesion site due to the breakage of blood brain barrier have been described to adversely impact regenerating axons (Horn et al., 2008; Busch et al., 2009). Taxol reduces cell migration including that of the macrophages after atherosclerotic lesions (Ogasawara et al., 2001; Wiskirchen et al., 2004; Maranhao et al., 2008). This prompted us to investigate whether Taxol can reduce the migration of macrophages around the ON lesion site and thereby positively influence axon regeneration. We performed ONC on rats and treated the lesion site with either Gelfoam soaked in a solution of Taxol (1 μM) or PBS. CD68-positive cells (infiltrating macrophages/activated microglia) around the lesion site were quantified after both treatments. At 24 h as well as 72 h after surgery, the numbers of CD68-positive cells were strongly increased after PBS treatment compared to controls (ON lesion site 2 h after ONC). However, Taxol treatment strongly reduced the infiltrating macrophages and activated microglia around the lesion site 24 h after surgery. Moreover, 72 h after ONC, Taxol treatment significantly decreased the numbers of CD68-positive cells around the lesion site; eventhough the reduction observed was not as marked as compared to 24 h after Taxol treatment (Fig. 24 A, B). This suggests that Taxol affected the migration of macrophages/activated microglia around the ON lesion site and contributed to the enhanced axon regeneration.

A

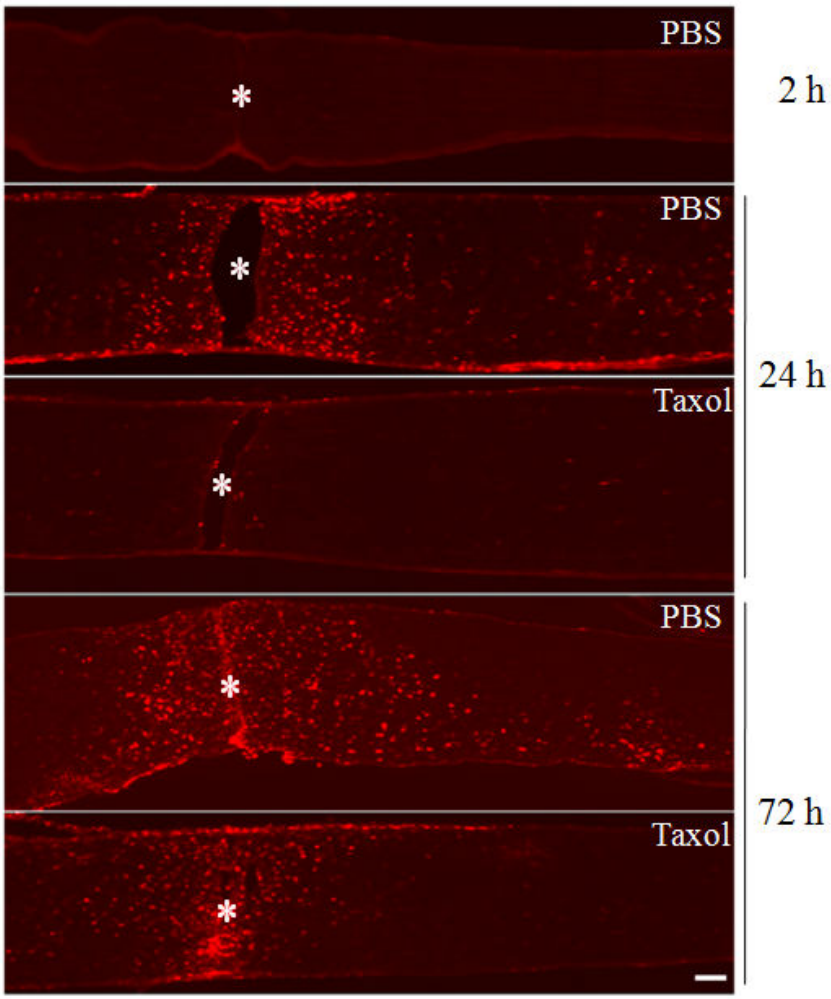

B

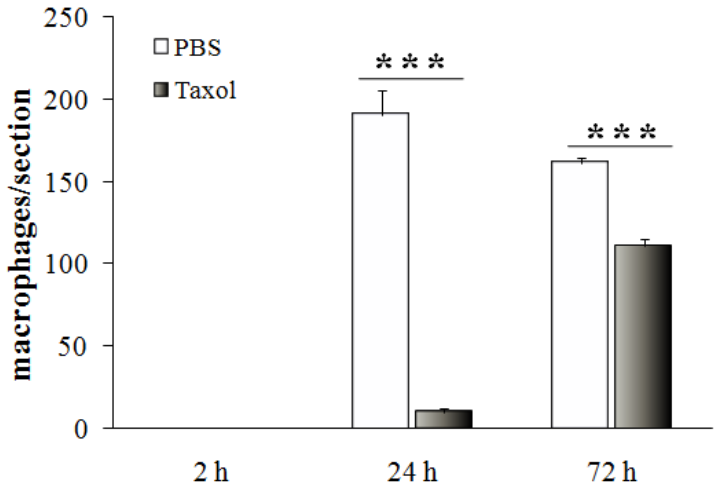

Fig. 24. Taxol delays infiltration of macrophages and activated microglia around the ON lesion site. A. Longitudinal sections of the ON stained for CD68/ED-1 positive cells -

2, 24 and 72 h after ONC and treatment of the lesion site with gelfoam soaked in a solution of PBS/Taxol (1 μM). Asterisks indicate the lesion site. Scale bar = 100 μm. B. Quantification of CD68/ED-1 positive cells from the optic nerve sections of groups described in A. Treatment effects: ***$p < 0.001$.

3.10 Taxol delays the astrocytic cellular responses around the lesion site

After ONC, astrocytic hypertrophy (characterized by high levels of GFAP expression, proliferation and branched morphology of astrocytes) occurs around the lesion site and contribute to glial scar formation (Fitch and Silver, 2008). Taxol has been previously known to reduce cell proliferation (Wiskirchen et al., 2004; Janardhanan et al., 2009). Hence, we examined whether local Taxol application around the lesion site might affect the astrocytic response to injury. ONC was performed on rats and the lesion site was treated with Gelfoam soaked in a solution of PBS or Taxol (1 μM) for 3 or 14 d. ON sections were then stained with GFAP to detect the astrocytic responses. We observed that 3 d after Taxol treatment, GFAP/astrocyte-free gap was markedly larger compared to PBS treated controls. However, 14 d after surgery, the lesion site was completely covered with GFAP positive cells (Fig. 25 A, B). This indicates that Taxol transiently delayed the astrocytic proliferation around the ON lesion site.

A

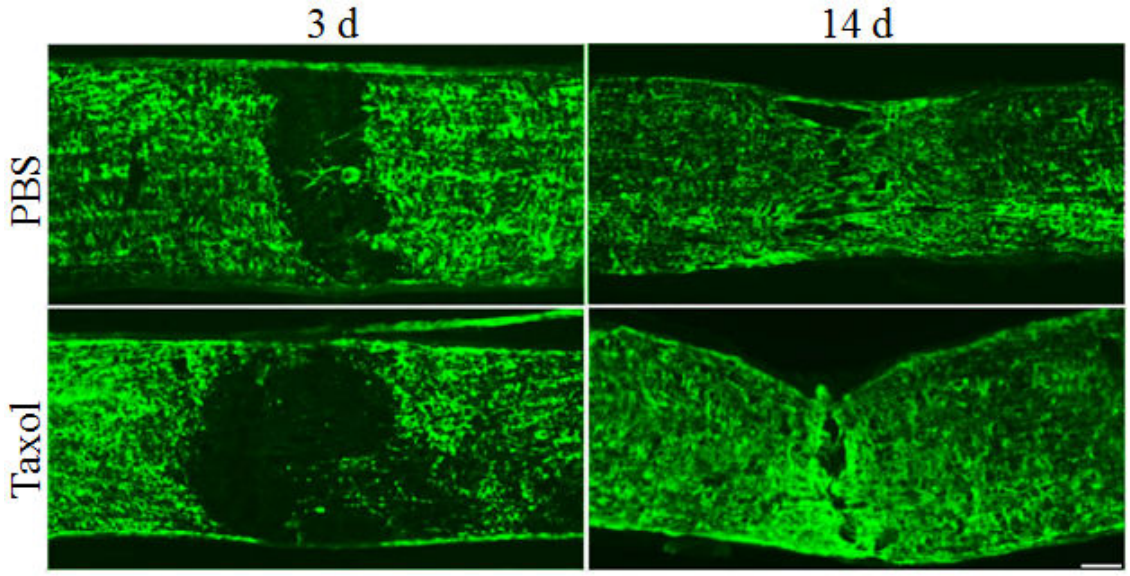

B

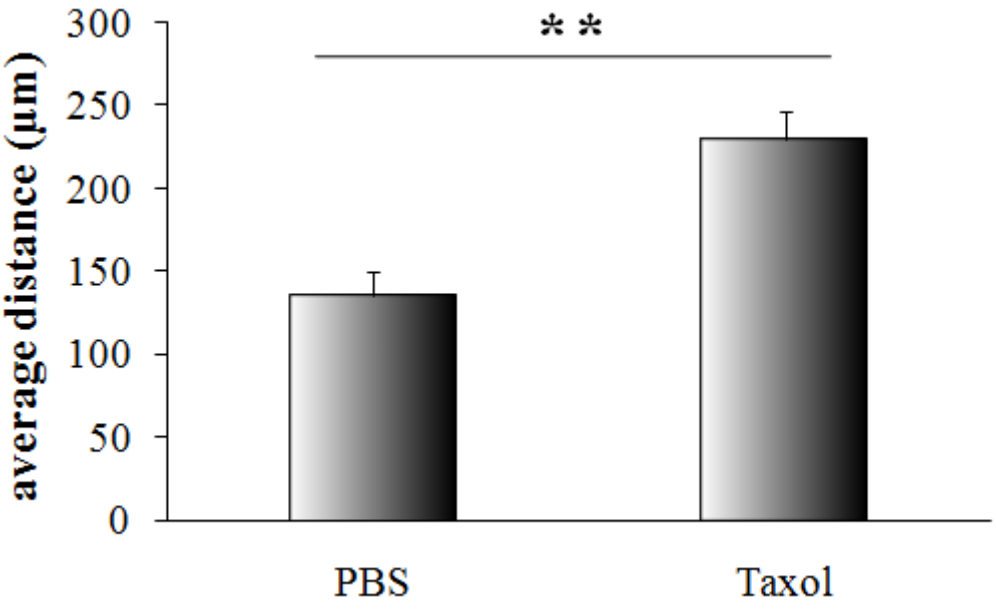

Fig. 25. Taxol decreases glial reactivity around the lesion site. A. Longitudinal sections of ON stained with GFAP - 3 and 14 d after ONC and treatment of the lesion site with gelfoam soaked in a solution of PBS/Taxol (1 µM). Scale bar = 100 µm. B. Quantification of the average length of the GFAP free area/gap around the lesion site 3 d after surgery. Treatment effects: ***$p < 0.01$.

3.11 Taxol delays the proliferation of primary astrocytes *in vitro*

To confirm the observation that Taxol treatment transiently delayed the proliferation of astrocytes around the ON lesion site, we prepared primary astrocyte cultures. [Note: The astrocyte cultures were a gift from Dr. Anke Witting, Department of Neurology, Universität Ulm]. After the astrocytes were confluent, we performed a scratch injury which resulted in a cell free gap of ~500 μm. We cultured the cells that were subjected to scratch injury either in the absence or presence of increasing concentrations of Taxol (3, 10, 50 and 100 nM). Untreated cells almost completely covered the astrocyte free gap 24 h after scratch injury, whereas Taxol treated cells displayed a reduction in the gap closure corresponding to the concentrations in which it is added to the medium. Taxol at a concentration of 3 nM slightly, but significantly delayed the formation of monolayer, whereas 100 nM concentration of Taxol resulted in a cell free gap similar to the size observed at the time of scratch injury (Fig. 26 A, B). These data confirm that Taxol only transiently delayed the proliferation of astrocytes and supported axon regeneration after ON injury *in vivo*.

A

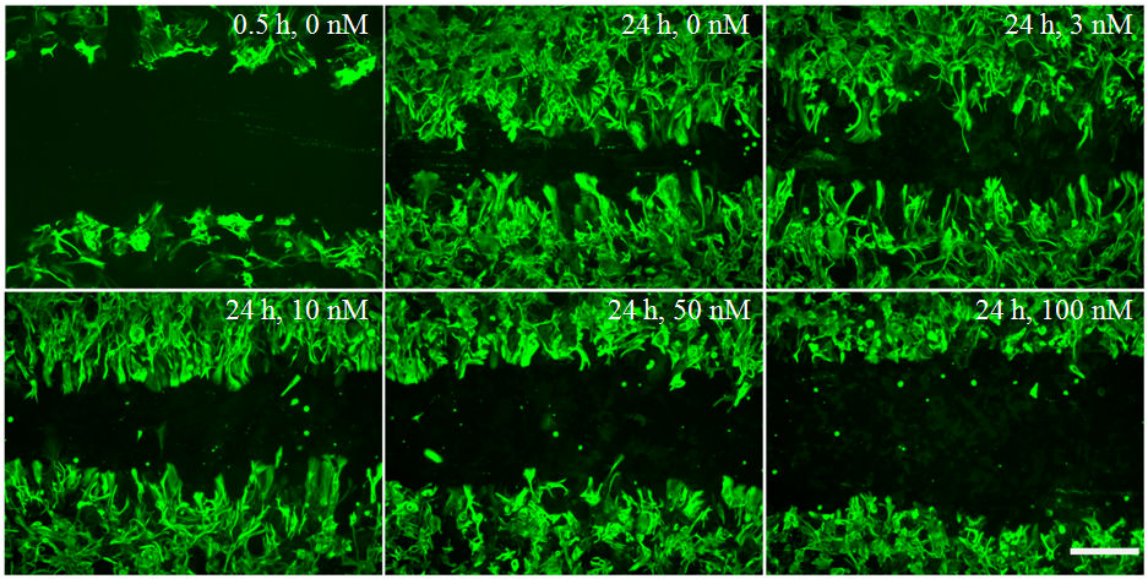

B

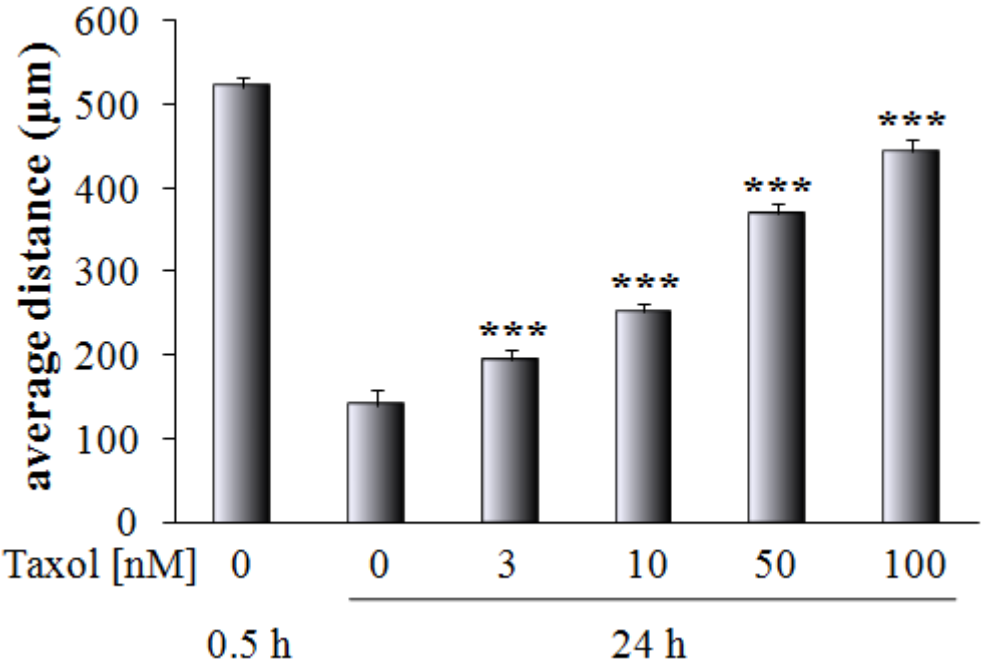

Fig. 26. Taxol also delays monolayer formation (gap closure) in primary astrocytes after scratch injury. A. GFAP stained primary astrocyte cultures after scratch injury and treatment with various concentrations of Taxol for 24 h as indicated. Scale bar = 200 µm. B. Quantification of the average width of the gap in the astrocyte monolayer 0.5 and 24 h after scratch injury. Treatment effects: ***$p < 0.001$.

3.12 Taxol reduces CSPG expression at the lesion site

CSPGs are expressed by proliferating astrocytes at the CNS lesion site, released into the extracellular matrix and contribute to the inhibitory responses toward axon regeneration (McKeon et al., 1995; Asher et al., 2001; Jones et al., 2003). Since, Taxol transiently delayed the proliferation of astrocytes we investigated whether Taxol also reduced the CSPG expression around the ON lesion site. We performed ONC and treated the lesion site with Gelfoam soaked in a solution of Taxol (1 μM) or PBS. At 2 h after injury (controls) no detectable CSPG staining could be found in PBS treated animals. In addition, no strong increase in CSPG levels could be observed 24 h after Taxol or PBS treatment. However, CSPG expression was strongly increased after 72 h in PBS treated groups and Taxol treated animals showed significant reduction in CSPG expression (Fig. 27 A, B).

A

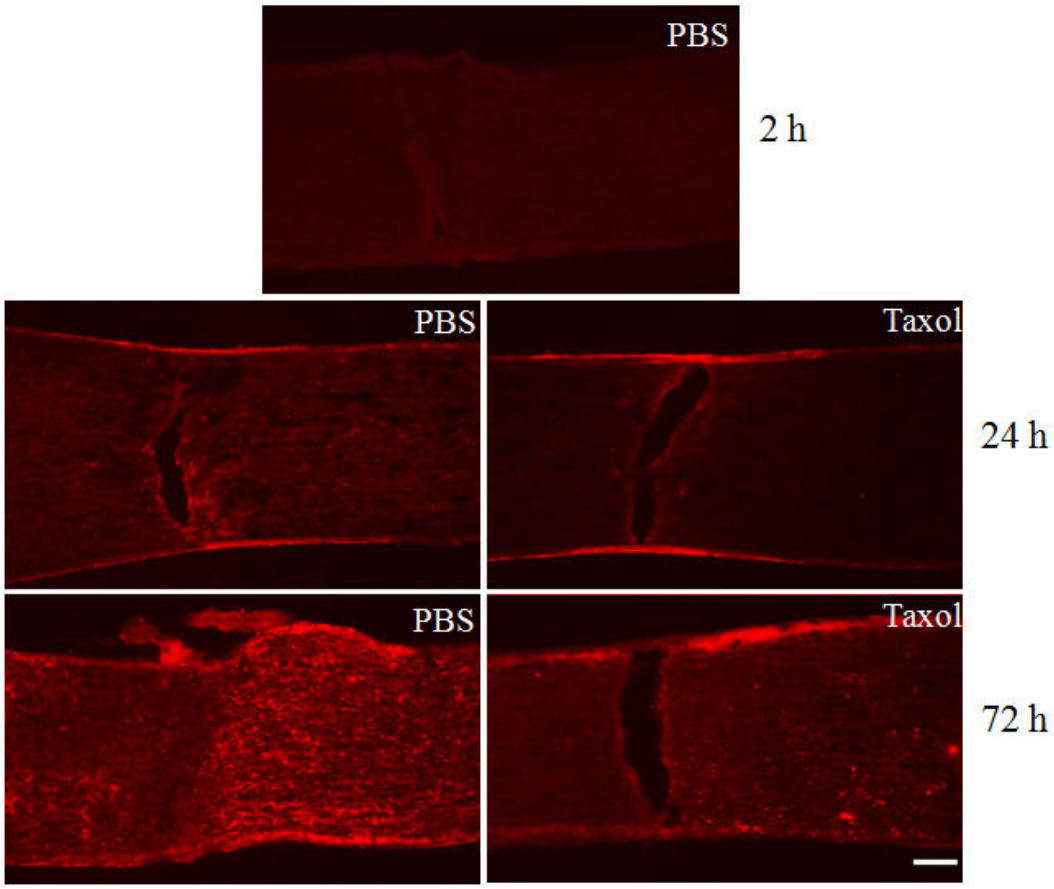

B

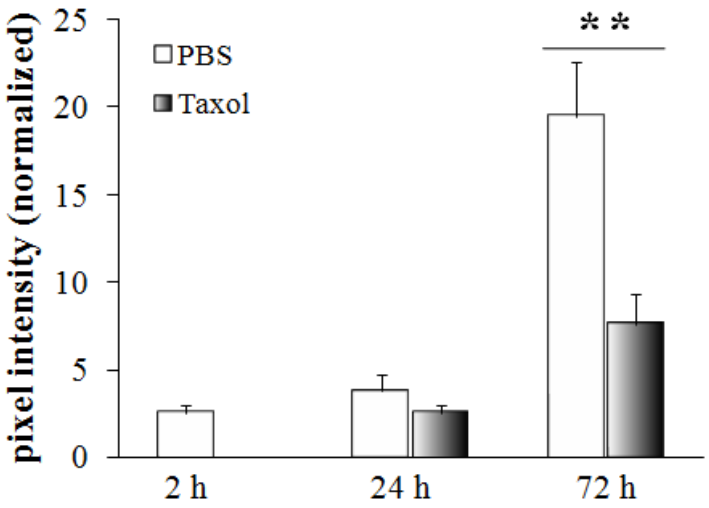

Fig. 27. Taxol reduces CSPG expression aroud the lesion site. A. Longitudinal sections of ON stained for CS-56 (CSPGs) - 2, 24 and 72 h after ONC and treatment of the lesion

site with gelfoam soaked in a solution of PBS/Taxol (1 µM). Scale bar = 100 µm. B. Quantification of pixel intensity (normalized to control optic nerve sections) of CSPG staining from equal area distal to the lesion site for groups described in A. Treatment effects: **$p < 0.01$.

The specificity of CSPG staining was confirmed through incubation of PBS treated ON sections with chondroitinase ABC enzyme which digests the sugar chains of CSPGs found at the lesion site. After treatment with the enzyme no detectable staining could be observed in the ON sections (Fig. 28). These data open the possibility that the delay in astrocytic proliferation and concomitant reduction in CSPG expression after Taxol treatment contributed to the enhanced axon regeneration after ON injury.

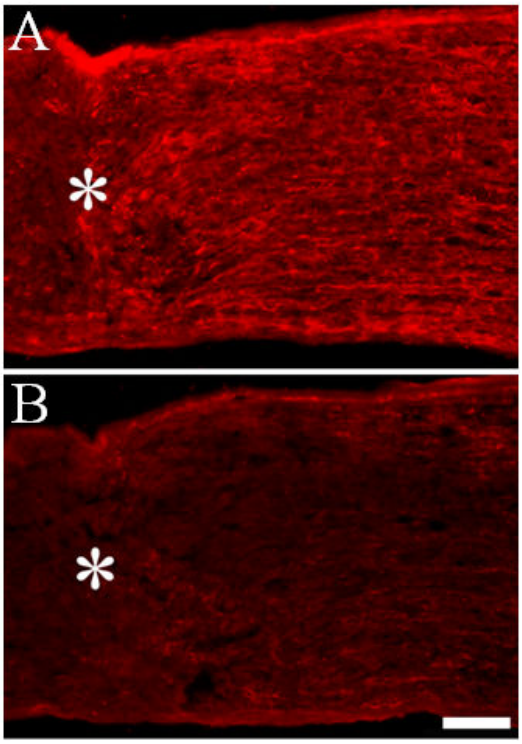

Fig. 28. CSPG staining specificity of CS-56 antibody. Longitudinal sections of optic nerve 3 d after optic nerve crush and treatment of the lesion site with gelfoam soaked PBS stained with CS-56 antibody. Asterisks indicate the lesion site. A. Strong staining of CSPG could be detected after treatment of the sections with digestion buffer alone. B. Adjacent sections treated with chondroitinase ABC in digestion buffer removed most of the CSPG molecules present at the lesion site. Scale bar = 100 µm.

4. Discussion

4.1 General Discussion

Major obstacles that limit axon regeneration after CNS injury are the inhibitory environment that prevails at the injury site in addition to the intrinsic inability of mature CNS neurons to regenerate axons (Silver and Miller, 2004; Yiu and He, 2006; Sun and He, 2010). As typical of CNS neurons, RGCs do not exhibit the propensity to regenerate axons after optic nerve injury (Benowitz and Yin, 2007; Benowitz and Yin, 2008; Berry et al., 2008). Significant levels of axon regeneration could be achieved after the stimulation of intrinsic regenerative state of RGCs through LI or intravitreal injections of lens crystallins, zymosan, Pam_3Cys (Fischer et al., 2000; Leon et al., 2000; Fischer et al., 2001; Lorber et al., 2005; Fischer et al., 2008; Hauk et al., 2009; Lorber et al., 2009). However, CNS myelin inhibitors including Nogo, MAG, OMgp and non-myelin inhibitors like CSPGs, tenascin, ephrin and semaphorin still hinders axon regeneration (Mukhopadhyay et al., 1994; GrandPre et al., 2000; Prinjha et al., 2000; Wang et al., 2002b; Filbin, 2003; Atwal et al., 2008; Llorens et al., 2011). Hence, implementation of combinatorial treatments that overcome the CNS inhibitory environment together with measures that activate the intrinsic regenerative state of neurons significantly enhances axon regeneration (Cui et al., 2003; Fischer et al., 2004b; Muller et al., 2007; Lingor et al., 2008; Ahmed et al., 2009). Strategies employed to overcome CNS inhibitory environment that includes the blockade of CNS inhibitory molecules *per se* or compromising their receptor activation enhances axon regeneration (Schnell and Schwab, 1990; Brosamle et al., 2000; GrandPre et al., 2002; Fischer et al., 2004a; Li et al., 2005). In addition, disruption of RhoA/ROCK pathway which mediates the downstream signaling of several inhibitory ligand-receptor complexes and ultimately affects cytoskeletal (actin and MT) organization/polymerization in the growth cone also promotes CNS axon regeneration (Lehmann et al., 1999; Fournier et al., 2003; Fischer et al., 2004b; Bertrand et al., 2005; Kubo et al., 2007). Conversely, in our current study we directly targeted MTs using Taxol and found that, a) MT stabilization by Taxol enhances neurite extension and is sufficient to overcome myelin and CSPGs inhibition in mature RGCs as well as PC12 cells *in vitro*, b) Taxol prevents myelin induced growth cone collapse of RGCs and PC12 cells, c) Taxol desensitizes growth cones toward inhibitory myelin without influencing RhoA activation, d) local application of Taxol at the ON injury site synergistically facilitates enhanced axon regeneration when combined with

LI which stimulates the intrinsic regenerative state of RGCs, e) Taxol treatment does not alter the intrinsic growth state of RGCs after ONC/LI, f) Taxol affects the components that contribute to the inhibitory glial scar formation – infiltrating macrophages/activated microglia, reactive astrocytes and expression of CSPGs.

4.2 Relevance of Taxol concentrations to improve axon regeneration

Our study indicates that only low concentrations of Taxol can enhance neurite outgrowth *in vitro* and regeneration of axons *in vivo*. We found that Taxol at a concentration of 3 nM significantly improves the neurite outgrowth of normal adult as well as intrinsic growth stimulated RGCs (Sengottuvel et al., 2011). However, Taxol at concentrations of 10 nM or 50 nM did not exert any positive effect or drastically reduces neurite outgrowth respectively. These results are consistent with previous studies which portray the importance of MT dynamics on axon growth. Taxol at higher concentrations permanently stabilizes the MTs, thereby affecting their dynamics and ultimately reduces neurite outgrowth of cortical neurons (Chuckowree and Vickers, 2003). In addition, disruption of MT dynamics adversely affects forward translocation of growth cone and axon growth (Tanaka et al., 1995). Treatment with MT destabilizing compound, nocodazole converts growth cones into retraction bulb like structures *in vivo* (as well as *in vitro*) and hinders regeneration of spinal cord axons (Erturk et al., 2007). In contrast, lower concentrations of Taxol increase the polymerization rate of MTs, without affecting their dynamics (Derry et al., 1995; Derry et al., 1997). Hence, as observed in our study, lower concentrations of Taxol enhance MT polymerization and significantly improves neurite outgrowth. To facilitate axon regeneration *in vivo* we used Taxol at higher concentrations than used in the *in vitro* studies. This anomaly could be explained by the fact that high-concentration gradients of a drug are necessary to permeate from gelfoam to reach effective concentrations in the injured ON tissue to promote axon regeneration. In addition, most of the drug might also diffuse in the intraorbital space and does not reach the lesioned ON. Regeneration of axons *in vivo* occurs at a broad concentration range of Taxol (1-1000 μM) which could be possibly due to the reasons described above to obtain effective Taxol concentrations at the lesion site. Importantly, animals treated with the lowest tested Taxol concentration in the study displayed maximal levels of axon regeneration. These data imply the significance of low concentrations of Taxol necessary to potentiate axon regeneration.

4.3 Modalities of Taxol mediated axon regeneration

Our study demonstrates that local Taxol treatment at the ON injury site does not affect LI induced intrinsic regenerative state stimulation as well as neuroprotection of RGCs. This could be ascertained from the results wherein the spontaneous neurite outgrowth of RGCs as well as retinal GAP-43 expression remain unaltered after local Taxol application (Sengottuvel et al., 2011). Moreover, the hallmarks of LI including STAT3 activation, endogenous retinal CNTF and LIF expression (Muller et al., 2007; Leibinger et al., 2009; Muller et al., 2009) which are necessary for the transformation of RGCs into a regenerative state remain unchanged after local Taxol treatment at the ON lesion site (Sengottuvel et al., 2011). A previous study on transgenic mice illustrates the important role of these cytokines for regenerative state stimulation as well as neuroprotection. Knock down of both CNTF and LIF leads to very limited axon regeneration and a significant reduction in RGC survival after LI compared to wild type animals (Leibinger et al., 2009). However, it is paramount to note that the significantly increased neurite outgrowth observed *in vitro* after combinatorial treatments either with CNTF or from intrinsic growth stimulated RGCs clearly denotes the synergistic influences of Taxol to enhance axon growth (Sengottuvel et al., 2011). The synergistic effects of Taxol could also be confirmed *in vivo* since ONC+LI together with local Taxol application at the lesion site markedly enhances axon regeneration. Another recent study had also reported that a combinatorial treatment which involves the stimulation of the intrinsic regenerative state of dorsal root ganglion neurons through peripheral nerve conditioning lesion together with local Taxol treatment at the lesion site significantly improves axon regeneration and functional recovery after spinal cord injury (Hellal et al., 2011). The results from our study also clarify that only local Taxol treatment at the injury site and not the intravitreal injections enhance axon regeneration. Taxol stabilizes the MTs and increases the polymerization rate without affecting the MT dynamics completely. This phenomenon could be confirmed from our study wherein the application of nocodazole, a drug which increases the catastrophe rate of MTs and affects MT polymerization drastically reduces the neurite outgrowth of RGCs (Sengottuvel et al., 2011). In addition, nocodazole application also adversely affects the enhanced neurite outgrowth observed after Taxol treatment (Sengottuvel et al., 2011). Hence, the key mechanism underlying the action of Taxol is MT stabilization at the regenerating axon tips and the resultant desensitization of growth cones toward inhibitory molecules. In addition, the delay in glial scar formation and macrophage infiltration also partially contributes to the improved axon regeneration.

4.4 Taxol desensitizes growth cone toward myelin and CSPGs inhibition

Myelin components at the lesion site of the ON activate RhoA/ROCK signaling pathway which leads to actin depolymerization, MT disassembly and ultimately reduces axon growth (Gallo and Letourneau, 2004; Mimura et al., 2006; Berry et al., 2008). It has also been reported that PTPσ receptor activation and RhoA/ROCK signaling mediates the inhibitory effects of CSPGs on axon growth (Monnier et al., 2003; Jain et al., 2004; Shen et al., 2009). A previous study had reported that the myelin component - MAG induces ROCK mediated phosphorylation of CRMP-2, down regulates MT assembly and inhibits axon extension (Mimura et al., 2006). In contrast, overexpression of CRMP-2 *per se* facilitates MT assembly/axon growth, and overexpression of non-phosphorylated forms of CRMP-2 compromises the MAG induced effects on MT disassembly (Inagaki et al., 2001; Mimura et al., 2006). Consistent with these studies on relevance of MT assembly to improve axon growth and overcome myelin inhibition, we demonstrate that MT stabilization by Taxol abrogates the inhibitory effects of myelin components/CSPGs on neurite outgrowth *in vitro* and on regenerating axon tips *in vivo*. A previous study had also described that Taxol could overcome neurite outgrowth inhibition by myelin on neonatal cerebellar granule neurons *in vitro*, whereas they did not observe any improved neurite outgrowth (Erturk et al., 2007). This is due to the concentration of Taxol (10 nM) used in their study, which did not lead to increased neurite outgrowth in our experiments as well. However, in another recent study the same group obtained enhanced neurite outgrowth on both normal and inhibitory substrates after Taxol treatment at low nanomolar concentrations [1 or 5 nM] (Hellal et al., 2011). Hence, results from different neuronal cell types clearly denote the consistent effects and importance of low nanomolar Taxol concentrations to improve neurite outgrowth and overcome myelin/CSPGs inhibition. We also identified that Taxol overcomes myelin inhibition without influencing RhoA activation. This suggests that Taxol acts downstream of RhoA to promote axon growth most probably through MT stabilization. Moreover, consistent with our results, another recent study also found that Taxol averts the growth cone collapse/shrinkage that occurs in the presence of myelin (Hellal et al., 2011). The disinhibitory effects of Taxol could be as a result of disentanglement of the MT and actin interactions in growth cone thereby making MT polymerization independent of actin polymerization which allows unhindered MT growth into filopodia and stabilizing the overall growth cone structure. Another possible explanation stems from the findings which report that the enhanced MT polymerization and dynamics also promotes actin polymerization through activation of Rac-1 (Waterman-

Storer et al., 1999; Grabham et al., 2003). Eventhough, a detailed mechanism underlying the beneficial effects of Taxol could not be deciphered in our study, it is plausible that disinhibition toward myelin and CSPG molecules contributes to the enhanced axon regeneration observed *in vivo*.

4.5 Taxol impedes glial scar formation

Glial scar formation after CNS injury elicited through the activation of microglia and infiltration of macrophages from the blood stream together with the hypertrophic astrocytic response at the injury site acts as a significant barrier to initial axon regeneration (Fitch and Silver, 1997; Silver and Miller, 2004; Fitch and Silver, 2008). Reactive astrocytes are characterized by increased GFAP immunoreactivity, proliferation as well as branched morphology and releases inhibitory molecules (CSPGs, tenascin, ephrin, semaphorin) into extracellular matrix which prevents neurite outgrowth/axon regeneration *in vitro*/*in vivo* respectively (McKeon et al., 1991; Lefrancois et al., 1997). We observed that local Taxol treatment markedly widened the GFAP free area around the lesion site 3 d after ON injury. Nevertheless, GFAP-positive cells completely overhaul the lesion site 14 d after injury. This suggests that a transient delay in astrocytic response around the injury site after Taxol application might have allowed the regenerating axons to cross the inhibitory environment. It should be also noted that the reactive astrocytes have certain degree of beneficial effects by protecting the tissue from secondary damage after injury. It also helps to repair the breakage in blood brain barrier (BBB) which is essential for regeneration of neurons and physiological functions (Faulkner et al., 2004). Consistent with our *in vivo* results, a delay in the formation of monolayer could be observed after treatment of Taxol to the primary astrocytes in culture after scratch injury. Moreover, another recent study also found that Taxol treatment delays the migration of meningeal fibroblasts in culture (Hellal et al., 2011). These data indicate that Taxol affects various cell types that are involved in glial scar formation. The integrity of the ON lesion site tissue provides an interesting observation, since Taxol treated nerves were relatively tender when compared to PBS treated nerves. This could be due to the influence of Taxol on glial scar formation, for instance delaying the astrocyte proliferation as well as meningeal fibroblast migration. CSPGs derived from reactive astrocytes have been reported to exert negative influence on axon regeneration after ON and spinal cord injury (Silver and Miller, 2004). Our study also demonstrates that local Taxol treatment strongly down regulates the expression of CSPGs around the lesion site. This might be possibly due to the delay in astrocyte proliferation

after ON injury, since astrocytes are one of the major sources of CSPGs expression and their release into extracellular matrix at the lesion site (Asher et al., 2000). To lend further support to this hypothesis, a previous study had shown that the treatment of cell cycle inhibitor olomoucine to the spinal cord injury site significantly reduces the expression of CSPGs (Tian et al., 2006). Taxol treatment of primary astrocytes also compromises the TGFβ signaling involved in glial scar formation, providing another mechanism for the reduced CSPG expression (Hellal et al., 2011). MT destabilization that occurs after CNS injury augments TGFβ signaling through phosphorylation and translocation of MT bound Smads from cytoplasm into the nucleus (Dong et al., 2000). However, MT stabilization by Taxol affects the translocation of Smads to the nucleus; and thereby inhibits TGFβ signaling and the resultant increase in CSPG expression (Hellal et al., 2011). In addition to the proliferating astrocytes, infiltrating macrophages are described to be the source of TGFβ around the CNS lesion site (Buss et al., 2008). Since we also observed that Taxol treatment delays the macrophage infiltration after ON injury, this might have reduced the TGFβ levels at the lesion site.

Activated macrophages have been shown to interact with dystrophic growth cones and induce axon retraction resulting in the failure of regeneration after spinal cord injury. Moreover, depletion of macrophages from the lesion site prevents axon retraction significantly (Horn et al., 2008). We found that Taxol treatment at the ON lesion site drastically reduces the infiltration of macrophages 1 d after ONC and significant reduction in numbers of macrophages could be observed even after 3 d. This is consistent with previous studies which report that Taxol treatment decrease macrophage infiltration and cell migration (Ogasawara et al., 2001; Wiskirchen et al., 2004; Maranhao et al., 2008). These data indicate that the delayed macrophage infiltration observed after Taxol treatment around the lesion site enhances axon regeneration. However, the role of macrophages at the lesion site has grown complex considering the recent reports which described the presence different subsets of macrophages – M1 and M2. M1 macrophages are the classically activated inflammatory macrophages which deleteriously affect axon regeneration while M2 macrophages enhance regeneration of axons (Kigerl et al., 2009). Hence, the delay in macrophage infiltration through Taxol treatment might have even limited the beneficial effects of macrophages, but was overcompensated by other mechanisms (MT stabilization, desensitization toward myelin and CSPGs inhibitory molecules, decreased reactive astrocytic response and CSPG expression) described before. Hence, these results clearly

suggest that Taxol impedes the inhibitory environment around the CNS injury site and promotes axon regeneration.

In conclusion, the results of our current study illustrates that Taxol application at the lesion site of the ON enhances axon regeneration in combination with treatments that stimulate the intrinsic regenerative state of RGCs. Taxol, an FDA approved drug is currently being used to treat cancer patients, hence it offers great scope to be applied for the treatment of patients suffering from various CNS injures. A previous study had reported that the systemic treatment of Taxol after spinal cord injury improves functional recovery, eventhough the mechanisms underlying the beneficial effects were not clearly outlined (Perez-Espejo et al., 1996). Moreover, another recent study had shown that a combinatorial treatment of Taxol and intrinsic regenerative stimulation after spinal cord injury supports functional recovery (Hellal et al., 2011). Taxol dosages applied to promote axon regeneration must be carefully screened to avoid any potential detrimental effects, since we had observed in our study that only low concentrations of Taxol are beneficial. The effective drug concentrations at low nanomolar range are promising since it alleviates any adverse effects associated with toxicity. Topical application of Taxol at the injury site of ON or spinal cord are extremely challenging. Hence, administration of Taxol through common modalities of drug delivery (e.g. intravenous injections) must be considered to provide required concentrations of Taxol at the site of CNS injury. Long-term application of Taxol could also be investigated to enhance the axon regeneration of CNS. It is paramount to note that the beneficial effects of LI to promote the intrinsic regenerative state and survival of RGCs could be sustained only for a limited duration of 2-3 weeks. After this time point a dramatic decline occurs in both RGC survival as well as regeneration of axons (Leon et al., 2000). However, this problem could be circumvented since LI can also be mimicked through intravitreal injections of Pam_3Cys (Hauk et al., 2010) or through continuous expression of CNTF/LIF (Leaver et al., 2006a; Leaver et al., 2006b), [unpublished results] and further potentiated by co-application of cAMP (Cui et al., 2003; Park et al., 2004; Muller et al., 2007). Hence, intrinsic regenerative state stimulation could be combined with Taxol application to achieve potent axon regeneration. Therefore strategies that integrate MT stabilization with various growth promoting paradigms can help to restore axon regeneration after CNS injuries.

5. Summary

Traumatic injuries to the CNS lead to several debilitating conditions including paralysis and irreversible blindness. Damaged CNS axons fail to regenerate owing to the inhibitory milieu present at the injury site - contributed by myelin derived from oligodendrocytes that ensheath axons and CSPGs synthesized, deposited into the extracellular matrix by reactive astrocytes. Additional contributors to the impaired axonal regeneration are the inflammatory macrophages/activated microglia dispersed around the injury site. Myelin and CSPG inhibitors activate RhoA/ROCK signaling cascade at the neuronal growth cones leading to actin filament depolymerization and microtubule destabilization. Most of the strategies to overcome inhibitory components employ disruption of ligands, their corresponding receptors or downstream signaling pathways. However, sufficient axon regeneration could not be achieved through these approaches since CNS neurons also lack the intrinsic growth capacity to regenerate axons after injury. Hence, combinatorial treatments aimed at compromising inhibitory components together with stimulation of the neuronal intrinsic growth state are pursued to progress toward attaining functional axon regeneration.

Taxol, a well known anti-cancer compound, at low nanomolar concentrations, can promote polymerization of MTs without adversely affecting MT dynamics. Hence in our study, we utilized this phenomenon of Taxol to enhance as well as overcome the inhibitory components mediated negative influence on axonal regeneration. We have shown that in dissociated mixed adult rat retinal cell cultures, Taxol treatment enhances the neurite outgrowth of RGCs only at low nanomolar concentrations. However, at high concentrations, Taxol drastically reduces neurite outgrowth, possibly due to hyper-stabilization of MTs. Taxol also enhances neurite outgrowth of PC12 cells which denotes that the beneficial effects on neurite extension were not restricted to specific neuronal cell types. As described in previous studies, CNTF treatment markedly improves neurite outgrowth of RGCs in dissociated mixed retinal cell cultures. Importantly, Taxol acts synergistically with CNTF to significantly promote neurite outgrowth. Taxol mediated microtubule stabilization assists RGCs to overcome both CNS myelin and CSPGs mediated inhibition of neurite outgrowth. Taxol also allays the inhibitory effect of CNS myelin on neurite outgrowth of PC12 cells. Moreover, Taxol prevents CNS myelin induced growth cone collapse/shrinkage in both RGCs and PC12 cells. The disinhibitory effects of

Taxol toward myelin are independent of RhoA activation as confirmed through co-immunoprecipitation assay. This suggests that Taxol acts downstream of common inhibitory pathways.

In rat ON model system which is widely used to study regenerative failure of CNS axons, local application of Taxol at the lesion site after ONC alone markedly improves regeneration of axons. Combinatorial treatment of Taxol and LI after ONC significantly enhances axon regeneration. In addition, only a local Taxol treatment at the lesion site facilitates early axonal sprouting, since intravitreal Taxol injections did not improve axon regeneration. After ONC+LI, local Taxol application at the lesion site neither alters the intrinsic regenerative state of RGCs and their survival as studied through dissociated mixed retinal cell cultures nor the cellular responses in the retina as determined through western blot assay all of which are necessary to achieve enhanced regeneration of axons. These data suggest that Taxol exerts its beneficial effects most probably through MT stabilization by specifically acting at the regenerating axon tips. Indirect effects of Taxol by delaying the activation/infiltration of microglia/macrophages, astrocytic scar formation and reduction in CSPG expression also contributes to improved axon regeneration. Thus, MT stabilization offers an alternate novel therapeutic strategy in combination with intrinsic regenerative state stimulation approaches to potently improve axon regeneration in CNS.

6. Reference(s):

Aguayo AJ, Rasminsky M, Bray GM, Carbonetto S, McKerracher L, Villegas-Perez MP, Vidal-Sanz M, Carter DA (1991) Degenerative and regenerative responses of injured neurons in the central nervous system of adult mammals. Philos Trans R Soc Lond B Biol Sci 331:337-343.

Ahmed Z, Berry M, Logan A (2009) ROCK inhibition promotes adult retinal ganglion cell neurite outgrowth only in the presence of growth promoting factors. Mol Cell Neurosci 42:128-133.

Ahmed Z, Dent RG, Suggate EL, Barrett LB, Seabright RJ, Berry M, Logan A (2005) Disinhibition of neurotrophin-induced dorsal root ganglion cell neurite outgrowth on CNS myelin by siRNA-mediated knockdown of NgR, p75NTR and Rho-A. Mol Cell Neurosci 28:509-523.

Akassoglou K, Yu WM, Akpinar P, Strickland S (2002) Fibrin inhibits peripheral nerve remyelination by regulating Schwann cell differentiation. Neuron 33:861-875.

Asher RA, Morgenstern DA, Moon LD, Fawcett JW (2001) Chondroitin sulphate proteoglycans: inhibitory components of the glial scar. Prog Brain Res 132:611-619.

Asher RA, Morgenstern DA, Fidler PS, Adcock KH, Oohira A, Braistead JE, Levine JM, Margolis RU, Rogers JH, Fawcett JW (2000) Neurocan is upregulated in injured brain and in cytokine-treated astrocytes. J Neurosci 20:2427-2438.

Atwal JK, Pinkston-Gosse J, Syken J, Stawicki S, Wu Y, Shatz C, Tessier-Lavigne M (2008) PirB is a functional receptor for myelin inhibitors of axonal regeneration. Science 322:967-970.

Bandtlow CE, Schmidt MF, Hassinger TD, Schwab ME, Kater SB (1993) Role of intracellular calcium in NI-35-evoked collapse of neuronal growth cones. Science 259:80-83.

Barres BA, Jacobson MD, Schmid R, Sendtner M, Raff MC (1993) Does oligodendrocyte survival depend on axons? Curr Biol 3:489-497.

Barron KD (1995) The microglial cell. A historical review. J Neurol Sci 134 Suppl:57-68.

Bauer S, Kerr BJ, Patterson PH (2007) The neuropoietic cytokine family in development, plasticity, disease and injury. Nat Rev Neurosci 8:221-232.

Benowitz L, Yin Y (2008) Rewiring the injured CNS: lessons from the optic nerve. Exp Neurol 209:389-398.

Benowitz LI, Yin Y (2007) Combinatorial treatments for promoting axon regeneration in the CNS: strategies for overcoming inhibitory signals and activating neurons' intrinsic growth state. Dev Neurobiol 67:1148-1165.

Berkelaar M, Clarke DB, Wang YC, Bray GM, Aguayo AJ (1994) Axotomy results in delayed death and apoptosis of retinal ganglion cells in adult rats. J Neurosci 14:4368-4374.

Berry M, Ahmed Z, Lorber B, Douglas M, Logan A (2008) Regeneration of axons in the visual system. Restor Neurol Neurosci 26:147-174.

Bertrand J, Winton MJ, Rodriguez-Hernandez N, Campenot RB, McKerracher L (2005) Application of Rho antagonist to neuronal cell bodies promotes neurite growth in compartmented cultures and regeneration of retinal ganglion cell axons in the optic nerve of adult rats. J Neurosci 25:1113-1121.

Bradbury EJ, Moon LD, Popat RJ, King VR, Bennett GS, Patel PN, Fawcett JW, McMahon SB (2002) Chondroitinase ABC promotes functional recovery after spinal cord injury. Nature 416:636-640.

Bradke F, Dotti CG (1997) Neuronal polarity: vectorial cytoplasmic flow precedes axon formation. Neuron 19:1175-1186.

Brosamle C, Huber AB, Fiedler M, Skerra A, Schwab ME (2000) Regeneration of lesioned corticospinal tract fibers in the adult rat induced by a recombinant, humanized IN-1 antibody fragment. J Neurosci 20:8061-8068.

Buck KB, Zheng JQ (2002) Growth cone turning induced by direct local modification of microtubule dynamics. J Neurosci 22:9358-9367.

Busch SA, Horn KP, Silver DJ, Silver J (2009) Overcoming macrophage-mediated axonal dieback following CNS injury. J Neurosci 29:9967-9976.

Buss A, Pech K, Kakulas BA, Martin D, Schoenen J, Noth J, Brook GA (2008) TGF-beta1 and TGF-beta2 expression after traumatic human spinal cord injury. Spinal Cord 46:364-371.

Cai D, Qiu J, Cao Z, McAtee M, Bregman BS, Filbin MT (2001) Neuronal cyclic AMP controls the developmental loss in ability of axons to regenerate. J Neurosci 21:4731-4739.

Challacombe JF, Snow DM, Letourneau PC (1997) Dynamic microtubule ends are required for growth cone turning to avoid an inhibitory guidance cue. J Neurosci 17:3085-3095.

Chen MS, Huber AB, van der Haar ME, Frank M, Schnell L, Spillmann AA, Christ F, Schwab ME (2000) Nogo-A is a myelin-associated neurite outgrowth inhibitor and

an antigen for monoclonal antibody IN-1. Nature 403:434-439.

Chen ZL, Yu WM, Strickland S (2007) Peripheral regeneration. Annu Rev Neurosci 30:209-233.

Chuckowree JA, Vickers JC (2003) Cytoskeletal and morphological alterations underlying axonal sprouting after localized transection of cortical neuron axons in vitro. J Neurosci 23:3715-3725.

Collins BE, Yang LJ, Mukhopadhyay G, Filbin MT, Kiso M, Hasegawa A, Schnaar RL (1997) Sialic acid specificity of myelin-associated glycoprotein binding. J Biol Chem 272:1248-1255.

Conde C, Caceres A (2009) Microtubule assembly, organization and dynamics in axons and dendrites. Nat Rev Neurosci 10:319-332.

Cui Q, Benowitz L, Yin Y (2008) Does CNTF mediate the effect of intraocular inflammation on optic nerve regeneration? Brain 131:e96; author reply e97.

Cui Q, Yin Y, Benowitz LI (2009) The role of macrophages in optic nerve regeneration. Neuroscience 158:1039-1048.

Cui Q, Yip HK, Zhao RC, So KF, Harvey AR (2003) Intraocular elevation of cyclic AMP potentiates ciliary neurotrophic factor-induced regeneration of adult rat retinal ganglion cell axons. Mol Cell Neurosci 22:49-61.

David S, Aguayo AJ (1981) Axonal elongation into peripheral nervous system "bridges" after central nervous system injury in adult rats. Science 214:931-933.

Davis S, Aldrich TH, Stahl N, Pan L, Taga T, Kishimoto T, Ip NY, Yancopoulos GD (1993) LIFR beta and gp130 as heterodimerizing signal transducers of the tripartite CNTF receptor. Science 260:1805-1808.

DeBellard ME, Tang S, Mukhopadhyay G, Shen YJ, Filbin MT (1996) Myelin-associated glycoprotein inhibits axonal regeneration from a variety of neurons via interaction with a sialoglycoprotein. Mol Cell Neurosci 7:89-101.

Dergham P, Ellezam B, Essagian C, Avedissian H, Lubell WD, McKerracher L (2002) Rho signaling pathway targeted to promote spinal cord repair. J Neurosci 22:6570-6577.

Derry WB, Wilson L, Jordan MA (1995) Substoichiometric binding of taxol suppresses microtubule dynamics. Biochemistry 34:2203-2211.

Derry WB, Wilson L, Khan IA, Luduena RF, Jordan MA (1997) Taxol differentially modulates the dynamics of microtubules assembled from unfractionated and purified beta-tubulin isotypes. Biochemistry 36:3554-3562.

DiProspero NA, Meiners S, Geller HM (1997) Inflammatory cytokines interact to modulate extracellular matrix and astrocytic support of neurite outgrowth. Exp

Neurol 148:628-639.

Dong C, Li Z, Alvarez R, Jr., Feng XH, Goldschmidt-Clermont PJ (2000) Microtubule binding to Smads may regulate TGF beta activity. Mol Cell 5:27-34.

Erturk A, Hellal F, Enes J, Bradke F (2007) Disorganized microtubules underlie the formation of retraction bulbs and the failure of axonal regeneration. J Neurosci 27:9169-9180.

Faulkner JR, Herrmann JE, Woo MJ, Tansey KE, Doan NB, Sofroniew MV (2004) Reactive astrocytes protect tissue and preserve function after spinal cord injury. J Neurosci 24:2143-2155.

Fawcett JW, Keynes RJ (1990) Peripheral nerve regeneration. Annu Rev Neurosci 13:43-60.

Fernandez-Valle C, Bunge RP, Bunge MB (1995) Schwann cells degrade myelin and proliferate in the absence of macrophages: evidence from in vitro studies of Wallerian degeneration. J Neurocytol 24:667-679.

Filbin MT (2003) Myelin-associated inhibitors of axonal regeneration in the adult mammalian CNS. Nat Rev Neurosci 4:703-713.

Fischer D (2008) CNTF, a key factor mediating the beneficial effects of inflammatory reactions in the eye. Brain.

Fischer D (2010) What are the principal mediators of optic nerve regeneration after inflammatory stimulation in the eye? Proc Natl Acad Sci U S A 107:E8.

Fischer D, Pavlidis M, Thanos S (2000) Cataractogenic lens injury prevents traumatic ganglion cell death and promotes axonal regeneration both in vivo and in culture. Invest Ophthalmol Vis Sci 41:3943-3954.

Fischer D, Heiduschka P, Thanos S (2001) Lens-injury-stimulated axonal regeneration throughout the optic pathway of adult rats. Exp Neurol 172:257-272.

Fischer D, He Z, Benowitz LI (2004a) Counteracting the Nogo receptor enhances optic nerve regeneration if retinal ganglion cells are in an active growth state. J Neurosci 24:1646-1651.

Fischer D, Petkova V, Thanos S, Benowitz LI (2004b) Switching mature retinal ganglion cells to a robust growth state in vivo: gene expression and synergy with RhoA inactivation. J Neurosci 24:8726-8740.

Fischer D, Hauk TG, Muller A, Thanos S (2008) Crystallins of the beta/gamma-superfamily mimic the effects of lens injury and promote axon regeneration. Mol Cell Neurosci 37:471-479.

Fischer P, Lehmann U, Sobota RM, Schmitz J, Niemand C, Linnemann S, Haan S,

Behrmann I, Yoshimura A, Johnston JA, Muller-Newen G, Heinrich PC, Schaper F (2004c) The role of the inhibitors of interleukin-6 signal transduction SHP2 and SOCS3 for desensitization of interleukin-6 signalling. Biochem J 378:449-460.

Fisher D, Xing B, Dill J, Li H, Hoang HH, Zhao Z, Yang XL, Bachoo R, Cannon S, Longo FM, Sheng M, Silver J, Li S (2011) Leukocyte common antigen-related phosphatase is a functional receptor for chondroitin sulfate proteoglycan axon growth inhibitors. J Neurosci 31:14051-14066.

Fitch MT, Silver J (1997) Activated macrophages and the blood-brain barrier: inflammation after CNS injury leads to increases in putative inhibitory molecules. Exp Neurol 148:587-603.

Fitch MT, Silver J (2008) CNS injury, glial scars, and inflammation: Inhibitory extracellular matrices and regeneration failure. Exp Neurol 209:294-301.

Fitch MT, Doller C, Combs CK, Landreth GE, Silver J (1999) Cellular and molecular mechanisms of glial scarring and progressive cavitation: in vivo and in vitro analysis of inflammation-induced secondary injury after CNS trauma. J Neurosci 19:8182-8198.

Fournier AE, McKerracher L (1997) Expression of specific tubulin isotypes increases during regeneration of injured CNS neurons, but not after the application of brain-derived neurotrophic factor (BDNF). J Neurosci 17:4623-4632.

Fournier AE, GrandPre T, Strittmatter SM (2001) Identification of a receptor mediating Nogo-66 inhibition of axonal regeneration. Nature 409:341-346.

Fournier AE, Takizawa BT, Strittmatter SM (2003) Rho kinase inhibition enhances axonal regeneration in the injured CNS. J Neurosci 23:1416-1423.

Fournier AE, Gould GC, Liu BP, Strittmatter SM (2002) Truncated soluble Nogo receptor binds Nogo-66 and blocks inhibition of axon growth by myelin. J Neurosci 22:8876-8883.

Freund P, Schmidlin E, Wannier T, Bloch J, Mir A, Schwab ME, Rouiller EM (2006) Nogo-A-specific antibody treatment enhances sprouting and functional recovery after cervical lesion in adult primates. Nat Med 12:790-792.

Gallo G, Letourneau PC (2004) Regulation of growth cone actin filaments by guidance cues. J Neurobiol 58:92-102.

Garcia-Valenzuela E, Gorczyca W, Darzynkiewicz Z, Sharma SC (1994) Apoptosis in adult retinal ganglion cells after axotomy. J Neurobiol 25:431-438.

Geraldo S, Gordon-Weeks PR (2009) Cytoskeletal dynamics in growth-cone steering. J Cell Sci 122:3595-3604.

Goldberg JL (2004) Intrinsic neuronal regulation of axon and dendrite growth. Curr Opin Neurobiol 14:551-557.

Goldberg JL, Klassen MP, Hua Y, Barres BA (2002a) Amacrine-signaled loss of intrinsic axon growth ability by retinal ganglion cells. Science 296:1860-1864.

Goldberg JL, Espinosa JS, Xu Y, Davidson N, Kovacs GT, Barres BA (2002b) Retinal ganglion cells do not extend axons by default: promotion by neurotrophic signaling and electrical activity. Neuron 33:689-702.

Grabham PW, Reznik B, Goldberg DJ (2003) Microtubule and Rac 1-dependent F-actin in growth cones. J Cell Sci 116:3739-3748.

GrandPre T, Li S, Strittmatter SM (2002) Nogo-66 receptor antagonist peptide promotes axonal regeneration. Nature 417:547-551.

GrandPre T, Nakamura F, Vartanian T, Strittmatter SM (2000) Identification of the Nogo inhibitor of axon regeneration as a Reticulon protein. Nature 403:439-444.

Grimpe B, Silver J (2002) The extracellular matrix in axon regeneration. Prog Brain Res 137:333-349.

Grozdanov V, Muller A, Sengottuvel V, Leibinger M, Fischer D (2010) A method for preparing primary retinal cell cultures for evaluating the neuroprotective and neuritogenic effect of factors on axotomized mature CNS neurons. Curr Protoc Neurosci Chapter 3:Unit3 22.

Hauk TG, Muller A, Lee J, Schwendener R, Fischer D (2008) Neuroprotective and axon growth promoting effects of intraocular inflammation do not depend on oncomodulin or the presence of large numbers of activated macrophages. Exp Neurol 209:469-482.

Hauk TG, Leibinger M, Muller A, Andreadaki N, Knippschild U, Fischer D (2009) Intravitreal application of the Toll-like receptor 2 agonist Pam3Cys stimulates axon regeneration in the mature optic nerve. Invest Ophthalmol Vis Sci.

Hauk TG, Leibinger M, Muller A, Andreadaki A, Knippschild U, Fischer D (2010) Stimulation of axon regeneration in the mature optic nerve by intravitreal application of the toll-like receptor 2 agonist Pam3Cys. Invest Ophthalmol Vis Sci 51:459-464.

Heinrich PC, Behrmann I, Haan S, Hermanns HM, Muller-Newen G, Schaper F (2003) Principles of interleukin (IL)-6-type cytokine signalling and its regulation. Biochem J 374:1-20.

Hellal F, Hurtado A, Ruschel J, Flynn KC, Laskowski CJ, Umlauf M, Kapitein LC, Strikis D, Lemmon V, Bixby J, Hoogenraad CC, Bradke F (2011) Microtubule

stabilization reduces scarring and causes axon regeneration after spinal cord injury. Science 331:928-931.

Hellstrom M, Pollett MA, Harvey AR (2011) Post-injury delivery of rAAV2-CNTF combined with short-term pharmacotherapy is neuroprotective and promotes extensive axonal regeneration after optic nerve trauma. J Neurotrauma.

Horn KP, Busch SA, Hawthorne AL, van Rooijen N, Silver J (2008) Another barrier to regeneration in the CNS: activated macrophages induce extensive retraction of dystrophic axons through direct physical interactions. J Neurosci 28:9330-9341.

Huang JK, Phillips GR, Roth AD, Pedraza L, Shan W, Belkaid W, Mi S, Fex-Svenningsen A, Florens L, Yates JR, 3rd, Colman DR (2005) Glial membranes at the node of Ranvier prevent neurite outgrowth. Science 310:1813-1817.

Huber AB, Weinmann O, Brosamle C, Oertle T, Schwab ME (2002) Patterns of Nogo mRNA and protein expression in the developing and adult rat and after CNS lesions. J Neurosci 22:3553-3567.

Inagaki N, Chihara K, Arimura N, Menager C, Kawano Y, Matsuo N, Nishimura T, Amano M, Kaibuchi K (2001) CRMP-2 induces axons in cultured hippocampal neurons. Nat Neurosci 4:781-782.

Inatani M, Honjo M, Otori Y, Oohira A, Kido N, Tano Y, Honda Y, Tanihara H (2001) Inhibitory effects of neurocan and phosphacan on neurite outgrowth from retinal ganglion cells in culture. Invest Ophthalmol Vis Sci 42:1930-1938.

Jain A, Brady-Kalnay SM, Bellamkonda RV (2004) Modulation of Rho GTPase activity alleviates chondroitin sulfate proteoglycan-dependent inhibition of neurite extension. J Neurosci Res 77:299-307.

Janardhanan R, Butler JT, Banik NL, Ray SK (2009) N-(4-Hydroxyphenyl) retinamide potentiated paclitaxel for cell cycle arrest and apoptosis in glioblastoma C6 and RG2 cells. Brain Res 1268:142-153.

Jo SA, Wang E, Benowitz LI (1999) Ciliary neurotrophic factor is and axogenesis factor for retinal ganglion cells. Neuroscience 89:579-591.

Johnson PW, Abramow-Newerly W, Seilheimer B, Sadoul R, Tropak MB, Arquint M, Dunn RJ, Schachner M, Roder JC (1989) Recombinant myelin-associated glycoprotein confers neural adhesion and neurite outgrowth function. Neuron 3:377-385.

Jones LL, Margolis RU, Tuszynski MH (2003) The chondroitin sulfate proteoglycans neurocan, brevican, phosphacan, and versican are differentially regulated following spinal cord injury. Exp Neurol 182:399-411.

Kigerl KA, Gensel JC, Ankeny DP, Alexander JK, Donnelly DJ, Popovich PG (2009) Identification of two distinct macrophage subsets with divergent effects causing either neurotoxicity or regeneration in the injured mouse spinal cord. J Neurosci 29:13435-13444.

Kim JE, Liu BP, Park JH, Strittmatter SM (2004) Nogo-66 receptor prevents raphespinal and rubrospinal axon regeneration and limits functional recovery from spinal cord injury. Neuron 44:439-451.

Koprivica V, Cho KS, Park JB, Yiu G, Atwal J, Gore B, Kim JA, Lin E, Tessier-Lavigne M, Chen DF, He Z (2005) EGFR activation mediates inhibition of axon regeneration by myelin and chondroitin sulfate proteoglycans. Science 310:106-110.

Kottis V, Thibault P, Mikol D, Xiao ZC, Zhang R, Dergham P, Braun PE (2002) Oligodendrocyte-myelin glycoprotein (OMgp) is an inhibitor of neurite outgrowth. J Neurochem 82:1566-1569.

Kubo T, Hata K, Yamaguchi A, Yamashita T (2007) Rho-ROCK inhibitors as emerging strategies to promote nerve regeneration. Curr Pharm Des 13:2493-2499.

Kuhlmann T, Wendling U, Nolte C, Zipp F, Maruschak B, Stadelmann C, Siebert H, Bruck W (2002) Differential regulation of myelin phagocytosis by macrophages/microglia, involvement of target myelin, Fc receptors and activation by intravenous immunoglobulins. J Neurosci Res 67:185-190.

Kurimoto T, Yin Y, Omura K, Gilbert HY, Kim D, Cen LP, Moko L, Kugler S, Benowitz LI (2010) Long-distance axon regeneration in the mature optic nerve: contributions of oncomodulin, cAMP, and pten gene deletion. J Neurosci 30:15654-15663.

Lai C, Watson JB, Bloom FE, Sutcliffe JG, Milner RJ (1987) Neural protein 1B236/myelin-associated glycoprotein (MAG) defines a subgroup of the immunoglobulin superfamily. Immunol Rev 100:129-151.

Lauren J, Airaksinen MS, Saarma M, Timmusk T (2003) Two novel mammalian Nogo receptor homologs differentially expressed in the central and peripheral nervous systems. Mol Cell Neurosci 24:581-594.

Leaver SG, Cui Q, Bernard O, Harvey AR (2006a) Cooperative effects of bcl-2 and AAV-mediated expression of CNTF on retinal ganglion cell survival and axonal regeneration in adult transgenic mice. Eur J Neurosci 24:3323-3332.

Leaver SG, Cui Q, Plant GW, Arulpragasam A, Hisheh S, Verhaagen J, Harvey AR (2006b) AAV-mediated expression of CNTF promotes long-term survival and regeneration of adult rat retinal ganglion cells. Gene Ther 13:1328-1341.

Lee JK, Geoffroy CG, Chan AF, Tolentino KE, Crawford MJ, Leal MA, Kang B, Zheng B (2010) Assessing spinal axon regeneration and sprouting in Nogo-, MAG-, and OMgp-deficient mice. Neuron 66:663-670.

Lefrancois T, Fages C, Peschanski M, Tardy M (1997) Neuritic outgrowth associated with astroglial phenotypic changes induced by antisense glial fibrillary acidic protein (GFAP) mRNA in injured neuron-astrocyte cocultures. J Neurosci 17:4121-4128.

Lehmann M, Fournier A, Selles-Navarro I, Dergham P, Sebok A, Leclerc N, Tigyi G, McKerracher L (1999) Inactivation of Rho signaling pathway promotes CNS axon regeneration. J Neurosci 19:7537-7547.

Leibinger M, Muller A, Andreadaki A, Hauk TG, Kirsch M, Fischer D (2009) Neuroprotective and axon growth-promoting effects following inflammatory stimulation on mature retinal ganglion cells in mice depend on ciliary neurotrophic factor and leukemia inhibitory factor. J Neurosci 29:14334-14341.

Leon S, Yin Y, Nguyen J, Irwin N, Benowitz LI (2000) Lens injury stimulates axon regeneration in the mature rat optic nerve. J Neurosci 20:4615-4626.

Li S, Kim JE, Budel S, Hampton TG, Strittmatter SM (2005) Transgenic inhibition of Nogo-66 receptor function allows axonal sprouting and improved locomotion after spinal injury. Mol Cell Neurosci 29:26-39.

Li S, Liu BP, Budel S, Li M, Ji B, Walus L, Li W, Jirik A, Rabacchi S, Choi E, Worley D, Sah DW, Pepinsky B, Lee D, Relton J, Strittmatter SM (2004) Blockade of Nogo-66, myelin-associated glycoprotein, and oligodendrocyte myelin glycoprotein by soluble Nogo-66 receptor promotes axonal sprouting and recovery after spinal injury. J Neurosci 24:10511-10520.

Lingor P, Tonges L, Pieper N, Bermel C, Barski E, Planchamp V, Bahr M (2008) ROCK inhibition and CNTF interact on intrinsic signalling pathways and differentially regulate survival and regeneration in retinal ganglion cells. Brain 131:250-263.

Llorens F, Gil V, del Rio JA (2011) Emerging functions of myelin-associated proteins during development, neuronal plasticity, and neurodegeneration. FASEB J 25:463-475.

Logan A, Ahmed Z, Baird A, Gonzalez AM, Berry M (2006) Neurotrophic factor synergy is required for neuronal survival and disinhibited axon regeneration after CNS injury. Brain 129:490-502.

Lorber B, Berry M, Logan A (2005) Lens injury stimulates adult mouse retinal ganglion cell axon regeneration via both macrophage- and lens-derived factors. Eur J Neurosci 21:2029-2034.

Lorber B, Berry M, Douglas MR, Nakazawa T, Logan A (2009) Activated retinal glia promote neurite outgrowth of retinal ganglion cells via apolipoprotein E. J Neurosci Res.

Loschinger J, Bandtlow CE, Jung J, Klostermann S, Schwab ME, Bonhoeffer F, Kater SB (1997) Retinal axon growth cone responses to different environmental cues are mediated by different second-messenger systems. J Neurobiol 33:825-834.

Ludwin SK (1990) Oligodendrocyte survival in Wallerian degeneration. Acta Neuropathol 80:184-191.

Maranhao RC, Tavares ER, Padoveze AF, Valduga CJ, Rodrigues DG, Pereira MD (2008) Paclitaxel associated with cholesterol-rich nanoemulsions promotes atherosclerosis regression in the rabbit. Atherosclerosis 197:959-966.

Margolis RK, Margolis RU (1993) Nervous tissue proteoglycans. Experientia 49:429-446.

McKeon RJ, Hoke A, Silver J (1995) Injury-induced proteoglycans inhibit the potential for laminin-mediated axon growth on astrocytic scars. Exp Neurol 136:32-43.

McKeon RJ, Schreiber RC, Rudge JS, Silver J (1991) Reduction of neurite outgrowth in a model of glial scarring following CNS injury is correlated with the expression of inhibitory molecules on reactive astrocytes. J Neurosci 11:3398-3411.

McKerracher L, David S, Jackson DL, Kottis V, Dunn RJ, Braun PE (1994) Identification of myelin-associated glycoprotein as a major myelin-derived inhibitor of neurite growth. Neuron 13:805-811.

Mi S, Lee X, Shao Z, Thill G, Ji B, Relton J, Levesque M, Allaire N, Perrin S, Sands B, Crowell T, Cate RL, McCoy JM, Pepinsky RB (2004) LINGO-1 is a component of the Nogo-66 receptor/p75 signaling complex. Nat Neurosci 7:221-228.

Miao T, Wu D, Zhang Y, Bo X, Subang MC, Wang P, Richardson PM (2006) Suppressor of cytokine signaling-3 suppresses the ability of activated signal transducer and activator of transcription-3 to stimulate neurite growth in rat primary sensory neurons. J Neurosci 26:9512-9519.

Mikol DD, Gulcher JR, Stefansson K (1990) The oligodendrocyte-myelin glycoprotein belongs to a distinct family of proteins and contains the HNK-1 carbohydrate. J Cell Biol 110:471-479.

Mimura F, Yamagishi S, Arimura N, Fujitani M, Kubo T, Kaibuchi K, Yamashita T (2006) Myelin-associated glycoprotein inhibits microtubule assembly by a Rho-kinase-dependent mechanism. J Biol Chem 281:15970-15979.

Monnier PP, Sierra A, Schwab JM, Henke-Fahle S, Mueller BK (2003) The Rho/ROCK pathway mediates neurite growth-inhibitory activity associated with the chondroitin

sulfate proteoglycans of the CNS glial scar. Mol Cell Neurosci 22:319-330.

Moon LD, Asher RA, Rhodes KE, Fawcett JW (2001) Regeneration of CNS axons back to their target following treatment of adult rat brain with chondroitinase ABC. Nat Neurosci 4:465-466.

Moore DL, Blackmore MG, Hu Y, Kaestner KH, Bixby JL, Lemmon VP, Goldberg JL (2009) KLF family members regulate intrinsic axon regeneration ability. Science 326:298-301.

Mueller BK (1999) Growth cone guidance: first steps towards a deeper understanding. Annu Rev Neurosci 22:351-388.

Mukhopadhyay G, Doherty P, Walsh FS, Crocker PR, Filbin MT (1994) A novel role for myelin-associated glycoprotein as an inhibitor of axonal regeneration. Neuron 13:757-767.

Muller A, Hauk TG, Fischer D (2007) Astrocyte-derived CNTF switches mature RGCs to a regenerative state following inflammatory stimulation. Brain 130:3308-3320.

Muller A, Hauk TG, Leibinger M, Marienfeld R, Fischer D (2009) Exogenous CNTF stimulates axon regeneration of retinal ganglion cells partially via endogenous CNTF. Mol Cell Neurosci 41:233-246.

Oertle T, van der Haar ME, Bandtlow CE, Robeva A, Burfeind P, Buss A, Huber AB, Simonen M, Schnell L, Brosamle C, Kaupmann K, Vallon R, Schwab ME (2003) Nogo-A inhibits neurite outgrowth and cell spreading with three discrete regions. J Neurosci 23:5393-5406.

Ogasawara M, Matsubara T, Suzuki H (2001) Screening of natural compounds for inhibitory activity on colon cancer cell migration. Biol Pharm Bull 24:720-723.

Park JB, Yiu G, Kaneko S, Wang J, Chang J, He XL, Garcia KC, He Z (2005) A TNF receptor family member, TROY, is a coreceptor with Nogo receptor in mediating the inhibitory activity of myelin inhibitors. Neuron 45:345-351.

Park K, Luo JM, Hisheh S, Harvey AR, Cui Q (2004) Cellular mechanisms associated with spontaneous and ciliary neurotrophic factor-cAMP-induced survival and axonal regeneration of adult retinal ganglion cells. J Neurosci 24:10806-10815.

Park KK, Liu K, Hu Y, Smith PD, Wang C, Cai B, Xu B, Connolly L, Kramvis I, Sahin M, He Z (2008) Promoting axon regeneration in the adult CNS by modulation of the PTEN/mTOR pathway. Science 322:963-966.

Pasterkamp RJ, De Winter F, Giger RJ, Verhaagen J (1998) Role for semaphorin III and its receptor neuropilin-1 in neuronal regeneration and scar formation? Prog Brain Res 117:151-170.

Pasterkamp RJ, Giger RJ, Ruitenberg MJ, Holtmaat AJ, De Wit J, De Winter F, Verhaagen J (1999) Expression of the gene encoding the chemorepellent semaphorin III is induced in the fibroblast component of neural scar tissue formed following injuries of adult but not neonatal CNS. Mol Cell Neurosci 13:143-166.

Perez-Espejo MA, Haghighi SS, Adelstein EH, Madsen R (1996) The effects of taxol, methylprednisolone, and 4-aminopyridine in compressive spinal cord injury: a qualitative experimental study. Surg Neurol 46:350-357.

Pernet V, Di Polo A (2006) Synergistic action of brain-derived neurotrophic factor and lens injury promotes retinal ganglion cell survival, but leads to optic nerve dystrophy in vivo. Brain 129:1014-1026.

Pignot V, Hein AE, Barske C, Wiessner C, Walmsley AR, Kaupmann K, Mayeur H, Sommer B, Mir AK, Frentzel S (2003) Characterization of two novel proteins, NgRH1 and NgRH2, structurally and biochemically homologous to the Nogo-66 receptor. J Neurochem 85:717-728.

Prinjha R, Moore SE, Vinson M, Blake S, Morrow R, Christie G, Michalovich D, Simmons DL, Walsh FS (2000) Inhibitor of neurite outgrowth in humans. Nature 403:383-384.

Richardson PM, Issa VM (1984) Peripheral injury enhances central regeneration of primary sensory neurones. Nature 309:791-793.

Schachtrup C, Lu P, Jones LL, Lee JK, Lu J, Sachs BD, Zheng B, Akassoglou K (2007) Fibrinogen inhibits neurite outgrowth via beta 3 integrin-mediated phosphorylation of the EGF receptor. Proc Natl Acad Sci U S A 104:11814-11819.

Schnell L, Schwab ME (1990) Axonal regeneration in the rat spinal cord produced by an antibody against myelin-associated neurite growth inhibitors. Nature 343:269-272.

Schnell L, Schwab ME (1993) Sprouting and regeneration of lesioned corticospinal tract fibres in the adult rat spinal cord. Eur J Neurosci 5:1156-1171.

Schreyer DJ, Skene JH (1993) Injury-associated induction of GAP-43 expression displays axon branch specificity in rat dorsal root ganglion neurons. J Neurobiol 24:959-970.

Schwab ME, Kapfhammer JP, Bandtlow CE (1993) Inhibitors of neurite growth. Annu Rev Neurosci 16:565-595.

Sengottuvel V, Leibinger M, Pfreimer M, Andreadaki A, Fischer D (2011) Taxol facilitates axon regeneration in the mature CNS. J Neurosci 31:2688-2699.

Shamash S, Reichert F, Rotshenker S (2002) The cytokine network of Wallerian degeneration: tumor necrosis factor-alpha, interleukin-1alpha, and interleukin-

1beta. J Neurosci 22:3052-3060.

Shao Z, Browning JL, Lee X, Scott ML, Shulga-Morskaya S, Allaire N, Thill G, Levesque M, Sah D, McCoy JM, Murray B, Jung V, Pepinsky RB, Mi S (2005) TAJ/TROY, an orphan TNF receptor family member, binds Nogo-66 receptor 1 and regulates axonal regeneration. Neuron 45:353-359.

Shen Y, Tenney AP, Busch SA, Horn KP, Cuascut FX, Liu K, He Z, Silver J, Flanagan JG (2009) PTPsigma is a receptor for chondroitin sulfate proteoglycan, an inhibitor of neural regeneration. Science 326:592-596.

Silver J, Miller JH (2004) Regeneration beyond the glial scar. Nat Rev Neurosci 5:146-156.

Skoff RP, Vaughn JE (1971) An autoradiographic study of cellular proliferation in degenerating rat optic nerve. J Comp Neurol 141:133-155.

Smith PD, Sun F, Park KK, Cai B, Wang C, Kuwako K, Martinez-Carrasco I, Connolly L, He Z (2009) SOCS3 deletion promotes optic nerve regeneration in vivo. Neuron 64:617-623.

Steinmetz MP, Horn KP, Tom VJ, Miller JH, Busch SA, Nair D, Silver DJ, Silver J (2005) Chronic enhancement of the intrinsic growth capacity of sensory neurons combined with the degradation of inhibitory proteoglycans allows functional regeneration of sensory axons through the dorsal root entry zone in the mammalian spinal cord. J Neurosci 25:8066-8076.

Sun F, He Z (2010) Neuronal intrinsic barriers for axon regeneration in the adult CNS. Curr Opin Neurobiol 20:510-518.

Sun F, Park KK, Belin S, Wang D, Lu T, Chen G, Zhang K, Yeung C, Feng G, Yankner BA, He Z (2011) Sustained axon regeneration induced by co-deletion of PTEN and SOCS3. Nature.

Tanaka E, Ho T, Kirschner MW (1995) The role of microtubule dynamics in growth cone motility and axonal growth. J Cell Biol 128:139-155.

Tang BL (2003) Inhibitors of neuronal regeneration: mediators and signaling mechanisms. Neurochem Int 42:189-203.

Tian DS, Yu ZY, Xie MJ, Bu BT, Witte OW, Wang W (2006) Suppression of astroglial scar formation and enhanced axonal regeneration associated with functional recovery in a spinal cord injury rat model by the cell cycle inhibitor olomoucine. J Neurosci Res 84:1053-1063.

Vargas ME, Barres BA (2007) Why is Wallerian degeneration in the CNS so slow? Annu Rev Neurosci 30:153-179.

Vidal-Sanz M, Bray GM, Villegas-Perez MP, Thanos S, Aguayo AJ (1987) Axonal regeneration and synapse formation in the superior colliculus by retinal ganglion cells in the adult rat. J Neurosci 7:2894-2909.

Villegas-Perez MP, Vidal-Sanz M, Rasminsky M, Bray GM, Aguayo AJ (1993) Rapid and protracted phases of retinal ganglion cell loss follow axotomy in the optic nerve of adult rats. J Neurobiol 24:23-36.

Vinson M, Strijbos PJ, Rowles A, Facci L, Moore SE, Simmons DL, Walsh FS (2001) Myelin-associated glycoprotein interacts with ganglioside GT1b. A mechanism for neurite outgrowth inhibition. J Biol Chem 276:20280-20285.

Vyas AA, Patel HV, Fromholt SE, Heffer-Lauc M, Vyas KA, Dang J, Schachner M, Schnaar RL (2002) Gangliosides are functional nerve cell ligands for myelin-associated glycoprotein (MAG), an inhibitor of nerve regeneration. Proc Natl Acad Sci U S A 99:8412-8417.

Vyas DM, Kadow JF (1995) Paclitaxel: a unique tubulin interacting anticancer agent. Prog Med Chem 32:289-337.

Wang KC, Kim JA, Sivasankaran R, Segal R, He Z (2002a) P75 interacts with the Nogo receptor as a co-receptor for Nogo, MAG and OMgp. Nature 420:74-78.

Wang KC, Koprivica V, Kim JA, Sivasankaran R, Guo Y, Neve RL, He Z (2002b) Oligodendrocyte-myelin glycoprotein is a Nogo receptor ligand that inhibits neurite outgrowth. Nature 417:941-944.

Wang X, Chun SJ, Treloar H, Vartanian T, Greer CA, Strittmatter SM (2002c) Localization of Nogo-A and Nogo-66 receptor proteins at sites of axon-myelin and synaptic contact. J Neurosci 22:5505-5515.

Waterman-Storer CM, Worthylake RA, Liu BP, Burridge K, Salmon ED (1999) Microtubule growth activates Rac1 to promote lamellipodial protrusion in fibroblasts. Nat Cell Biol 1:45-50.

Whitford KL, Ghosh A (2001) Plexin signaling via off-track and rho family GTPases. Neuron 32:1-3.

Winzeler AM, Mandemakers WJ, Sun MZ, Stafford M, Phillips CT, Barres BA (2011) The lipid sulfatide is a novel myelin-associated inhibitor of CNS axon outgrowth. J Neurosci 31:6481-6492.

Wiskirchen J, Schober W, Schart N, Kehlbach R, Wersebe A, Tepe G, Claussen CD, Duda SH (2004) The effects of paclitaxel on the three phases of restenosis: smooth muscle cell proliferation, migration, and matrix formation: an in vitro study. Invest Radiol 39:565-571.

Witte H, Neukirchen D, Bradke F (2008) Microtubule stabilization specifies initial neuronal polarization. J Cell Biol 180:619-632.

Wong EV, David S, Jacob MH, Jay DG (2003) Inactivation of myelin-associated glycoprotein enhances optic nerve regeneration. J Neurosci 23:3112-3117.

Wong ST, Henley JR, Kanning KC, Huang KH, Bothwell M, Poo MM (2002) A p75(NTR) and Nogo receptor complex mediates repulsive signaling by myelin-associated glycoprotein. Nat Neurosci 5:1302-1308.

Yamashita T, Higuchi H, Tohyama M (2002) The p75 receptor transduces the signal from myelin-associated glycoprotein to Rho. J Cell Biol 157:565-570.

Yin Y, Cui Q, Li Y, Irwin N, Fischer D, Harvey AR, Benowitz LI (2003) Macrophage-derived factors stimulate optic nerve regeneration. J Neurosci 23:2284-2293.

Yiu G, He Z (2006) Glial inhibition of CNS axon regeneration. Nat Rev Neurosci 7:617-627.

Zheng B, Ho C, Li S, Keirstead H, Steward O, Tessier-Lavigne M (2003) Lack of enhanced spinal regeneration in Nogo-deficient mice. Neuron 38:213-224.

Zheng B, Atwal J, Ho C, Case L, He XL, Garcia KC, Steward O, Tessier-Lavigne M (2005) From the Cover: Genetic deletion of the Nogo receptor does not reduce neurite inhibition in vitro or promote corticospinal tract regeneration in vivo. Proc Natl Acad Sci U S A 102:1205-1210.

7. Acknowledgements

I sincerely thank the following people who have helped me through the course of my thesis project duration. It would have been impossible to carry out this project without their unstinted support.

First, I would like to thank my principal supervisor, **Prof. Dr. Dietmar Fischer** for giving me the opportunity to work in his lab in the exciting field of axon regeneration in the central nervous system. I am grateful for his support during each step of my thesis work and for providing me deep insights through fruitful discussions to understand the nuances of scientific details and constructive criticisms to develop myself in my research career.

I am grateful to my second supervisor, **Prof. Dr. Uwe Knippschild** for his support and evaluating my thesis. I am also grateful to **Prof. Dr. Ralf Marienfeld** and **Prof. Dr. Stefan Schumacher** for accepting to be my thesis examiners.

I would like to express my sincere gratitude to all the members of Prof. Fischer's lab, especially **Marco Leibinger** and **Anastasia Andreadaki** for their valuable help during my thesis work. I also thank **Mariana Pfreimer**, Department of Pharmacology and **Dr. Anke Witting**, Department of Neurology, Universität Ulm for their support.

I am greatly indebted to **my parents**, **family members** and **friends** who have helped me through my journey in research career and life.

8. Curriculum Vitae

Personal information

Name	Vetrivel Sengottuvel
Date of Birth	10 June 1982
Place of Birth	Rasipuram, Tamilnadu, India
Nationality	Indian
Contact address	Brinckmannstrasse 13 A 40225 Düsseldorf Germany

Education

June 2000 – May 2003	: **Bachelor of Science** (**B.Sc**) in **Zoology** at Loyola College, Chennai, India.
June 2003 – May 2005	: **Master of Science** (**M.Sc**) in **Biotechnology** at University of Madras, Chennai, India.
June 2008 – present	: **PhD student** on **"**Optic nerve regeneration**"** at Department of Experimental Neurology, Universität Ulm and Universität Düsseldorf, Germany.

Research Experience

May – June 2004	: **Summer Traineeship project** on **"**DNA- protection against gamma radiation by synthetic and natural compounds**"**, at Bhabha Atomic Research Centre, India.
January-May 2005	: **M.Sc Thesis project** on **"**Persistent Infections with Japanese Encephalitis Virus**"**, at National Institute of Virology, India.
December 2005 – September 2007	: **Project Fellow** on **"**HIV-1 neuropathogenesis**"**, at National Brain Research Centre, India.
October 2007 – May 2008	: **Research student** on **"**Signaling pathways during neuroinflammation**"**, at University of Bonn, Germany.

List of Scientific publications

Sengottuvel V, Leibinger M, Pfreimer M, Andreadaki A, Fischer D (2011) Taxol facilitates axon regeneration in the mature CNS. J Neurosci 31:2688-2699.

Grozdanov V, Muller A, Sengottuvel V, Leibinger M, Fischer D (2010) A method for preparing primary retinal cell cultures for evaluating the neuroprotective and neuritogenic effect of factors on axotomized mature CNS neurons. Curr Protoc Neurosci Chapter 3:Unit3 22.

Sengottuvel Vetrivel and Pankaj Seth. (2007) HIV-1 associated dementia in the pre and post HAART era. Annals of Neurosciences. Volume 14, No 2: 41-49.
[Official journal of Indian Academy of Neurosciences]

Mishra M, Vetrivel S, Siddappa NB, Ranga U, Seth P (2008) Clade-specific differences in neurotoxicity of human immunodeficiency virus-1 B and C Tat of human neurons: significance of dicysteine C30C31 motif. Ann Neurol 63:366-376.

Poster presentations

Sengottuvel V, Leibinger M, Pfreimer M, Andreadaki A, Fischer D. (2011) Taxol facilitates axon regeneration in the mature CNS. NeuroVisionen7 Symposium, held at Universitätsklinikum Essen, Germany.

Vetrivel S, Gandhi NM, Nair CKK. (2005) *in vitro* and *in vivo* protection of DNA and membrane damages from *gamma* radiation by Terminalia chebula extract. International Conference on Antioxidants & Free Radicals in Health-Nutrition & Radio-protectors and IV Annual Conference of Society for Free Radical Research in India, held at St.John's Medical College, Bangalore, India.